

*M.A. Rahman, S. Sritharan*

**Force-Based Vs. Displacement-Based Design of  
Jointed Precast Prestressed Wall Systems**

**ISU-CCEE Report 01/11  
Submitted to the  
Precast/Prestressed Concrete Institute**

**JUNE 2011**

**Final**

---

***REPORT***

---

**IOWA STATE UNIVERSITY**  
OF SCIENCE AND TECHNOLOGY

**Department of Civil, Construction  
and Environmental Engineering**

# **Force-Based Vs. Displacement-Based Design of Jointed Precast Prestressed Wall Systems**

**by**

**Mohammad Aatur Rahman**  
Graduate Research Assistant

**Sri Sritharan**  
Professor

**ISU-CCEE Report 01/11**

**A Final Report to the Precast/Prestressed Concrete**

Department of Civil, Construction and Environmental Engineering  
Iowa State University  
Ames, IA 50011

**June 2011**

*Intentionally blank*

## **ABSTRACT**

This study focuses on the multiple-level seismic performance in terms of structural and non-structural damages of jointed precast post-tensioned wall systems through a dynamic analysis of precast buildings subjected to spectrum compatible ground motions of various intensities. The maximum transient interstory drift, residual interstory drift, and floor acceleration are considered as acceptance criteria for evaluating seismic performance of these systems subjected by four levels of ground motions. Interstory drift and floor acceleration are directly related to structural and non-structural damages, respectively. Two-dimensional non-linear finite element analytical models for jointed wall systems used in this study are validated against test results for a five-story test building. In designing this precast structural system, it is shown that traditional force-based design approach results in significantly higher level of design base shear compared to direct displacement-based design approach. After observing satisfactory performance in the five-story model building designed by the direct displacement-based approach, similar multiple-level seismic performance is evaluated for five-, seven- and ten-story buildings designed by the direct displacement-based method. These low to mid-rise full scale jointed precast post-tensioned wall systems also exhibit the maximum transition interstory drift, residual interstory drift, and floor acceleration within the acceptable limits. Therefore, it is recommended these systems may be utilized as primary lateral load resistant structural systems when designed by the economic approach of direct displacement-based design. Variation influence of building heights on the performance of this system is also examined.

## **ACKNOWLEDGMENTS**

The research described in this report was funded by the Precast/Prestressed Concrete Institute (PCI) through the Daniel P. Jenny Fellowship program, which is greatly acknowledged. Additionally the authors like to thank Dr. Ned Cleland, Dr. S. K. Ghosh and Ms. Suzanne Nakaki who served as advisors for the Daniel P. Jenny Fellowship award. The authors also like to acknowledge the support from Professor Eduardo Miranda at Stanford University, California, USA in providing the ground motion information. Help from former graduate students, Sriram Aaleti and Onur Celik, is appreciated.

Conclusions, opinions and recommendations expressed in this report are those of the authors alone, and should not be considered endorsed by the financial sponsor.

# TABLE OF CONTENTS

|  |           |
|--|-----------|
| <b>ABSTRACT</b> .....  | iii       |
| <b>ACKNOWLEDGMENTS</b> .....                                 | iv        |
| <b>TABLE OF CONTENTS</b> .....                               | v         |
| <b>LIST OF TABLES</b> .....                                  | viii      |
| <b>LIST OF FIGURES</b> .....                                 | ix        |
| <b>CHAPTER 1: GENERAL INTRODUCTION</b> .....                 | <b>1</b>  |
| 1.1 Introduction.....  | 1         |
| 1.2 Benefits of Precast Concrete.....                        | 2         |
| 1.3 Unbonded Precast Wall Systems .....                      | 3         |
| 1.4 Seismic Design Methods.....                              | 4         |
| 1.5 Multiple-Level Performance-Based Seismic Evaluation..... | 6         |
| 1.6 Previous Work .....                                      | 7         |
| 1.7 Scope of Research.....                                   | 14        |
| 1.8 Report Layout .....                                      | 15        |
| 1.9 References.....  | 17        |
| <b>CHAPTER 2: REVIEW OF LITERATURE</b> .....                 | <b>20</b> |
| 2.1 Introduction.....  | 20        |
| 2.2 Unbonded Post-Tensioned Precast Wall Systems .....       | 20        |
| 2.2.1 Single wall system .....                               | 20        |
| 2.2.1.1 Kurama et al. (1999); Kurama et al. (2002).....      | 20        |
| 2.2.2 Precast jointed wall systems .....                     | 23        |
| 2.2.2.1 Priestley et al. (1999).....                         | 23        |
| 2.2.2.2 Thomas (2003); Thomas and Sritharan (2004).....      | 23        |
| 2.2.2.3 Sritharan et al. (2006); Aaleti (2005).....          | 25        |
| 2.3 References.....  | 32        |

|   |           |
|---|-----------|
| <b>CHAPTER 3: AN EVALUATION OF FORCE-BASED DESIGN VS. DIRECT DISPLACEMENT-BASED DESIGN OF JOINTED PRECAST POST-TENSIONED WALL SYSTEMS.....</b>                            | <b>34</b> |
| 3.1 Introduction.....   | 35        |
| 3.2 Unbonded Post Tensioning Precast Jointed Wall Systems.....  | 36        |
| 3.3 Analytical Model .....  | 38        |
| 3.4 Characteristics of Elements Used in the Analytical Model .....  | 40        |
| 3.5 Model Validation .....  | 41        |
| 3.6 Performance-Based Seismic Evaluation.....   | 42        |
| 3.6.1 Input ground motions.....   | 43        |
| 3.6.2 Interstory drift limits.....  | 44        |
| 3.6.3 Floor acceleration limits .....   | 44        |
| 3.7 Results from Earthquake Analysis of Jointed Wall Systems.....   | 45        |
| 3.8 Conclusions.....  | 48        |
| 3.9 Acknowledgments.....  | 49        |
| 3.10 References.....  | 51        |
| <b>CHAPTER 4: SEISMIC RESPONSE OF PRECAST POST-TENSIONED JOINTED WALL SYSTEMS DESIGN FOR LOW TO MID-RISE BUILDINGS USING THE DIRECT DISPLACEMENT-BASED APPROACH .....</b> | <b>67</b> |
| 4.1 Introduction.....   | 68        |
| 4.2 Unbonded Post Tensioning Precast Wall Systems in Five, Seven And Ten Story Buildings.....   | 69        |
| 4.3 Dynamic Analysis Models.....  | 70        |
| 4.4 Performance-Based Seismic Evaluation.....   | 72        |
| 4.6 Interstory drift limits.....  | 73        |
| 4.7 Floor acceleration limits .....   | 74        |
| 4.8 Analysis Results.....   | 74        |
| 4.9 Conclusions.....  | 80        |
| 4.10 Acknowledgments.....   | 81        |
| 4.11 References.....  | 82        |

|                                     |            |
|-------------------------------------|------------|
| <b>CHAPTER 5: CONCLUSIONS .....</b> | <b>105</b> |
| 5.1 Overview .....                  | 105        |
| 5.2 Conclusions.....                | 105        |
| 5.3 Future Research .....           | 106        |

## LIST OF TABLES

|  |    |
|--|----|
| Table 3.1 Dimensions of the jointed wall JWS1 and the properties of the analytical model shown in Fig. 3.5 .....   | 54 |
| Table 3.2 Different combinations of short-duration ground motions used for the performance based seismic evaluation of precast jointed wall systems .....                              | 55 |
| Table 3.3 List of ground motions selected for the performance-based seismic evaluation of precast jointed wall systems .....   | 55 |
| Table 4.1 Design base shear force calculated by force-based and direct displacement-based methods for low and mid-rise buildings .....   | 85 |
| Table 4.2 Dimensions of the jointed wall systems and the properties of the analytical models shown in Fig. 4.3 for the five, seven and ten story buildings.....                        | 85 |
| Table 4.3 List of long-duration ground motions selected for the performance-based evaluation of the ten, seven and five story precast jointed wall system buildings .....              | 86 |
| Table 4.4 List of combinations of short-duration ground motions used for the performance-based evaluation of the ten, seven and five story precast jointed wall system buildings ..... | 86 |
| Table 4.5 Maximum residual interstory drift of the seven and ten story buildings under long-duration motions.....  | 87 |

## LIST OF FIGURES

|  |    |
|--|----|
| Figure 1.1 Illustration of a jointed wall system .....   | 4  |
| Figure 1.2 A schematic of a design spectrum acceleration used in estimating design base shear force in force-based design method.....  | 5  |
| Figure 1.3 A schematic of a spectrum displacement used in estimating design base shear in direct displacement-based method (Priestley 2002) .....  | 6  |
| Figure 1.4 Floor plans of the PRESSSS test building (Sritharan et al. 2002).....   | 9  |
| Figure 1.5 The typical connection details of a precast hybrid frame (transverse reinforcements are omitted for clarity) .....  | 10 |
| Figure 1.6 Elevation view of the jointed wall system used in the PRESSSS test building (Sritharan et al. 2002) .....   | 11 |
| Figure 1.7 The PRESSSS building after erecting the wall system (Sritharan et al. 2002) .....   | 12 |
| Figure 1.8 Connection details of UFP connectors in the PRESSSS building (Sritharan et al. 2002) .....  | 13 |
| Figure 1.9 The 5% damped multiple-level acceleration response spectra, suggested for soil type Sc in high seismic zone as per Reference (Performance-Based Seismic Engineering Ad Hoc Subcommittee 2003).....        | 13 |
| Figure 2.1 Precast wall base shear-roof drift relationship (Kurama et al. 1999).....   | 21 |
| Figure 2.2 Comparison of roof drifts obtained from dynamic analysis of walls (Kurama et al. 1999) .....  | 22 |
| Figure 2.3 Force displacement response of a precast wall under cyclic loading (Kurama et al. 1999) .....   | 22 |
| Figure 2.4 Forces acting on a jointed two-wall system at base rotation $\theta$ ( $C$ = resultant compressive force and $T = P_D$ + force in the prestressing tendon) (Sritharan et al. 2006; Aaleti 2005) .....     | 28 |
| Figure 2.5 Forces acting on a jointed three-wall system at base rotation $\theta$ ( $C$ = resultant compressive force and $T = P_D$ + force in the prestressing tendon) (Sritharan et al., 2006; Aaleti, 2005) ..... | 29 |

|   |    |
|---|----|
| Figure 3.1 Illustration of the jointed wall system .....  | 56 |
| Figure 3.2 Plan view of the precast concrete prototype building (Nakaki et al. 1999) .....  | 56 |
| Figure 3.3 Plan view of the scaled post-tensioned precast wall system building .....  | 57 |
| Figure 3.4 The PRESSSS test building after erecting the jointed wall system.....  | 57 |
| Figure 3.5 Proposed analytical model for the building with the jointed wall system shown in<br>Fig. 3.3.....  | 58 |
| Figure 3.6 Illustration of rotations of walls and the corresponding UFP deformation at a base<br>rotation of $\theta$ .....   | 58 |
| Figure 3.7 Short-duration earthquake ground motions used for testing of the PRESSSS<br>building in the jointed wall direction .....   | 59 |
| Figure 3.8 The 5% damped multiple-level acceleration response spectra suggested for soil<br>type Sc in high seismic zone as per the Performance-Based Seismic Engineering<br>Ad Hoc Subcommittee (2003) of SEAOC..... | 59 |
| Figure 3.9 Comparison between the analytical and experimental lateral displacement at the<br>fifth floor of the PRESSSS test building in the jointed wall direction.....  | 60 |
| Figure 3.10 Comparison between the analytical and experimental base moment of the<br>PRESSSS test building in the jointed wall direction .....  | 60 |
| Figure 3.11 Comparison between the analytical and experimental UFP deformation at the<br>fifth floor of the PRESSSS test building in the jointed wall direction.....  | 61 |
| Figure 3.12 (a) The 5% damped acceleration response spectra of EQ-I, EQ-II and EQ-III with<br>those produced for scaled ground motions IM-a through IM-e listed in Table 3.3<br>.....                                 | 61 |
| Figure 3.12 (b) The 5% damped acceleration response spectra of EQ-IV with those produced<br>for scaled ground motions IM-f through IM-h listed in Table 3.3.....  | 62 |
| Figure 3.13 The maximum transient interstory drifts obtained for JWS1 (DDBD) and JWS2<br>(FBD) when subjected to various combinations of short-duration ground motions<br>summarized in Table 3.2.....                | 62 |
| Figure 3.14 The maximum floor accelerations obtained for JW1 (DDBD) and JW2 (FBD)<br>when subjected to various combinations of short-duration ground motions<br>summarized in Table 3.2.....                          | 63 |

|   |    |
|---|----|
| Figure 3.15 The maximum transient interstory drifts obtained for JWS1 (DDBD) and JWS2 (FBD) when subjected to various long-duration ground motions summarized in Table 3.3 .....  | 63 |
| Figure 3.16 The maximum floor accelerations obtained for JWS1 (DDBD) and JWS2 (FBD) when subjected to various long-duration ground motions summarized in Table 3.3 .....  | 64 |
| Figure 3.17 (a) Illustration of the influence of the number of UFP connectors on the maximum transient interstory drift of JWS1 using input motion IM-d .....   | 64 |
| Figure 3.17 (b) Illustration of the influence of the number of UFP connectors on the maximum residual interstory drift of JWS1 using input motion IM-d.....   | 65 |
| Figure 3.18 (a) Illustration of the influence of the number of UFP connectors on the maximum transient interstory drift of JWS1 using input motion IM-c.....  | 65 |
| Figure 3.18 (b) Illustration of the influence of the number of UFP connectors on the maximum residual interstory drift of JWS1 using input motion IM-c.....   | 66 |
| Figure 4.1 Illustration of a unbonded precast post tensioned jointed wall system .....  | 88 |
| Figure 4.2 Plan view for the five, seven and ten story prototype buildings .....  | 88 |
| Figure 4.3 Analytical model of the wall system in the ten story building .....  | 89 |
| Figure 4.4 Illustration of typical moment-rotation response of post-tensioning spring located at each wall base and force-displacement response of UFP spring placed between two walls .....  | 90 |
| Figure 4.5 The 5% damped multiple-level acceleration response spectra suggested for soil type Sc in high seismic zone as per the Performance-Based Seismic Engineering Ad Hoc Subcommittee (2003) of SEAOC. (The insert in the figure shows short-duration earthquake ground motions) ..... | 90 |
| Figure 4.6 (a) Deflected shape of the five story building when achieving at the maximum interstory drifts imposed by the four levels of ground motions.....   | 91 |
| Figure 4.6 (b) Deflected shape of the seven story building when achieving at the maximum interstory drifts imposed by the four levels of ground motions.....  | 91 |
| Figure 4.6 (c) Deflected shape of the ten story building when achieving at the maximum interstory drifts imposed by the four levels of ground motions.....  | 92 |

|   |     |
|---|-----|
| Figure 4.7 Correlation between the average and maximum interstory drifts obtained for the five, seven and ten story post-tensioned jointed wall system based on the responses to long-duration ground motions ..... | 92  |
| Figure 4.8 (a) Maximum transient interstory drift obtained for the five story jointed wall system building subjected to the long-duration ground motions .....  | 93  |
| Figure 4.8 (b) Maximum transient interstory drift obtained for the seven story jointed wall system building subjected to the long-duration ground motions .....   | 94  |
| Figure 4.8 (c) transient interstory drift obtained for the ten stories jointed wall system building subjected to long-duration ground motions .....   | 95  |
| Figure 4.9 (a) Maximum floor acceleration obtained for the five story jointed wall system building subjected to the long-duration ground motions .....  | 96  |
| Figure 4.9 (b) Maximum floor acceleration obtained for the seven story jointed wall system building subjected to the long-duration ground motions .....   | 97  |
| Figure 4.9 (c) Maximum floor acceleration obtained for the ten story jointed wall system building subjected to the long-duration ground motions .....   | 98  |
| Figure 4.10 (a) Maximum transient interstory drift obtained for the five story building when subjected to short-duration ground motions .....   | 99  |
| Figure 4.10 (b) Maximum transient interstory drift obtained for the seven story building when subjected to short-duration ground motions.....   | 99  |
| Figure 4.10 (c) Maximum transient interstory drift obtained for the ten story building when subjected to short-duration ground motions .....  | 100 |
| Figure 4.11(a) Maximum floor acceleration obtained for the five story building when subjected to short-duration ground motions .....  | 100 |
| Figure 4.11 (b) Maximum floor acceleration obtained for the seven story building when subjected to short-duration ground motions .....  | 101 |
| Figure 4.11 (c) Maximum floor acceleration obtained for the ten story building when subjected to short-duration ground motions .....  | 101 |
| Figure 4.12 The maximum transient interstory drift normalized by the acceptable interstory drift.....   | 102 |

|   |     |
|---|-----|
| Figure 4.13 The maximum floor acceleration normalized by the acceptable floor acceleration<br>.....   | 103 |
| Figure 4.14 Effect of moment of inertia of wall in controlling the maximum floor<br>acceleration when the ten story building was subjected to ground motion IM-h<br>..... | 103 |
| Figure 4.15 Effect of moment of inertia of wall in controlling the maximum floor<br>acceleration when the ten story building was subjected to ground motion IM-c<br>..... | 104 |

# CHAPTER 1: GENERAL INTRODUCTION

## 1.1 Introduction

Precast concrete structural systems benefit from advantages, such as improved quality of construction, efficient use of materials, reduced construction time, and cost efficiency. In addition, precast concrete allows architects and engineers to perform more innovative designs than traditional cast-in-place concrete design. Poor performance (Fintel 2002; Earthquake Engineering Research Institute 1996; Ghosh 2001; John A. Martin and Associates, Inc. 2003) of precast structures in past earthquakes has given designers, architects, and contractors a misconception that precast concrete may not be a desirable construction technology in seismic regions. This lower level of performance of several precast structures in past earthquakes was either due to the lack of a sufficient number of lateral load resisting systems in the structures or a result of using poor connection details between precast elements that contributed to brittle structural behavior (Vernu and Sritharan 2004). Recent advancements in research have introduced efficient precast structural systems (e.g., hybrid frame (Priestley et al. 1999) and unbonded jointed precast walls (Priestley et al. 1999) capable of maintaining structural integrity, as well as providing sufficient energy dissipation under cyclic loading; thus, improving the seismic performance of precast structural system. Both the hybrid frame system and unbonded jointed precast wall system use simple concepts. In a hybrid connection, the beam and column are connected through unbonded post-tensioning tendons and mild steel reinforcement across the beam-column interface. In a jointed precast wall system, individual walls are held to the foundation by post-tensioning from the top of the wall, and are connected to each other horizontally along the height using special energy dissipating connectors. Despite these huge potential developments for seismic resistance, sufficient analytical research to support their dynamic response under earthquake loads has not been completed. Such an investigation is expected to elevate the confidence of practicing engineers on using these innovative and economical precast structural systems in seismic regions.

In this study, seismic performance of precast jointed walls suitable for low- to mid-rise buildings will be investigated by conducting dynamic analyses using various levels of ground motions. Consequently, this study will help predict the seismic performance of this structural system. In addition, the difference in performance of currently available seismic design methods will be conducted through dynamic analysis of two similar precast jointed walls.

The remainder of this introductory chapter focuses on the general benefits of precast concrete, description of unbonded jointed precast wall systems, current seismic design methods, and performance-based seismic evaluation. A short description of previous work on this field will be presented, followed by the scope of research and the report layout.

## 1.2 Benefits of Precast Concrete

Concrete exhibits high compressive strength and low tensile strength due to its brittleness. Flexural cracks develop in concrete members at early stages of loading as flexural tensile stresses exceed the tensile strength of concrete. Development of undesirable flexural cracking in structures may be delayed or avoided under service conditions by prestressing the concrete. Precast concrete provides the following benefits over cast-in-place concrete systems.

- **High quality:** Precast concrete products exhibit higher quality and more uniform properties than cast-in-place counterparts because they are produced under controlled environment in a manufacturing plant, where curing conditions, such as temperature and humidity, are typically controlled and the dependency on craftsmanship is somewhat reduced. Moreover, efficient inspection of precast concrete production enhances the quality of the products (Park 1995).
- **Use of advance technology:** Robotics and computer-aided manufacturing are feasible for precast concrete construction, which will lead to more efficient production and erection of components (Priestly 1991).
- **Optimum use of materials:** A significant reduction to the concrete volume is achieved in precast concrete elements by using high strength concrete and steel. High strength materials help to achieve a longer life cycle (Vernu 2003).

- **Reduced construction time:** Construction of precast components requires a significantly reduced amount of formwork and temporary supports in the field compared to cast-in-place concrete construction. Using prefabricated concrete members helps to reduce construction time of structures in comparison to the cast-in-place concrete construction. Furthermore, time is not wasted due to bad weather conditions or for curing concrete.
- **Cost efficiency:** Faster erection time and quick factory production lead to reduction in construction and labor costs. Multiple uses of the same forms, for constructing standard precast members, also contribute to reducing construction costs (Priestly 1991).

### **1.3 Unbonded Precast Wall Systems**

Unbonded jointed precast walls can be used as the primary structural system for resisting seismic lateral forces. Individual precast walls are attached to the foundation by unbonded post-tensioning steel running from the top of the wall to the foundation. Two or more such post-tensioned walls are connected to each other, horizontally along the height, by shear connectors to form a jointed precast wall system (Fig. 1.1). When detailed with unbonded post-tensioning, a precast concrete wall can provide added benefits, such as reduced structural damage and minimum residual displacements when subjected to seismic lateral forces, due to concentration of flexural cracks and re-centering capability of prestressing tendon (Thomas and Sritharan 2004). The main disadvantage against single unbonded precast walls is the lack of energy dissipating capability, which is eliminated by incorporating shear connectors between the walls in jointed wall systems.

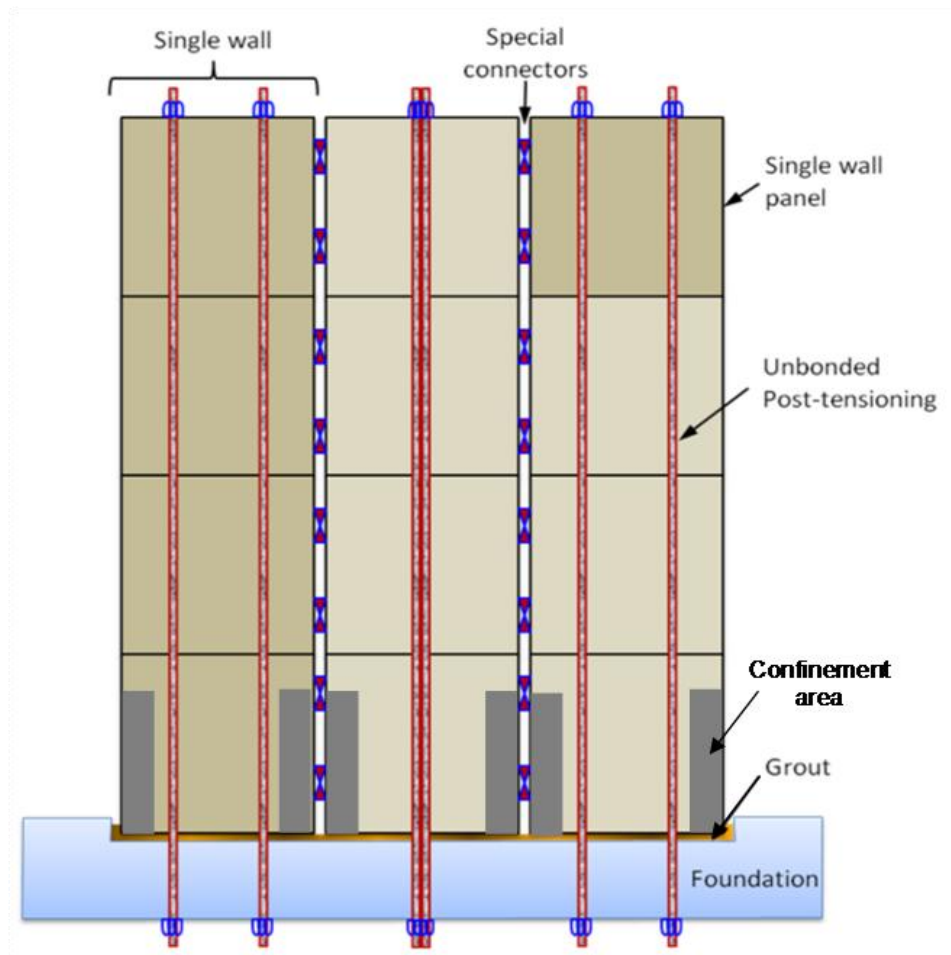


Figure 1.1 Illustration of a jointed wall system

## 1.4 Seismic Design Methods

In this report, applicability of two seismic design methods is investigated: (1) force-based design, and (2) direct displacement-based design. The traditional approach of seismic design is force-based, which is also widely used in design codes (e.g., Uniform Building Code 1997, International Building Code 2000). In this approach, the design base shear is obtained from the estimated fundamental period and total mass of the structure, incorporating the influence of seismic intensity in terms of spectral acceleration (Fig. 1.2). It does not involve target lateral displacement for the building, but the intent is to keep interstory drifts less than or equal to 2% when the building is subjected by design level earthquakes.

In contrast, a target displacement linked to the expected performance of the building is used in direct displacement-based design, which dictates the required effective natural

period of an equivalent single-degree-of-freedom system representing the structure, based on the seismic intensity in terms of spectral displacement (Priestley 2002). The total mass of the building, converted to an effective mass for the equivalent single-degree-of-freedom system, and the abovementioned effective period are used to calculate the effective stiffness of the building (Priestley 2002). Finally, the design base shear is obtained from the product between the target lateral displacement and effective stiffness (Fig. 1.3). Furthermore, it is demonstrated in Priestley (2002) that the direct displacement-based design approach typically results in a smaller design base shear than that obtained from the force-based design approach thus reducing the cost of the structure.

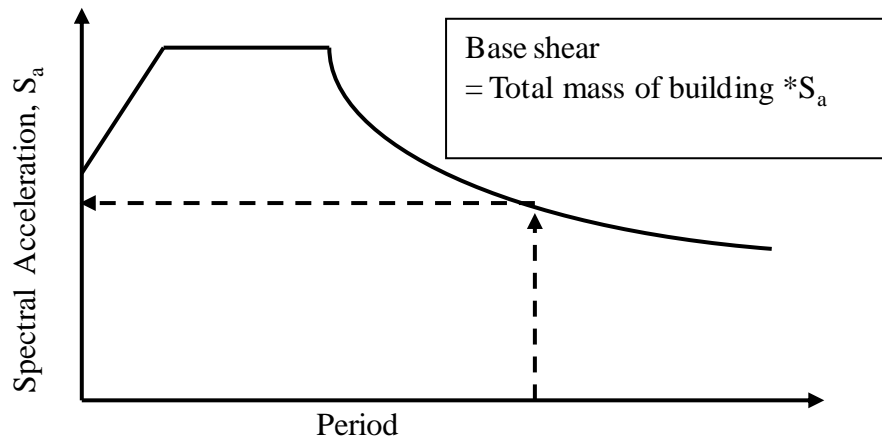


Figure 1.2 A schematic of a design spectrum acceleration used in estimating design base shear force in force-based design method

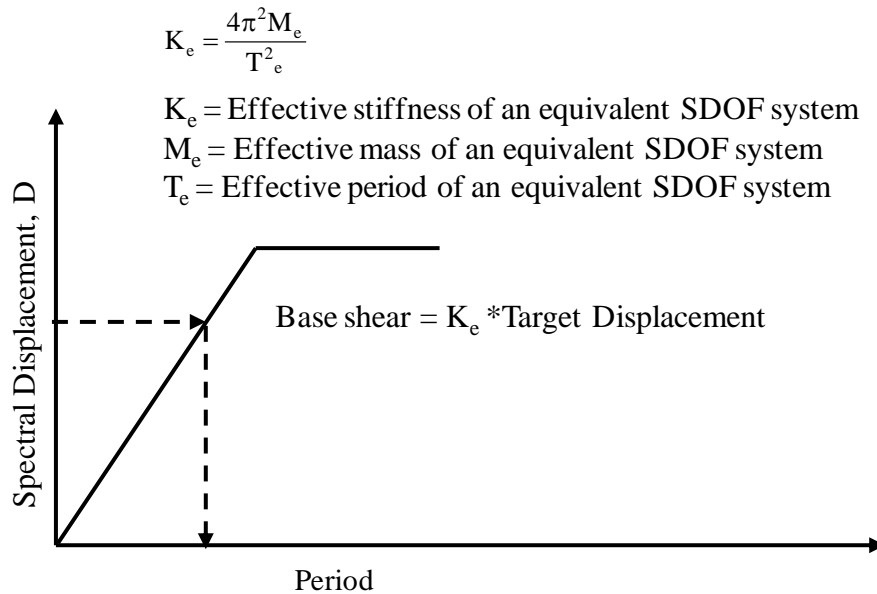


Figure 1.3 A schematic of a spectrum displacement used in estimating design base shear in direct displacement-based method (Priestley 2002)

## 1.5 Multiple-Level Performance-Based Seismic Evaluation

A multiple-level performance-based seismic evaluation ensures whether a building is capable of fulfilling specified levels of target performances when subjected to earthquakes of different intensities. The philosophy of multiple-level performance-based seismic evaluation should consist of controlling structural and non-structural performance for earthquakes that may be characterized as frequent, occasional, rare, and maximum considered events with mean return periods of 25, 72, 250 to 800, and 800 to 2500 years, respectively. The overall performance of a building, subjected to the aforementioned earthquakes levels, is expected to be operational, life safety, near collapse and collapse, respectively (Performance-Based Seismic Engineering Ad Hoc Subcommittee 2003; Seismology Committee 1999).

With the increased interest in performance-based earthquake engineering, the future of force-based design method can be questioned, because of a lack of direct connection of this approach with target displacement of the structure when estimating the design base shear. Another obvious disadvantage of this method is higher construction cost compared to the direct displacement-based approach due to the increased design base shear. To compare the performance of similar buildings designed by both approaches, a detailed dynamic

analytical investigation is appropriate under different levels of ground motions, representing various earthquake intensity levels. For this process, a multiple-level performance-based evaluation method may be necessary. If it can be shown through this investigation that the direct displacement-based solution can satisfy all acceptance criteria of performance, this solution will offer a structural design a more economical solution due to the reduced design base shear. Such a rigorous dynamic analytical investigation to realize this economical benefit is not available in present literature. The focus of this thesis is to conduct such a study for both hybrid frames and jointed wall systems.

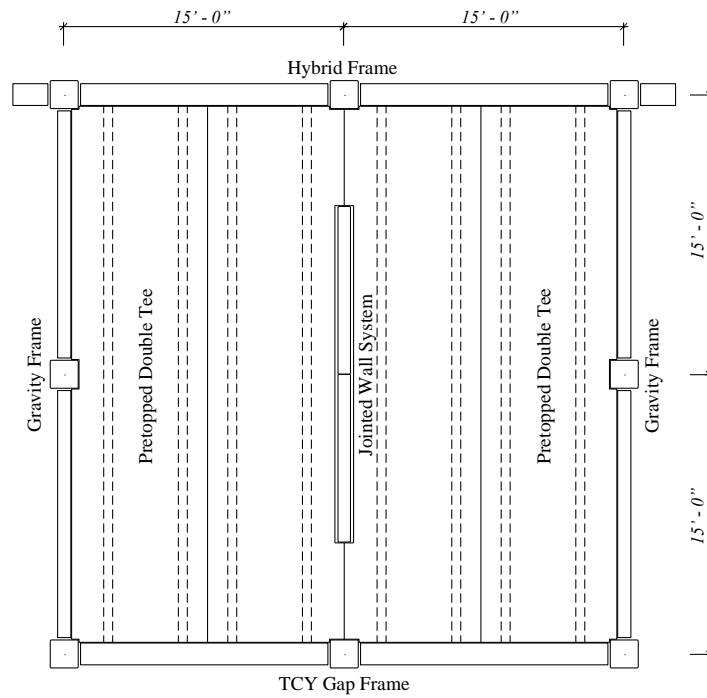
## **1.6 Previous Work**

The unbonded jointed wall system has been studied by various researchers (Nakaki 1999; Nakaki and Englekirk 1991; Priestley et al. 1999; Schultz and Magna 1996; Conely et al. 2002). Design procedures and recommendations for unbonded jointed wall system are available (Thomas 2004; Stanton and Nakaki 2002; Pampanin 2001; Aaleti 2005). A more detailed presentation of these works is presented in the literature review in Chapter 2.

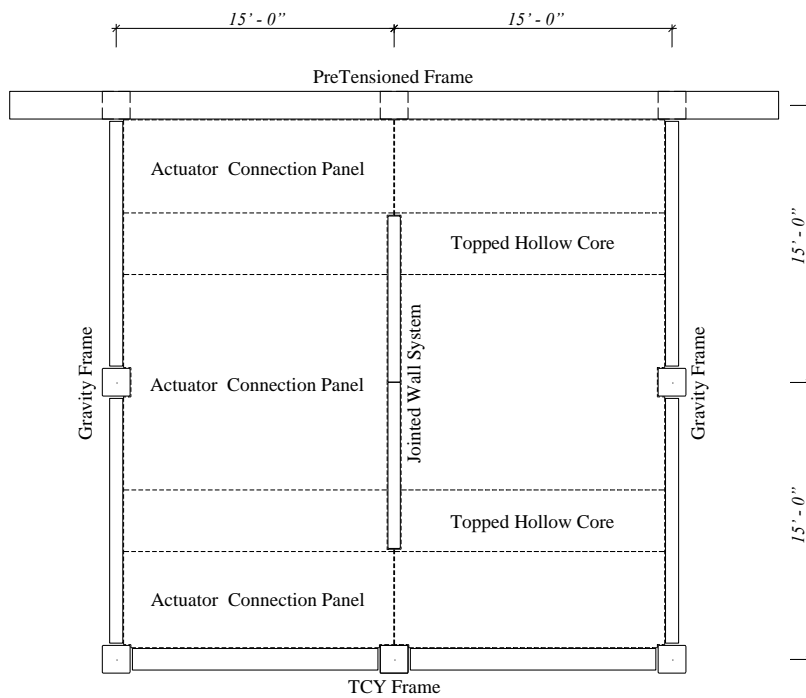
## **1.7 PREcast Seismic Structural Systems (PRESSSS) Research Program**

The PREcast Seismic Structural Systems (PRESSSS) research program, sponsored by the National Science Foundation (NSF), Precast/Prestressed Concrete Institute (PCI), and Precast/Prestressed Concrete Manufacturers Association of California (PCMAC) was initiated in the United States in the early 1990s, taking into account the exceptional performance of structural walls in past earthquakes, the benefits of precast concrete and the possible design restrictions that must be overcome. This program was initiated as a part of the United States-Japan protocol on large-scale testing for seismic response of precast concrete buildings. Two primary objectives of this program were to: (1) develop comprehensive and rational design recommendations based on fundamental and basic research data which emphasize the viability of precast construction in the various seismic zones, and (2) develop new materials, concepts and technologies for precast construction in the various seismic zones (Priestley 1991).

With a view of obtaining feedback from concrete producers, design engineers, and contractors on concept developments and connection classification projects of PRESSS, a concept development workshop was held in April 1991 (Nakaki and Englekirk 1991). Following the concept development workshop, and various testing and analytical models in the first two phases of the PRESSS program, a five-story precast test building was designed, built, and tested under simulated seismic loading at a 60% scale, in phase III of the PRESSS program, at the University of California at San Diego (Sritharan et al. 2002). This test building, with two bays by two bays, utilized two seismic frames with four different types of jointed moment resisting frames in one direction, while a jointed precast wall system served as a lateral load resisting component in the orthogonal direction. Figures 1.4 (a) and (b) show the hybrid and TCY-gap connections were used in the lower three stories of the two seismic frames; whereas, pretensioned and TCY connections (Sritharan et al. 2002) were utilized in the upper two floors. Figure 1.5 illustrates various components of a hybrid connection between the precast column and the beam. The wall was comprised of four panels, each was 2½ stories tall (18.75-ft) by 9-ft wide and 8-in thick (Figs. 1.6 and 1.7). Two walls, separated by a small gap, were formed by joining the panels vertically. These two walls were secured to the foundation using four unbonded post-tensioning bars and were connected horizontally by 20 U-shaped flexural plates (UFP connectors, see Fig. 1.8) placed along the vertical joint between the walls (Fig. 1.7). Figure 1.9 represents the 5% damped multiple-level acceleration response spectra, suggested for soil type  $S_c$  in a high seismic zone as per the Performance-Based Seismic Engineering Ad Hoc Subcommittee (2003). In the PRESSS test building, short segment ground motions compatible with acceleration response spectra of 1.5EQ-I, EQ-II and EQ-III shown in Fig. 1.10 were used for seismic testing.



(a) Lower three floors



(b) Upper two floors

Figure 1.4 Floor plans of the PRESSS test building (Sritharan et al. 2002)

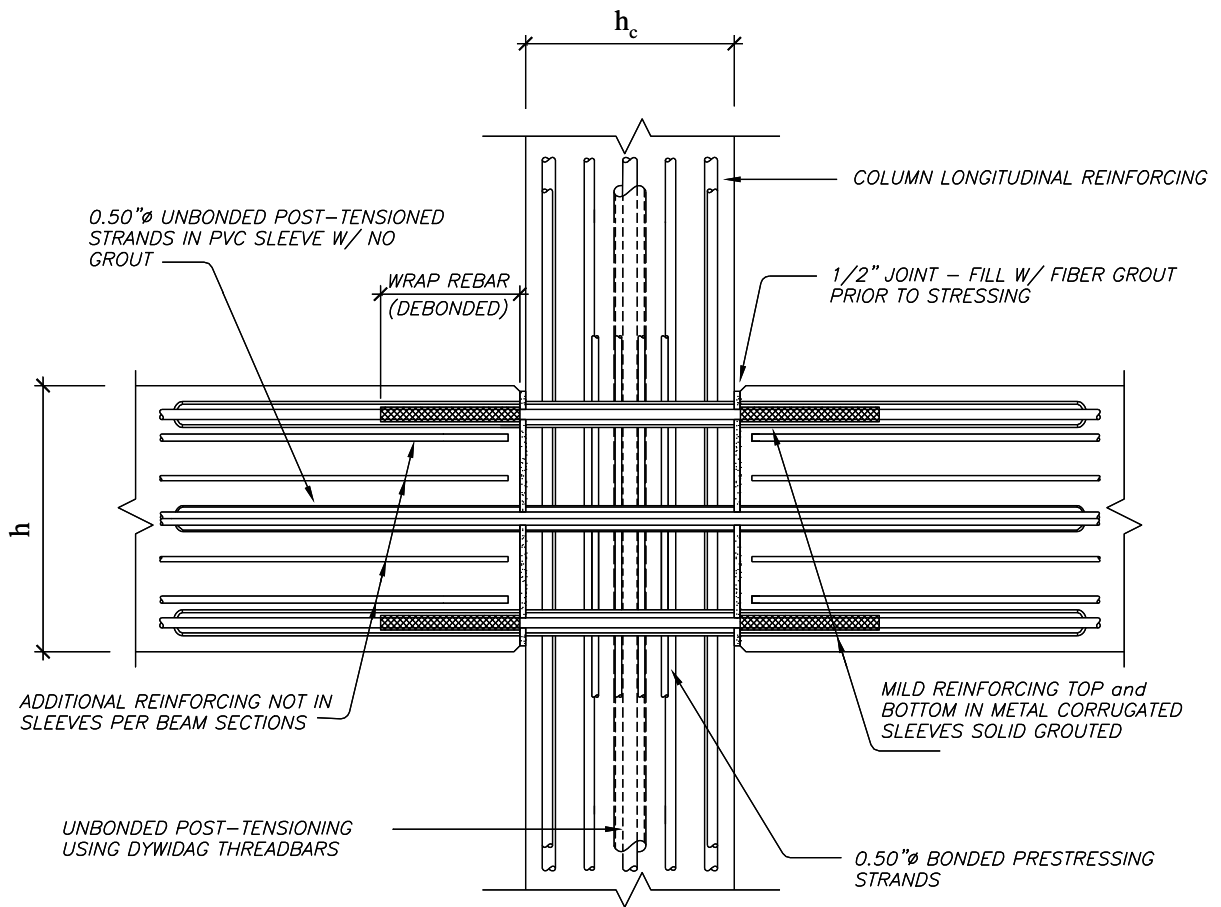


Figure 1.5 The typical connection details of a precast hybrid frame (transverse reinforcements are omitted for clarity)

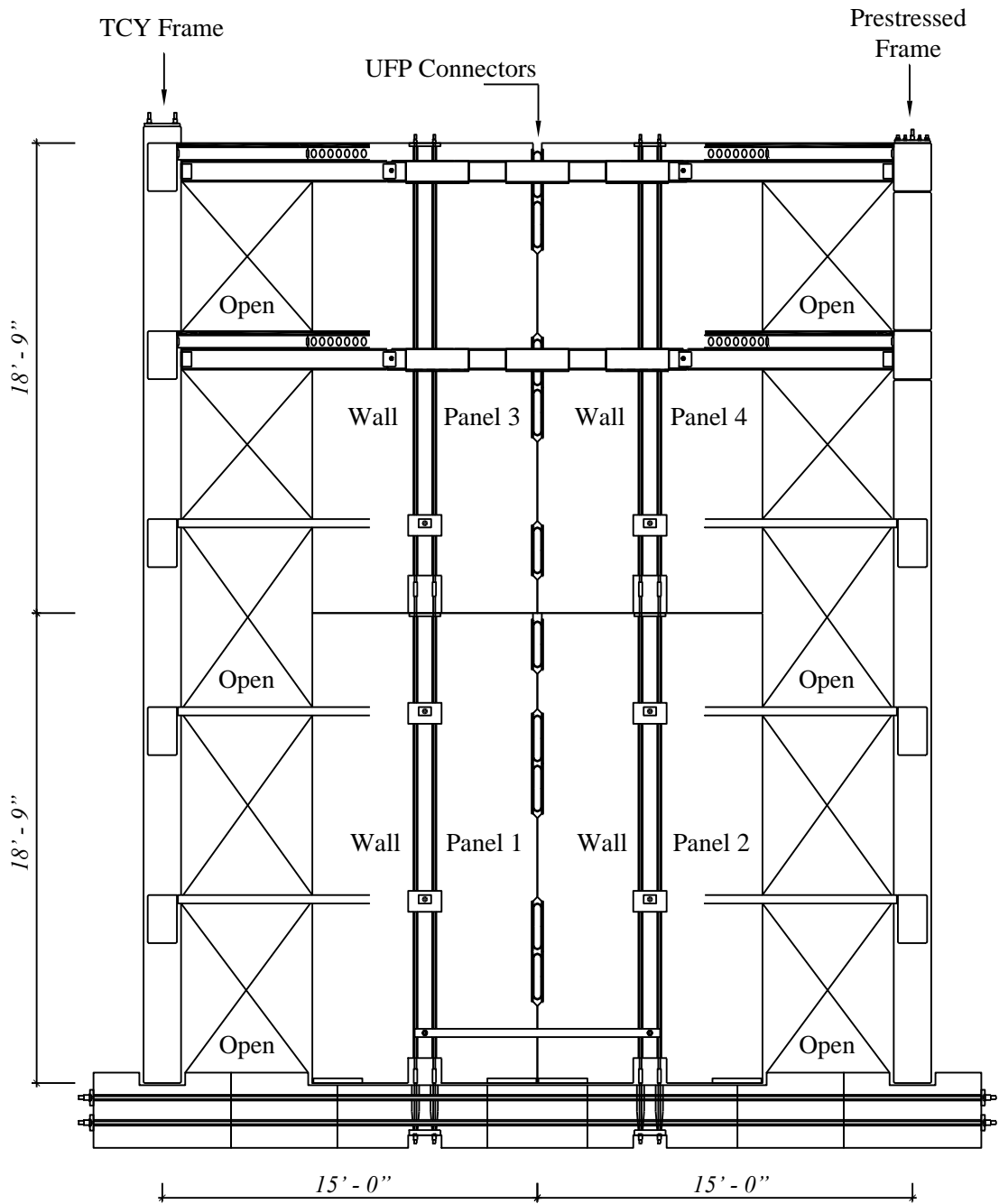


Figure 1.6 Elevation view of the jointed wall system used in the PRESSS test building (Sritharan et al. 2002)



Figure 1.7 The PRESSS building after erecting the wall system (Sritharan et al. 2002)

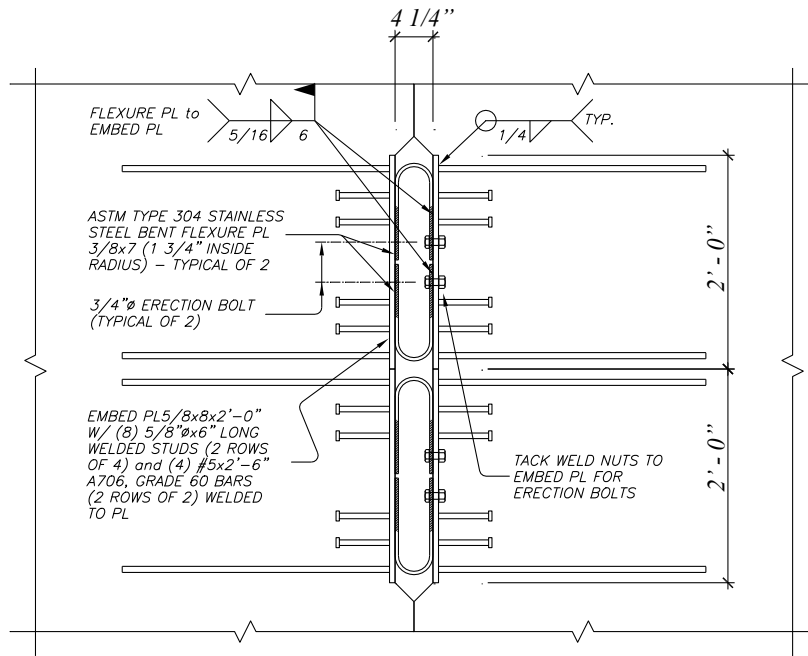


Figure 1.8 Connection details of UFP connectors in the PRESSS building (Sritharanet al. 2002)

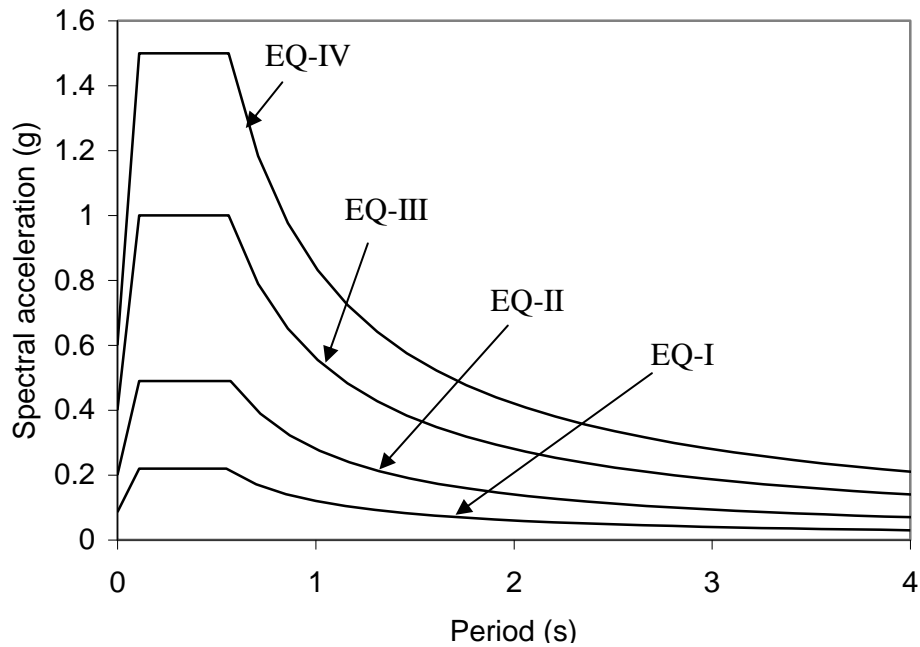


Figure 1.9 The 5% damped multiple-level acceleration response spectra, suggested for soil type Sc in high seismic zone as per Performance-Based Seismic Engineering Ad Hoc Subcommittee (2003)

Test results from the PRESSSS building is the only available document in the United States, providing information about the seismic performance of the precast structure comprised of hybrid frame and jointed unbonded precast walls, subjected to various levels of ground motions. However, test results of the PRESSSS program cannot be used to make a generalized prediction of multiple-level seismic performance of hybrid frame and jointed unbonded precast walls, because these tests were conducted only for a five-story building subjected by only short-duration ground motions. This study did not explore the effect of varying the height of the building. Performance of the test building under long-duration ground motion was not addressed. Moreover, the jointed walls had only one setup, comprising of two walls, connected by twenty UFP connectors, where incorporation of UFP connectors involved more cost to the structure. With this one setup of the jointed walls, it was not possible to evaluate the effect of varying the number of UFP connectors on seismic performance of the jointed wall system. In addition, test results could not provide comparison of performance between displacement-based and force-based design, because the only building tested was designed based on the direct displacement-based approach.

## **1.8 Scope of Research**

The overall scope of this research is to evaluate seismic performance of precast concrete buildings designed with jointed wall systems by subjecting them to earthquakes of different intensities. These buildings are designed using both the direct displacement-based and force-based design methods, such that the benefits of the two methods in designing these buildings can be realized. This research scope will be achieved by conducting dynamic analysis of several precast concrete buildings under several earthquake motions as classified in the following tasks:

- (1) Using the PRESSSS building configuration, a 60% scale five-story building is established as a displacement-based solution. This building will be designed by introducing jointed unbonded precast walls as lateral load resisting systems in two orthogonal directions. Analysis models for the wall system will be formulated independently for wall direction. Using the input ground motions from the PRESSSS building test, it will be ensured that the analytical models can adequately capture the

seismic response, which includes time history of top floor displacement, base moment resistance, and displacement of the connectors of the jointed wall system.

- (2a) A procedure for conducting performance-based evaluation will be developed, using the following references (Uniform Building Code 1997; International Building Code 2000; Performance-Based Seismic Engineering Ad Hoc Subcommittee 2003; Seismology Committee 1999) as the basis. Using this procedure, performance-based evaluation of jointed wall system buildings designed by both the direct displacement-based and force-based approach will be conducted. Four combinations of short-duration earthquake motions and eight long-duration ground motions, representing frequent to maximum considered earthquakes, will be used as the input motions. Performance will be evaluated with respect to the maximum transient inter-story drift limits, maximum residual inter-story drift limits, and floor acceleration limits.
- (2b) Pushover analysis will be conducted for both of the jointed wall systems designed by the displacement-based approach and force-based approaches. This analysis will result in a direct comparison of base shear vs. roof displacement of the two jointed wall systems. Moreover, influence of hysteric damping on the performance of the jointed wall system buildings will be investigated by changing the number of wall connectors.
- (3) In this task, five-, seven-, and ten-story high buildings comprised of jointed wall systems will be designed at 100% scale using the direct displacement-based design procedure. Performance-based seismic evaluation of the two buildings will be conducted using the analysis models developed for these buildings.

## **1.9 Report Layout**

The report comprises of five chapters including the general introduction presented in this chapter. Chapter 2 will contain literature review, which will include previous investigations on analysis and design of precast concrete seismic wall systems. An analytical model of a post tensioned precast concrete jointed wall system similar to that used in the PRESSS test building will be formulated in Chapter 3. After successful validation of this model, comparison of performance-based evaluation will be conducted for two similar buildings in the wall direction designed by using the direct displacement-based and force-

based methods at 60% scale.

In Chapter 4, five-, seven- and ten-story high full-scale precast jointed post-tensioned wall system buildings will be designed according to the direct displacement-based design method. Multiple level seismic performance of these low to mid-rise buildings will be presented. It will be shown that the performance of the buildings is satisfactorily under collapse level ground motions when they are designed by the direct displacement-based design method. This chapter will reveal the difference in performance of buildings containing post tensioned precast jointed wall system as a function of story height. The research material in Chapters 3 and 4 is presented in a journal article format. Chapter 5 presents conclusions and recommendations derived from this research along with recommendations for future research in this topic area.

## 1.9 References

- Fintel, M., 2002. Performance of Buildings with Shear Walls in Earthquakes of the Last Thirty Years, *PCI Journal*, Vol. 40, No. 3, 62-80.
- Earthquake Engineering Research Institute, 1996. Northridge Earthquake Reconnaissance Reports, *Earthquake Spectra*, 1995-1996, Supplement C to Vol. 11.
- Ghosh, S. K., 2001. Observations from the Bhuj Earthquake of January 26, *PCI Journal*, Vol. 46, No. 2, 34-42.
- John A. Martin and Associates, Inc., 2003. Earthquake Images: A Comprehensive Collection of Earthquake Related Slides and Photographs. Retrieved from <http://www.johnmartin.com/earthquakes/eqshow/index.htm> on 20-12-2003.
- Vernu, S., and Sritharan, S., 2004. Section, Member and System Level Analysis for Precast Concrete Hybrid Frames, ISU-ERI-Ames Report ERI-04635, June-2004, Iowa State University, Ames, Iowa, USA.
- Priestley, M. J. N., Sritharan, S., Conley, J. R., Pampanin, S., 1999. Preliminary Results and Conclusions From the PRESSS Five-Story Precast Concrete Test Building, *PCI Journal*, Vol. 44, No. 6, 42-67.
- Park, R., 1995. A Perspective on the Seismic Design of Precast Concrete Structures in New Zealand, *PCI Journal*, Vol. 40, No. 3, 40-59.
- Priestley, M. J. N., 1991. Overview of PRESSS Research Program, *PCI Journal*, Vol. 36, No. 4, 50-57.
- Vernu, S., 2003. Connection and Structural Level Analysis of Precast Hybrid Frame Systems, *Master Thesis*, Iowa State University, Ames, Iowa.
- Thomas, D. J., and Sritharan, S., 2004. An Evaluation of Seismic Design Guidelines Proposed for Precast Jointed Wall Systems, ISU-ERI-Ames Report ERI-04635, June 2004, Iowa State University, Ames, Iowa, USA.
- Uniform Building Code (UBC), 1997. International Conference of Building Officials, Whittier, California, USA, Vol. 2.

- International Building Code (IBC), 2000. International Code Council, Virginia, USA.
- Priestley, M. J. N., 2002. Direct Displacement-Based Design of Precast/Prestressed Concrete Buildings, *PCI Journal*, Vol. 47, No. 6, 67-79.
- Performance-Based Seismic Engineering Ad Hoc Subcommittee, 2003. SEAOC Blue Book, Revised Interim Guidelines, Performance-Based Seismic Engineering, Structural Engineers Association of California (SEAOC), California, USA.
- Seismology Committee, 1999. Recommended Lateral Force Requirements and Commentary, SEAOC Blue Book, Structural Engineers Association of California (SEAOC), California, USA.
- Sritharan, S., Pampanin, S., and Conley, J., 2002. Design Verification, Instrumentation and Test Procedures, PRESSS-3: The Five-Story Precast Test Building, Vol. 3-3. ISU-ERI-Ames Report ERI-03325, Iowa State University, Ames, Iowa, USA.
- Stanton, J. F. and Nakaki, S. D., 2002. Design Guidelines For Precast Concrete Seismic Structural Systems, *PRESSS* Report No. 01/03-09, UW Report No. SM 02-02, The University of Washington and The Nakaki Bashaw Group, Inc.
- Nakaki, S. D., Stanton, J. F., and Sritharan, S., 1999. An Overview of the PRESSS Five story Precast Test Building, *PCI Journal*, Special Report.
- Nakaki, S.D., Englekirk, R. E., 1991. PRESSS Industry Seismic Workshops: Concept Development, *PCI Journal*, Vol. 36, No. 5, 54-71.
- Priestley, M. J. N., Sritharan, S., Conley, J. R., Pampanin, S., 1999. Preliminary Results and Conclusions From the PRESSS Five-Story Precast Concrete Test Building, *PCI Journal*, Vol. 44, No. 6, 42-67.
- Schultz, A. E., and Magna, R. A., 1996. Seismic Behavior of Connections in Precast Concrete Walls”, Mete A. Sozen Symposium, Paper No. SP 162-12, American Concrete Institute, Farmington Hills, MI.
- Conely, J., Sritharan, S., and Priestley, M. J. N., 2002. Precast Seismic Structural Systems PRESSS-3: The Five-Story Precast Test Building Vol. 3-1, Wall Direction Response, Report No. SSRP-99/19, Department of Structural Engineering, University of California, San Diego, California.

- Pampanin, S., Priestley, M. J. N., and Sritharan, S., 2001. Analytical Modeling of the Seismic Behavior of Precast Concrete Frames Designed with Ductile Connections, *Journal of Earthquake Engineering*, Vol. 5, No. 3.

## **CHAPTER 2: REVIEW OF LITERATURE**

### **2.1 Introduction**

This chapter describes past experimental and analytical work of precast post-tensioned wall systems. Recent progress in development of precast jointed wall systems will be discussed. Design approaches recommended for this system in the literature will also be presented.

### **2.2 Unbonded Post-Tensioned Precast Wall Systems**

In consideration of the need for a non-emulative precast wall alternative, a concept for an unbonded post-tensioned precast concrete wall system was introduced. This was based on the concept suggested by Priestley and Tao (1993) for precast building frames with the idea that the post-tensioning would provide an improved restoring force. Kurama et al. (1999) and Kurama et al. (2002) recently investigated this option for precast walls, which consists of separate panels stacked vertically. The behavioral and analytical findings of their study as well as their design recommendations are discussed in this section.

#### **2.2.1 Single Wall system**

Researchers have analytically investigated the behavior of unbonded post-tensioned precast single wall systems in buildings as the primary lateral load resisting. Research work on precast single wall systems found in literature is presented below.

##### **2.2.1.1 Kurama et al. (1999); Kurama et al. (2002)**

###### *Behaviour and Analyses*

To identify seismic performance, the author specified four states for the lateral force-displacement response of a single unbonded post-tensioned precast wall system (Fig. 2.1). The *Decompression State* comes first, the point where the gap opening is initiated at the horizontal joint between the base of the wall and the foundation. The next state is the *Softening State*. This state is identified by the beginning of a significant reduction in the

lateral stiffness of the wall, due to a gap opening along the horizontal joints and non-linear behavior of the concrete in compression. The *Yielding State* is the third state, the point where the strain in the post-tensioning steel first reaches the limit of proportionality. In the *Failure State*, flexural failure of the wall occurs, with the triggering of concrete crushing at the toe locations of the walls.

The authors concluded the self-centering capability of the wall resulted from elastic behavior of the post-tensioning tendons. The nonlinear displacements occurred primarily due to gap opening along the horizontal joints. They recommended a tri-linear curve be used to represent the lateral load-displacement behavior of the unbonded post-tensioned wall by joining various wall states defined above. The unbonded post-tensioned wall exhibited larger displacements under seismic loading compared to a normal monolithic concrete wall. An opposite trend was observed for residual displacement (Fig. 2.2).

The non-linear elastic behavior of the wall demonstrated very little inelastic energy dissipation, resulting in a “slender” hysteresis (Fig. 2.3). Gap opening between the panels appeared to be smaller with the increase of initial prestressing. The base shear demands attained by analysis were found to be below those estimated by the design procedure. Therefore, the authors recommended the method of calculating base shear developed for cast-in-place monolithic concrete walls be applied to unbonded post-tensioned precast walls.

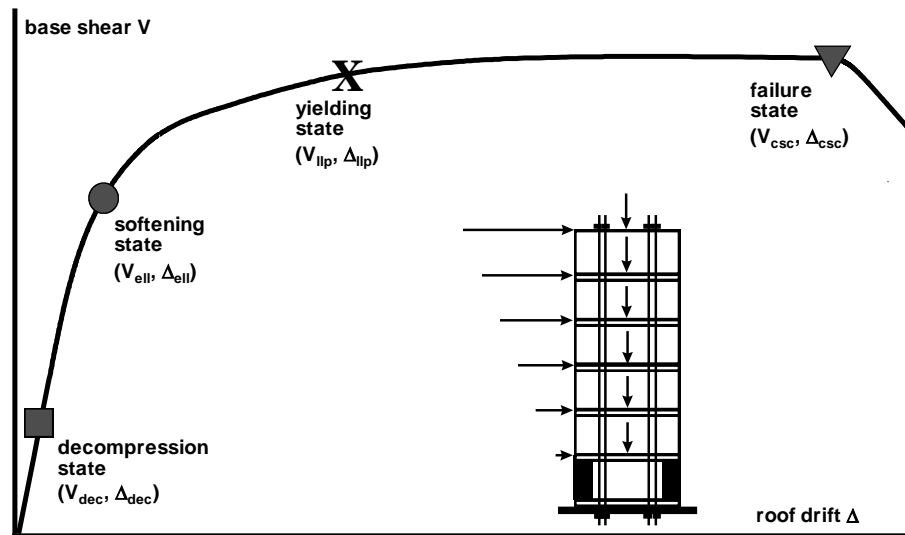


Figure 2.1 Precast wall base shear vs. roof drift relationship (Kurama et al. 1999)

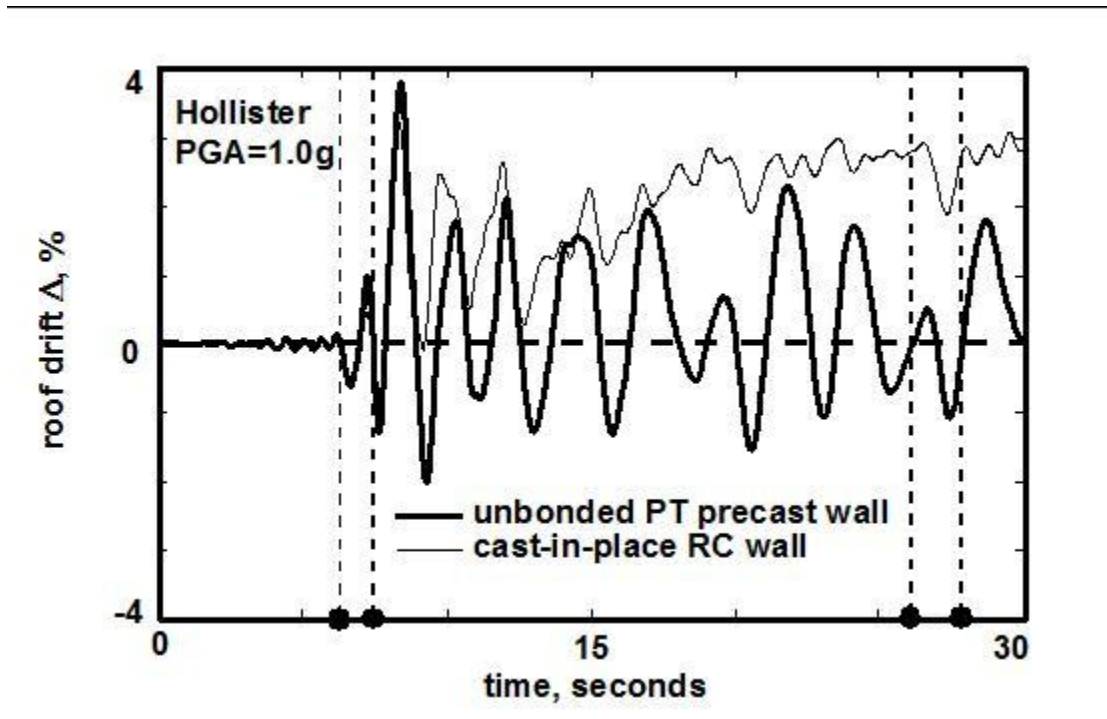


Figure 2.2 Comparison of roof drifts obtained from dynamic analysis of walls (Kurama et al. 1999)

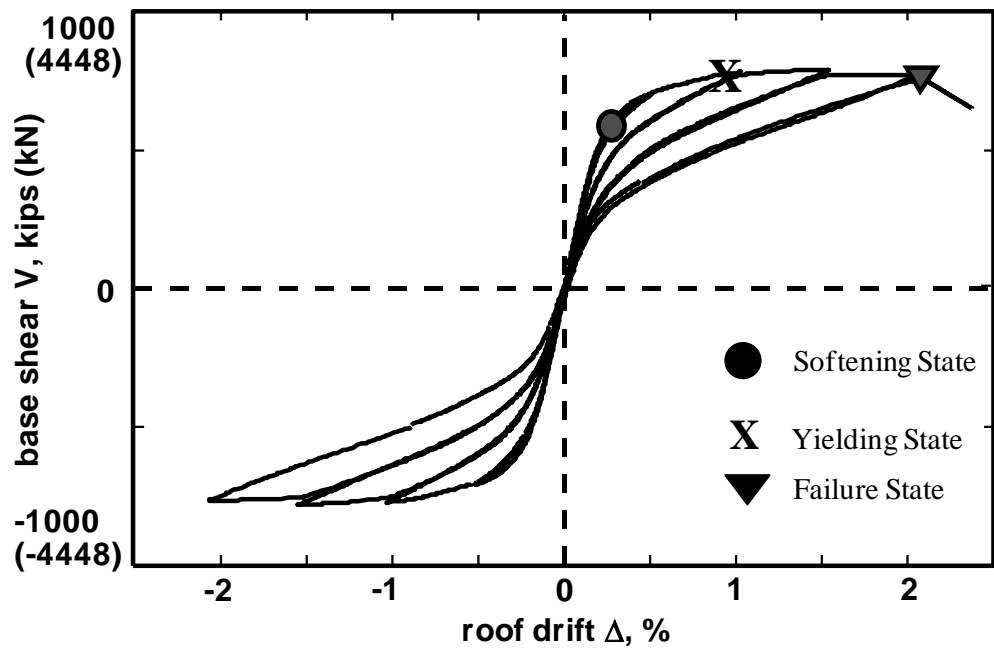


Figure 2.3 Force displacement response of a precast wall under cyclic loading (Kurama et al. 1999)

## 2.2.2 Precast Jointed Wall Systems

Researchers have investigated the use of unbonded post-tensioned precast jointed wall systems in buildings as the primary lateral load resisting elements in addition to the single wall systems. The connection between walls is constructed along the height of the wall. Energy dissipation and reduction of lateral drift are expected contributions from wall connectors. Research work on precast jointed wall systems found in the literature is presented below.

### 2.2.2.1 Priestley et al. (1999)

The PRESSS test building included an unbonded post-tensioned precast wall system with UFP connectors along the vertical joint direction. In the wall direction of loading under the design level earthquake, the wall experienced a peak recorded displacement of 8.3-in, just 8% below the target design displacement of 9-in. The wall experienced a maximum displacement of about 11.5-in. at an event 1.5 times the design level event. The base moment associated with this maximum displacement in the wall direction was approximately 100,000 kip-in with minor spalling in the cover concrete of the walls. During the entire wall direction testing, no structural damage was observed.

### 2.2.2.2 Thomas (2003); Thomas and Sritharan (2004)

These authors used the Monolithic Beam Analogy to develop a methodology for analyzing the unbonded post-tensioned jointed precast wall system. In this method, a relation between extreme concrete fiber strain and the neutral axis depth ( $c$ ), the base rotation ( $\theta$ ) has been established by setting the total displacement of jointed precast wall equal to the total displacement of equivalent monolithic wall.

$$\theta = (\phi_u - \phi_e)L_p = \left( \frac{\varepsilon_{c,ext}}{c} - \phi_e \right) L_p$$

where  $\varepsilon_{c,ext}$  is the extreme fiber concrete strain and  $L_p$  is the plastic hinge length.

The authors found that the plastic hinge length ( $L_p$ ) of  $0.06h_w$  gave a good prediction of the observed base moment vs. lateral displacement response for the PRESSS test building. Thus, the following expression was obtained,

$$\varepsilon_{c,ext} = c \left( \frac{\theta}{0.06h_w} + \phi_e \right) \quad \text{where } \phi_e = \frac{M}{E_c I_{eff}}.$$

The analysis procedure suggested by the authors is summarized below.

**Step 1:** Define wall dimensions and material properties, including yield strength of post-tensioning steel ( $f_{py}$ ), concrete strength ( $f_c'$ ), concrete density ( $\gamma_c$ ), modulus of elasticity for post-tensioning steel ( $E_p$ ), area of post-tensioning steel ( $A_p$ ), initial post-tensioning force ( $P_0$ ), height of wall ( $h_w$ ), length of wall panel ( $l_w$ ), thickness of wall ( $t_w$ ), connector force-displacement relationship, and number of panels ( $n$ ).

**Step 2:** Calculate wall moment capacity at the decompression point:  $M_{decomp} = \frac{(P_0 + W)I}{0.5t_w l_w l_w}$ ,

where  $I$  is the gross moment of inertia of the wall.

**Step 3:** Select base rotation ( $\theta$ ).

**Step 4:** Assume a neutral axis depth ( $c$ ) for the selected rotation.

**Step 5:** Determine the forces at the base rotation ( $\theta$ ) and neutral axis depth ( $c$ ), ensuring equilibrium is met.

- Find the tendon elongation:  $\Delta_p = \left( \frac{l_w}{2} - c \right) \theta$
- Find the increase in tendon stress:  $\Delta f_p = E_p \frac{\Delta_p}{h_w}$
- Find the total post-tensioning force ( $P$ ) and the total tension force ( $N$ ) under the current base rotation and assumed neutral axis depth:

$$P = \Delta f_p A_p + P_0$$

$$N = P + W$$

**Step 6:** Using a force versus vertical displacement curve determine the force contribution of the connectors ( $F_{sco}$ ). The compressive force ( $C$ ) can be determined from the equilibrium condition of the wall panel in the vertical direction:

$$C = N + F_{sc}, \text{ for leading wall}$$

$$C = N - F_{sc}, \text{ for trailing wall}$$

$F_{sc} = N_{con} F_{sco}$ , where  $N_{con}$  is total number of connectors in a vertical joint

**Step 7:** Determine the extreme fiber concrete strain for the assumed neutral axis depth ( $c$ ):

$$\varepsilon_{c,ext} = c \left( \frac{\theta}{0.06h_w} + \frac{M}{E_c I_{eff}} \right)$$

where  $M$  is the base moment resistance of the wall panel,  $E_c$  is the modulus of elasticity of concrete and  $I_{eff}$  is the effective moment of inertia of the wall.

**Step 8:** Calculate the compression force and its location utilizing the confinement model suggested by Mander et al. (1998). If the confined compressive force ( $C_{conf}$ ) is not equal to the compressive force established by equilibrium ( $C$ ), then the neutral axis depth is increased and steps 5 through 7 must be repeated until the two forces converge.

**Step 9:** Calculate the resisting moment of the wall panel by taking the moment about the corner of the each wall panel utilizing the distance ( $y$ ) from the edge of the wall to the resultant compression force.

$$M_{cap,panel1} = C(l_w - y) - 0.5Nl_w$$

$$M_{cap,panel2} = -C(y) + 0.5Nl_w$$

**Step 10:** Compute the total moment capacity of wall system:

$$M_{cap,wall} = M_{cap,panel1} + M_{cap,panel2}$$

### 2.2.2.3 Sritharan et al. (2006); Aaleti (2005)

These authors developed a simplified procedure for seismic design and monotonic analysis of precast post-tensioned jointed walls. The following assumptions, consistent with suggestions by Stanton and Nakaki (2002), were considered for the design of jointed precast wall systems:

- The wall will undergo in-plane deformations only. Torsion and out-of-plane deformations are prevented by providing adequate out-of-plane bracing.
- All individual walls are assumed to have identical dimensions, reinforcement details, and an initial prestressing force.

- All vertical joints contain an equal number of identical connectors, and a dependable force vs. displacement response envelope is available for the connector.
- All walls undergo the same lateral displacement at the floor and roof levels due to the rigid floor assumption.
- The post-tensioning steel is located at the center of each wall.
- The strength of fiber grout typically placed between the wall base and foundation is greater than the strength of concrete in the walls.
- The post-tensioning steel reaches the yield strain at the design drift. The corresponding rotation at the wall base is assumed to be  $\theta_{\text{design}}$ , which may be taken as 2%.
- The following seven steps are recommended for the design of the jointed wall systems.

***Step 1: Material Properties and Wall Dimensions***

- Establish the following material properties

Prestressing steel: Modulus of elasticity ( $E_p$ ) and yield strength ( $f_{py}$ ).

Concrete: Unconfined concrete strength ( $f'_c$ ), elastic modulus of concrete ( $E_c$ ), and appropriate coefficient of friction between the precast wall base and foundation ( $\mu$ ).

Connector: Force vs. displacement response envelope.

- Establish the wall dimensions

Select the total length of the wall system ( $L_s$ ) or length of a single wall ( $L_w$ ), wall height ( $H_w$ ), wall thickness ( $t_w$ ), and the number of walls ( $n$ ).

When deciding the number of walls in each system, use the smallest possible value for  $n$  with a suitable  $H_w/L_w$  ratio. Stanton and Nakaki (2002) suggest  $H_w/L_w$  should be more than 2.0 to ensure a flexural dominant behavior for the wall. If the length of each wall or the total length of the wall system is known, the other variable can be determined with the following expression.

$$L_w = \frac{L_s}{n}$$

Guidance to determine an initial value for the wall thickness:

1. Select a value in the range of  $h_{\text{story}}/16$  to  $h_{\text{story}}/25$ , where  $h_{\text{story}}$  is the story height (Englekirk, 2003).

2. The wall thickness should be sufficient to limit the shear stress in the wall to the permissible limit specified in the code (e.g., ACI 318-05 2005).
3. The wall thickness should be sufficient to accommodate the required confinement reinforcement at the wall ends.

**Step 2: Design Moment Resistance**

Establish the base moment resistance for the wall system ( $M_{design}$ ). Hence, the precast wall system should be designed such that  $\phi M_n \geq M_{design}$

where  $\phi$  is the flexural strength reduction factor and  $M_n$  is the nominal moment capacity of the wall system at the design drift.

**Step 3: Force Resisted by the Connector**

- Estimate the force in the connector ( $F_{con}$ ) at the design drift from the force-displacement envelope curve available for the connector with an assumption that vertical relative displacement between the walls is  $0.9L_w\theta_{design}$ .
- The number of connectors should be determined such that a desired level of equivalent damping is incorporated in the wall system. For UFP connectors, the required number of connectors may be established as given below, to ensure the wall system would have a desired level equivalent damping (Galusha 1999).

$$N_{con} = \frac{\pi \zeta_{eq} M_n}{1.25(n-1)F_{con}L_w}$$

where  $N_{con}$  is the number of connectors in each vertical joint between the precast walls and  $\zeta_{eq}$  is the required level of equivalent viscous damping.

**Step 4: Calculate Area of the Post-tensioning Steel**

- The design moment for the wall that would provide the largest moment resistance can be determined using the following expressions.

$$M_{design,wall} = \Omega \frac{M_{design}}{n\phi}; \quad \Omega = 1 + \frac{\lambda \phi N_{con} F_{con} L_w}{M_{design}}$$

where  $\Omega$  is the moment contribution factor and  $\lambda$  is a constant. When  $n = 2$  and  $\lambda = 0.9$ , and  $M_{design,wall}$  will correspond to the moment demand in the leading wall (i.e.,

$M_{design,lead}$ ). When  $n \geq 3$  and  $\lambda = 1.04$  and the  $M_{design,wall}$  will correspond to the moment in an intermediate wall (i.e.,  $M_{design,inter}$ ).

- Find the area of the post-tensioning steel ( $A_p$ ) in a jointed wall system of two walls using the expression developed based on moment equilibrium of forces acting on the base of the leading wall as given below (Fig. 2.4).

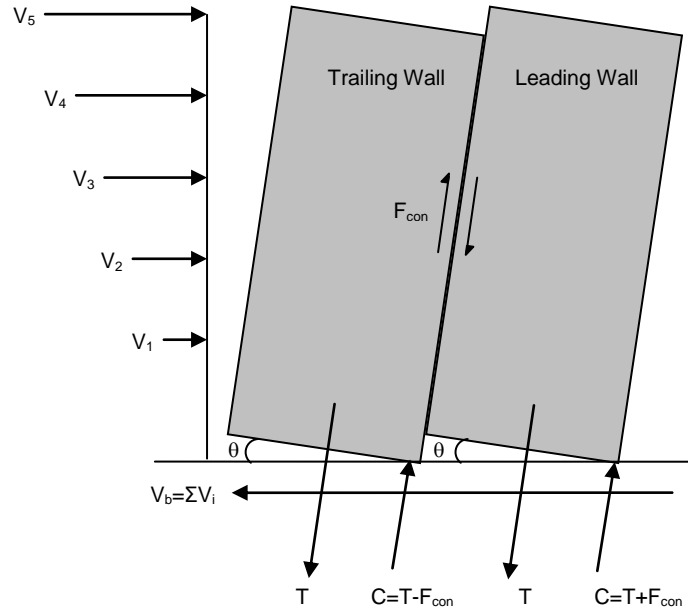


Figure 2.4 Forces acting on a jointed two-wall system at base rotation  $\theta$  ( $C$  = resultant compressive force and  $T = P_D +$  force in the prestressing tendon) (Sritharan et al. 2006; Aaleti 2005)

$$M_{design,lead} = (P_D + 0.95f_{py}A_p) * \left( \frac{L_w}{2} - \frac{P_D + 0.95f_{py}A_p + N_{con}F_{con}}{2 * (\alpha.f'_{cc})t_w} \right) + N_{con}F_{con} * \left( L_w - \frac{P_D + 0.95f_{py}A_p + N_{con}F_{con}}{2 * (\alpha.f'_{cc})t_w} \right)$$

where  $P_D$ , the summation of the wall self weight and superimposed live load, is equated to  $(\gamma_c L_w t_w H_w + W_{floor} L_w)$ ,  $\gamma_c$  is the unit weight of concrete,  $W_{floor}$  is the distributed superimposed live load at the base of wall from all floors,  $0.95f_{py}$  represents the expected stress in the post-tensioning steel in the critical wall at the

design drift, and  $\alpha.f'_{cc}$  approximates the expected confined concrete strength of the equivalent rectangular stress block with  $f'_{cc}$  representing the strength of the confined concrete. The value of  $\alpha$  may be obtained as follows.

$$\alpha = \frac{2 * r * (0.98 - 0.0022 * f'_c)}{r - 1 + 2r}$$

where 
$$r = 1.24 + 0.01 * \left( \frac{f'_c - 4.0}{0.25} \right)$$

- For a multi-wall system with  $n \geq 3$  (Fig. 2.5), the required area of the post-tensioning steel is established using the moment equilibrium of the forces acting at the base of an intermediate wall,

$$M_{design,inter} = (P_D + 0.95 f_{py} A_p) * \left( \frac{L_w}{2} - \frac{P_D + 0.95 f_{py} A_p}{2 * (\alpha * f'_{cc}) t_w} \right) + N_{con} F_{con} L_w$$

The connector forces acting on both sides of an intermediate wall are assumed to be the same.

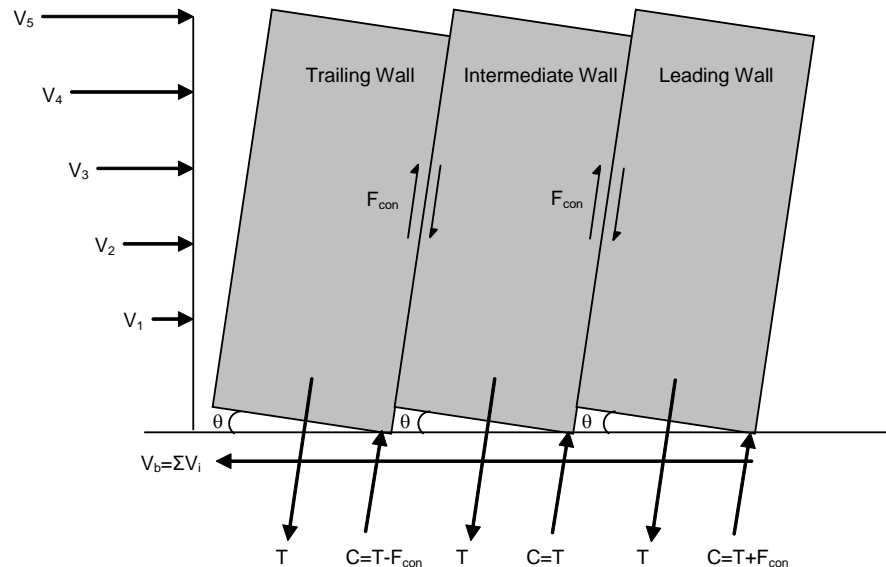


Figure 2.5 Forces acting on a jointed three-wall system at base rotation  $\theta$  ( $C$  = resultant compressive force and  $T = P_D +$  force in the prestressing tendon) (Sritharan et al., 2006; Aaleti, 2005)

### ***Step 5: Design the Initial Stress for the Post-tensioning Steel***

- Estimate the neutral axis depth at the base of the trailing wall at the design drift.

$$c_{design, trail} = \frac{P_D + f_{py} A_p - N_{con} F_{con}}{\beta * (\alpha \cdot f'_{cc}) t_w}$$

where the value of  $\beta$  can be approximated to 0.96.

- Assuming the post-tensioning steel reaches the yield limit state in the trailing wall at the design drift, the initial stress in the post-tensioning steel is established,

$$f_{pi} = f_{py} - \frac{(0.5L_w - c_{design, trail}) \theta_{design} E_p}{H_w}$$

### ***Step 6: Estimate the Moment Capacity***

The connector details, area of the post-tensioning steel and initial prestress designed in the previous steps may be used in all walls in the jointed system instead of designing the walls individually. With the help of a suitable analysis procedure (e.g., Thomas, 2003; Sritharan et al., 2006; Aaleti, 2005) calculate the total base moment resistance of the jointed wall system to verify the  $\phi M_n \geq M_{design}$  condition is fulfilled.

The proposed design method is expected to adequately satisfy  $\phi M_n \geq M_{design}$ .

However, wall dimensions may be modified to satisfy the condition  $\phi M_n \geq M_{design}$ .

### ***Step 7: Design of Confinement Reinforcement***

By observing the test results of the PRESSS building and identifying that the leading wall would face the maximum resultant compressive force at the base, the following expression has been suggested for estimating the maximum concrete strain demand in the compressive regions of the wall toes (Mander et al. 1998).

$$\varepsilon_{conc} = c_{max, lead} \left( \frac{M_{max, lead}}{E_c I_{gross}} + \frac{\theta_{max}}{0.06 H_w} \right)$$

where  $M_{max, lead}$  is the base moment resistance of the leading wall at the maximum expected drift, the corresponding base rotation is  $\theta_{max}$ , which may be taken as

$1.5*\theta_{design}$ ,  $I_{gross}$  is the gross moment of inertia of the wall and is equal to  $\frac{t_w L_w^3}{12}$ , and

$c_{max,lead}$  is the neutral axis depth at the base of the leading wall at  $\theta_{max}$ . The value of  $c_{max,lead}$  may be established as part of the analysis of the wall system in Step 6. Following an estimate for  $\epsilon_{conc}$ , quantify the required amount of confinement reinforcement in the wall toes using an appropriate confinement model.

The shear resistance at the base of the wall should be ensured using a shear friction mechanism. If an interface material such as grout is placed between the precast walls and foundation, this should be reflected in the value of  $\mu$ . Since the stress in the post-tensioning steel and the connector force increase with drift, it will be necessary to perform this check at both  $\theta_{design}$  and  $\theta_{max}$

## 2.3 References

- Priestley, M. J. N., and Tao, J. T., 1993. Seismic Response of Precast Prestressed Concrete Frames with Partially Debonded Tendons, *PCI Journal*, Vol. 38, No. 1, 58-69.
- Stanton, J. F. and Nakaki, S. D., 2002. Design Guidelines For Precast Concrete Seismic Structural Systems, *PRESSS Report No. 01/03-09, UW Report No. SM 02-02*, The University of Washington and The Nakaki Bashaw Group, Inc.
- Kurama, Y., Pessiki, S., Sause, R., and Lu, L., 1999. Seismic Behavior and Design of Unbonded Post-Tensioned Precast Concrete Walls, *PCI Journal*, Vol. 44, No. 3.
- Kurama, Y., Pessiki, S., Sause, R., and Lu, L., 1999. Lateral Load Behavior and Seismic Design of Unbonded Post-Tensioned Precast Concrete Walls, *ACI Structural Journal*, Vol. 96, No. 4, 622-632.
- Kurama, Y., Pessiki, S., Sause, R., and Lu, L., 2002. Seismic Response Evaluation of Unbonded Post-Tensioned Precast Walls, *ACI Structural Journal*, Vol. 99, No. 5, 641-651.
- Priestley, M. J. N., Sritharan, S., Conley, J.R., and Pampanin, S., 1999. Preliminary Results and Conclusions from the PRESSS Five-Story Precast Concrete Test Building, *PCI Journal*.
- Thomas, D., J., 2003. Analysis and Validation of a Seismic Design Method Proposed for Precast Jointed Wall Systems, M.S. Thesis, Department of Civil, Construction and Environmental Engineering, Iowa State University, Ames, Iowa, USA.
- Thomas, D., J., and Sritharan, S., 2004. An Evaluation of Seismic Design Guidelines Proposed for Precast Jointed Wall Systems, *ISU-ERI-Ames Report ERI-04635*, Iowa State University, Ames, Iowa, USA.
- Mander, J. B., Priestly, M. J. N., and Park, R., 1998. Theoretical Stress-Strain Model for Confined Concrete, *Journal of Structural Engineering*, Vol. 114, No. 8.
- Sritharan, S., Aaleti, D., and Thomas, D. J., Seismic Analysis and Design of Precast Concrete Jointed Wall Systems, *ISU-ERI-Ames Report ERI-07404*, Iowa State University, Ames, Iowa, USA, December 2007.

- Aaleti, S., 2005. Design and analysis of unbonded post-tensioned precast wall systems, *M.S. Thesis*, Department of Civil, Construction and Environmental Engineering, Iowa State University, Ames, Iowa, USA.
- Englekirk, R. E., 2003. *Seismic Design of Reinforced and Precast Concrete Buildings*, John Wiley and Sons, Inc., New Jersey, USA.
- Galusha, J.G., 1999. *Precast, Post-Tensioned Concrete Walls Designed to Rock*, M.S. Thesis, Department of Civil Engineering, University of Washington, USA.

# **CHAPTER 3: AN EVALUATION OF FORCE-BASED DESIGN Vs. DIRECT DISPLACEMENT-BASED DESIGN OF JOINTED PRECAST POST-TENSIONED WALL SYSTEMS**

(A paper accepted in *Earthquake Engineering and Engineering Vibration Journal*)

**M. Ataur Rahman<sup>1</sup> and Sri Sritharan<sup>2</sup>**

## **Abstract**

The unique features of jointed post-tensioned wall systems, which include minimum structural damage and re-centering capability when subjected to earthquake lateral loads, are the result of using unbonded post-tensioning to attach the walls to the foundation, along with employing energy dissipating shear connectors between the walls. Using acceptance criteria defined in terms of inter-story drift, residual drift, and floor acceleration, this study presents a multiple-level performance-based seismic evaluation of two five-story unbonded post-tensioned jointed precast wall systems. The design and analyses of these two wall systems, established as the direct displacement-based and force-based solutions for a prototype building used in the PREcast Seismic Structural Systems (PRESSSS) program, were performed at 60% scale so that the analyses model could be validated using the PRESSSS test data. Both buildings satisfied the performance criteria at four levels of earthquake motions although the design base shear of the direct displacement-based jointed wall system was 50% of that demanded by the force-based design method. The study also investigated the feasibility of controlling the maximum transient inter-story drift in a jointed wall system by

---

<sup>1</sup>PhD Candidate, Department of Civil, Construction and Environmental Engineering, Iowa State University, Ames, IA 50011, USA

<sup>2</sup>Associate Professor, Department of Civil, Construction and Environmental Engineering, e-mail: [sri@iastate.edu](mailto:sri@iastate.edu), tel.: 515-294-5238, fax: 515-294-7424, Iowa State University, Ames, IA 50011, USA

increasing the number of energy dissipating shear connectors between the walls without significantly affecting its re-centering capability.

### **3.1 Introduction**

Jointed precast wall systems with unbonded post-tensioning can be used as the primary structural system for resisting earthquake lateral forces in high seismic regions. In these systems, individual precast wall is secured to the foundation using unbonded prestress tendons running from the top of the wall to the foundation. Two or more of such post-tensioned walls are connected horizontally to each other using shear connectors, which are distributed along the wall height, to form a jointed precast wall system (Fig. 3.1). The basic concept of this wall system is to allow the walls to rock individually at the base when subjected to a ground excitation of significant magnitude and return to its original vertical position after the event has concluded (Priestley et al. 1999; Thomas and Sritharan 2004). The vertical post-tensioning contributes to overturning moment resistance and ensures transfer of shear forces between the walls and foundation through a friction mechanism. The shear connectors between the walls contribute to both moment overturning moment resistance as well as hysteretic energy dissipation.

When designed with unbonded post-tensioning, a precast concrete wall provides additional benefits under seismic loading condition, which include reduced damage due to concentration of flexural cracking at the base and negligible residual displacements as a result of its re-centering capability. Instead of joining the walls, researchers have also investigated the possibility of using single precast walls connected to the foundation using unbonded post-tensioning. A significant drawback of these walls is that they have limited energy dissipation capacity and thus they can experience significantly large transient inter-story drifts (Conley et al. 2002; Kurama et al. 1999a; Kurama et al. 1999b; Kurama et al. 2002).

In seismic regions, design base shear of jointed precast wall system may be established using two methods. The traditional approach is to follow the force-based design (FBD) approach as recommended in refs. (Uniform Building Code (UBC) 1997; International Building Code (IBC) 2000). In this approach, design base shear is obtained

from the estimated fundamental period and total mass of the structure, incorporating the influence of seismic intensity in terms of a design spectral acceleration. In this method, the target level lateral displacement of the building is not directly used to quantify the design base shear. In contrast, the direct displacement-based design (DDBD) method uses the target displacement that is selected to match the expected performance of the building to establish the design base shear. In this approach, the base shear is determined using an effective period for the fundamental mode and seismic intensity in terms of a design spectral displacement (Priestley 2002). By representing the hysteretic action with equivalent viscous damping, the effective period is established using an effective mass for the fundamental mode of the building, which is determined by assuming a suitable displacement profile for this mode. The effective period is used to determine the effective stiffness of the building. Finally, the design base shear is calculated by multiplying the equivalent target displacement and effective stiffness. More detailed presentation of the DDBD method is available elsewhere (Priestley 2002).

Using acceptance criteria defined in terms of inter-story drift, residual drift, and floor acceleration, this paper presents a multiple-level performance-based seismic evaluation of FBD and DDBD solutions for a five-story precast unbonded post-tensioned jointed wall system. The significance of studying the two approaches to design a five-story jointed wall system is that they lead to drastically different design base shear forces, and thus a systematic seismic evaluation of the systems based on the two design forces have economical implications for the design of jointed precast walls.

### **3.2 Unbonded Post Tensioning Precast Jointed Wall Systems**

Figure 3.2 shows the plan view of a five-story precast concrete building chosen for the investigation reported in this paper. The building primarily uses four jointed walls to resist lateral forces in the transverse direction of the building. As with the PRESSSS test building (see Fig. 3.4) (Nakaki et al. 1999; Priestley et al. 1999; Sritharan 2002), the consequences of using the FBD and DDBD to design the jointed wall systems was conducted on 25% of the building at 60% scale (see Fig 3.3 for the plan view of the reduced building).

This approach was necessary to ensure satisfactory modeling of jointed wall system using the PRESSS test data

In model scale building shown in Figs. 3.3 and 3.4, one jointed wall system consisting of two precast walls is used. Each wall is secured to the foundation using unbonded post-tensioning bars located at the centroid of the wall. The walls are connected horizontally using U-shaped stainless steel flexural plates (also known as UFP connectors). Construction details and expected behavior of the UFP connectors may be found elsewhere (Nakaki et al. 1999; Thomas and Sritharan 2004). The combination of modeling a portion of the building and the use of reduced scale lead to the ratios of 0.6,  $0.6^2$ ,  $0.25 \times 0.6^2$ ,  $0.25 \times 0.6^3$ , 1.0,  $0.6^{-1}$  and 0.6, respectively, for the member dimension, member force, base shear, mass, stress, acceleration and time between the building model and the prototype structure.

The first jointed wall system, referred to as JWS1, was designed for the building Fig. 3.3 using DDBD as adopted for the design of the PRESSS building (Collins 1999, Galusha 1999, Priestley 2002; Sritharan et al. 2002). Using an equivalent viscous damping of 18% and a target inter-story design drift of 2% (as per ITG 5.1-XX (2006), Seismology Committee (1999) and Performance-Based Seismic Engineering Ad Hoc Subcommittee (2003) of the Structural Engineers Association of California (SEAOC)), the design base shear of 867.4 kN was found for JWS1. Because this design base shear is similar to that used for the jointed wall system in the PRESSS test building, the dimensions of the precast walls and details of unbonded post tensioning tendons and UFP connectors for JWS1 were taken the same as those used for the jointed wall in the PRESSS test building.

Base shear for the second building, referred to as JWS2, was calculated to be 1734.7 kN using FBD in accordance with the design codes used in current practice (e.g., UBC 1997; IBC 2000). This base shear was derived from the design base shear calculated for the prototype building with the code-based estimate for the fundamental period of 0.44 sec. Consequently, JWS1 and JWS2 should be considered as two contrasting solutions for the design of the jointed walls in Figs. 3.2 and 3.3, with the base shear of JWS1 being 50% less than that of JWS2. It should be noted that the design base shear in JWS2 was restricted by the code upper limit on the seismic coefficient. Without this limitation, the design base shear of JWS2 was 2185.13 kN, which was not given further consideration because it violated the

recommended design practice. For calculating the values of design base shear of both JWS1 and JWS2, the soil condition was assumed to be very dense soil or soft rock, with the shear wave velocity in the range of 366 m/s to 762 m/s, which is identified as Soil Profile Type  $S_C$  in UBC (1997) and Site Class C in IBC (2000). Because the design base shear forces differed by a factor of two between JWS2 and JWS1, it was decided that the FBD solution (i.e., JWS2) could be modeled using two JWS1 systems for evaluating the seismic performance. In other words, seismic analysis of both buildings could be evaluated using a single dynamic model with appropriate modifications to the seismic mass.

### **3.3 ANALYTICAL MODEL**

For the analysis of the jointed wall system, a 2-D analytical model was developed using the finite element computer program RAUMOKO (Carr 2003). Figure 4.5 includes the model of the jointed wall system comprised of two unbonded post-tensioned precast walls, in which each unbonded post-tensioned wall is represented using an elastic beam-column element positioned at the wall centerline. The rotational capacity of each unbonded post-tensioned wall is represented by a non-linear rotational spring at the base of the beam-column element. Although there are twenty UFP connectors positioned between the two unbonded walls, their combined effect is modeled equally at each floor level, resulting in five non-linear inelastic vertical direction springs with each modeling four UFPs. These springs are connected to rigid beam-column elements extending from the centerline of each wall towards the centerline of the jointed wall system as seen in Fig. 3.5.

In the PRESS test building, the lateral load resistance in the wall direction was assisted by two gravity columns and the framing action resulting from out-of-plane response of the two seismic frames and precast floor at the lower three floor levels (Thomas and Sritharan 2004). Including these contributions in the analytical model was considered essential for validation of the analysis model; however they were excluded during the performance-based evaluation of JWS1 and JWS2. A one bay frame, rigidly connected in series to the left side of the jointed wall model, represents the framing action resulting from the seismic frames and precast floors. Similarly, a beam-column element is added to the right side of the jointed wall model to account for the effect of the two gravity columns (see Fig.

3.5). Seismic mass of the building, lumped at five floor levels, was assigned to the five nodes of the element modeling the gravity columns (Fig. 3.5). Properties of various elements used in Fig. 3.5 for modeling the building are presented in the subsequent sections.

With the description of the jointed wall model described above, it should be realized that the distance between the wall elements is fixed at  $L_w$ , which is the length of each wall. Consequently, it is assumed that the distance between the centers of rotation at the wall bases remains unchanged as depicted in Figure 3.6. In reality, the compression ends of the wall bases cannot significantly deform beyond the rigid foundation, causing overestimation of the UFP connectors. For a given rotation at the wall bases, the value of the UFP deformation calculated for the model, the UFP deformation expected in the structure and the ratio between these two deformations are given by equations (1), (2) and (3), respectively:

$$d_m = \left( \frac{L_w}{2} \times \theta \right) \times 2 = L_w \times \theta \quad (1)$$

$$d_a = (L_w - N) \times \theta \quad (2)$$

$$F = \frac{d_a}{d_m} = \frac{L_w - N}{L_w} \quad (3)$$

where,

$d_m$  = UFP deformation calculated for the model

$d_a$  = UFP deformation expected in the actual structure

$L_w$  = length of one unbonded wall

$\theta$  = rotation in base of wall

$N$  = neutral axis depth at the wall base

$F$  = ratio of between the UFP deformations in the actual and model wall systems

To compensate for the error in the UFP deformation in the model, the elastic and inelastic stiffnesses of the UFP springs were modified by multiplying them by factor  $F$  determined from Eq. 3. The test data from the PRESS building confirmed that the floor displacement and UFP deformation were approximately linearly correlated. Similar trend

was found in the analytical results of the present model because of utilizing the rigid links between the walls and the UFP springs.

### **3.4 Characteristics of Elements used in the Analytical Model**

Properties of various elements, used in the analytical model, were derived based on their material properties and geometric dimensions, which are included in Table 3.1. The material properties were taken identical to those established for the PRESSSS test building. Since each wall in the jointed system was expected to undergo negligible damage with inelastic actions concentrated at the wall base, the walls in the analytical model were represented by elastic beam-column elements with their stiffness based on their gross section properties. Each wall element was connected to the foundation using an elastic bi-linear rotational spring to model the flexural resistance of the wall at the base and the corresponding concentrated crack opening at this location. Moment-rotation behavior of the rotational springs, which were found by analyzing the wall behavior using the procedure recommended in (Aaleti 2005), are reported in Table 3.1.

Each of the two columns, included in the one bay seismic frame model (see Fig. 3.5), represented three seismic columns shown in the plan view of the structure shown in Fig. 3. These columns were modeled as linear elastic beam-column elements with the effective moment of inertia equal to 70% of the gross moment of inertia of the column section in the first story and 100% of the gross moment of inertia in the upper stories. This approach was followed to capture the effect of observed flexural cracking on the seismic columns during the wall direction testing of the PRESSSS test building (Priestley et al. 1999).

The beams in the one bay seismic frame model (Fig. 3.5) represented the floor systems at the five floor levels. These beams were modeled using linear elastic beam-column elements. The beams in the first three floor levels included elasto-plastic rotational springs at the ends, whereas the beams at the fourth and fifth floor levels were connected to the columns using pin connections. Such rotational springs and pin connections were incorporated in the model to adequately capture the behavior of actual connections between the floor and seismic frames as used in the PRESSSS test building as well as the expected framing action resulting from the seismic frames and flooring systems. More descriptions of

these connections and their expected behavior may be found in Thomas and Sritharan (2004). The effects of two gravity columns seen in Fig. 3.3 were modeled using a single gravity column, which was placed in series with the jointed wall system model as shown in Fig. 3.5. Uncracked section properties were used to model these columns using an elastic beam-column element. The base of this element was attached to the foundation using a non-linear rotational spring with the Modified Takeda hysteretic rule available in RAUMOKO (Carr 2003), which was to satisfactorily capture the moment-rotation behavior of the gravity column at this location. The moment-rotation properties of this spring were obtained from ref. (Thomas 2003) and are included in Table 3.1.

Based on the force-displacement test results reported for UFP connectors by Thomas (2003), equivalent bi-linear inelastic axial springs modeled the contribution of UFPs. These springs (Fig. 3.5), whose properties are summarized in Table 3.1, were mainly responsible for the hysteretic energy dissipation of the jointed wall systems. Rayleigh damping model (Carr 2003) was used to introduce viscous damping in dynamic analysis. The percentage of critical damping at the first and fifth modes was given as input parameters to define the damping matrix as a function of mass and stiffness matrices.

The elastic modulus, moment of inertia, and cross sectional area values of a wall member were multiplied by  $10^3$ ,  $10^4$ , and  $10^8$ , respectively, to establish the properties of rigid beam-column elements, which linked wall elements to the UFP springs. These high values for the element properties ensured adequate behavior for the rigid elements. As previously noted, the lateral load resistance of the seismic frame and gravity columns was included to adequately validate the analytical model. However, for comparing multiple level performance of the two unbonded post-tensioned jointed precast wall systems (i.e., JWS1 and JWS2), these contributions were not included.

### **3.5 Model Validation**

In the wall direction, the PRESSS test building was subjected to five levels of short-duration ground motions as shown in Fig. 3.7, and they were referred as 0.75EQ-I, 1.5EQ-I, EQ-II, EQ-III and -1.5EQ-III. EQ-I, EQ-II, EQ-III and EQ-IV represent four levels of seismic hazard expressed in terms of spectral accelerations (see Fig. 3.8), and were

established by the Performance-Based Seismic Engineering Ad Hoc Subcommittee (2003) of the Structural Engineers Association of California (SEAOC). Of these different seismic hazard levels, EQ-III represents the design-level earthquake ground motions, while EQ-IV, which is equivalent to 1.5 times EQ-III, correspond to the maximum considered earthquakes. For these four levels of seismic hazard, Sritharan et al. (1999 and 2002) created spectrum compatible short-duration ground motions. Three of these ground motions, multiplied by different scale factors, were used for the wall direction test of the PRESSSS building. Details for using different scale factors for the PRESSSS building test may be found in Rahman and Sritharan (2006). The analytical model of the PRESSSS building with the jointed wall described in Section 4 (see Fig. 3.5) was also subjected to these five levels of short-duration ground motions in Fig. 3.7. Figures 3.9 and 3.10 show that the comparison between the experiment and analytical results for the top floor displacement and base moment as a function of time. Good agreements between the analytical and experimental results are seen, which confirm the satisfactory representation of the analytical model. Furthermore, as shown in Fig. 3.11, the analytical model also satisfactorily captured the deformation of the UFP connectors as a function of time. All of these validations suggest that the jointed wall model incorporated in Fig. 3.5 can be used to satisfactorily evaluate the seismic performance of jointed wall systems JWS1 and JWS2.

### **3.6 Performance-Based Seismic Evaluation**

Seismic performance of JWS1 and JWS2 designed using DDBD and FBD was evaluated at EQ-I, EQ-II, EQ-III and EQ-IV using the maximum transient inter-story drift, maximum residual inter-story drift, and the maximum floor acceleration, where the inter-story drift is defined as the relative floor displacement divided by story height. According to the performance-based seismic design concept presented by the SEAOC Seismology Committee (1999), ordinary buildings with conventional structural systems when subjected to ground motions compatible with EQ-I, EQ-II, EQ-III and EQ-IV may be expected to produce operational, occupiable, life safety and near collapse performances for both structural and non-structural components. At the minimum, the precast jointed wall systems were expected to meet the same performance levels under the four earthquake levels.

The acceptable performance of the joined walls was arbitrated by comparing the maximum values of the inter-story drift, residual drift and floor acceleration against the limiting values. The limiting values for the transient inter-story drifts and residual drifts were defined in accordance with the recommendations of Seismology Committee (1999) and ITG 5.1-XX (2006.). However, the acceptable floor accelerations were defined using an IBC (2000) recommendation for the design of non-structural components. More details on multiple levels input ground motions and the limiting values for the inter-story drifts and floor acceleration are given below.

### **3.6.1 Input Ground Motions**

Two sets of earthquake input motions were used to evaluate the seismic performance of the jointed wall systems JWS1 and JWS2. The first set consisted of four combinations of short-duration spectrum compatible earthquake motions, while the second set consisted of eight scaled input motions recorded in past earthquakes. The motivation for using the first set of input motions was that it followed the procedure adopted for the pseudo dynamic testing of the PRESSSS building (Sritharan et al. 1999) and provided an opportunity to examine the validity of using short-duration input motions in performance-based seismic testing of structural systems.

Table 3.2 lists different combinations of the short-duration ground motions used in the seismic evaluation of the jointed wall systems, which were performed using each combination of records as one sequence with zero acceleration for about 13.3 s of duration between the records. This procedure enabled the free vibration response of the jointed walls to be examined after subjecting them to each earthquake segment. The original motions used to create the short-duration ground motions of 1.5EQ-I, EQ-II, EQ-III, EQ-IVa and EQ-IVb were recorded at stations with soil profile type  $S_C$  in the 1974 Hollister, 1971 San Fernando, 1940 Imperial Valley, 1993 Northridge and 1978 Tabas earthquakes, respectively. More descriptions of the input records and the process used for creating the short-duration input motions may be found in refs. (Sritharan et al. 1999; Sritharan et al. 2002; Rahman and Sritharan 2006).

Table 3.3 provides details of the eight scaled long-duration input motions used for evaluating the performance of the jointed wall systems. The original records of these input motions were obtained typically from stations with soil profile type  $S_C$  as defined in (UBC 1997). As detailed in Table 3.3, the original recorded motions were scaled such that their spectra would be comparable to the target spectra within a dominant period range, following the procedure developed in (Rahman and Sritharan 2006). Figures 3.12 (a) and (b) depict the acceleration response spectra for all modified long-duration ground motions listed in Table 3.3. Because the analyses of the jointed wall systems were conducted at 60 percent scale, the time step and accelerations of all input motions listed in Tables 3.2 and 3.3 were modified by scale factors of 0.6 and 1.67, respectively. These modifications were made when performing the analyses of the buildings.

### **3.6.2 Inter-Story Drift Limits**

The following inter-story drift limits were used as acceptable limits to evaluate the jointed wall system performances at the four earthquake intensity levels: maximum transient drifts of 0.4% (EQ-I), 1.2% (EQ-II), 2.0% (EQ-III) and 3.0% (EQ-IV); and maximum residual drifts of 0.1% (EQ-I), 0.3% (EQ-II), 0.5% (EQ-III) and 0.75% (EQ-IV). These limits were chosen based on the guidance given in the SEAOC Blue Book (Seismology Committee 1999), ITG 5.1-XX (2006) and considering the re-centering nature of the jointed wall systems.

### **3.6.3 Floor Acceleration Limits**

To limit damage to non-structural elements that may be anchored to the floors during seismic response of the precast buildings, a set of floor acceleration limits were imposed. These limits were derived in Rahman and Sritharan (2006) using the recommendations of Tong et al. (2004) and the IBC (2000) provision for estimating design forces required to anchor different types of non-structural elements to building floors under seismic condition. A controlling parameter of these floor acceleration limits is the spectral acceleration corresponding to a short period that is used to define the design response acceleration spectrum (IBC 2000). For the design spectra recommended by the SEAOC Performance-Based Seismic Engineering Ad Hoc Subcommittee (2003), the values of the sort-period

spectral acceleration ordinates are  $2.16 \text{ m/s}^2$ ,  $4.80 \text{ m/s}^2$ ,  $9.81 \text{ m/s}^2$  and  $14.72 \text{ m/s}^2$  for EQ-I, EQ-II, EQ-III and EQ-IV, respectively (Rahman and Sritharan 2006). The corresponding limiting floor accelerations are  $2.60 \text{ m/s}^2$ ,  $5.77 \text{ m/s}^2$ ,  $11.79 \text{ m/s}^2$  and  $17.68 \text{ m/s}^2$ . Including the scale factor of 0.6, the following limits are used in this study:  $4.33 \text{ m/s}^2$  (EQ-I),  $9.61 \text{ m/s}^2$  (EQ-II),  $19.65 \text{ m/s}^2$  (EQ-III) and  $29.47 \text{ m/s}^2$  (EQ-IV).

### **3.7 Results from Earthquake Analysis Of Jointed Wall Systems**

Figures 3.13 and 3.14 summarize the key results obtained by subjecting the two jointed wall systems, JWS1 and JWS2, to all combinations of short-duration earthquake motions. As expected due to the increased flexibility, the maximum transient inter-story drifts of JWS1 were higher than those obtained for JWS2 for all levels of ground motions (Fig. 3.13). The utmost difference between the maximum transient inter-story drifts of JWS1 and JWS2 were 112%, 132%, 191% and 245%, for EQ-I, EQ-II, EQ-III and EQ-IV level motions, respectively. This observation indicates that the highest difference between the maximum transient inter-story drifts of the two jointed walls increases as intensity of the ground motion increases. However, a similar trend is not observed for the smallest difference in the maximum transient inter-story drifts of JWS1 and JWS2, which were found to be 29%, 43%, 8% and 23%, for EQ-I, EQ-II, EQ-III and EQ-IV level motions, respectively. Furthermore, Figure 3.13 illustrates that both jointed walls exhibited acceptable performances in terms of the maximum transient inter-story drift for the four levels of short-duration ground motions. For EQ-I and EQ-II level motions, the maximum transient inter-story drifts of JWS1 and JWS2 were noticeably lower than the acceptable limits. When the two wall systems were subjected to the EQ-III level short-duration motions, the maximum transient inter-story drift recorded for JWS1 was 1.15%, which is 58% of the acceptable limit of 2% established for EQ-III level motions. Similarly, when all EQ-IV level motions were considered, JWS1 exhibited the maximum transient inter-story drift of 2.81%, which is 94% of the acceptable limit. In comparison, the highest level of the maximum transient inter-story drifts obtained for JWS2 were 0.82% (41% of acceptable limit) and 2.02% (67% of acceptable limit) for EQ-III and EQ-IV level motions, respectively. Such low values for the maximum transient inter-story drifts for JWS2 under EQ-III and EQ-IV level motions

suggest that the stiffness of JWS2 may be unnecessarily high and that JWS1 provides a more economical solution.

Figure 3.14 represents the maximum floor accelerations of JWS1 and JWS2 when subjected to short-duration ground motions. Generally, the maximum floor accelerations in JWS2 building were higher than those obtained for JWS1 by as much as 78%, 33%, 20% and 34% for EQ-I, EQ-II, EQ-III and EQ-IV level motions, respectively. However, for the EQ-III level motions in combination-1, combination-2 and combination-3 as well as for the EQ-IV level motion in combination-3, the maximum floor accelerations obtained for JWS2 were lower than those of JWS1, indicating the dependency of the jointed wall responses on the frequency contents of the input motions. The maximum floor accelerations in JWS1 for all levels of ground motions were appreciably below the acceptable limits. A similar trend was demonstrated by JWS2, except for the EQ-I level ground motions in combinations 1 and 2, for which the acceptable limit of the maximum floor acceleration was exceeded by 2%.

Figure 3.15 compares the maximum transient inter-story drifts obtained for the two jointed wall models when subjected to the long-duration ground motions, listed in Table 3.3. As previously witnessed for the short-duration motions, both buildings produced acceptable seismic performances in terms of the maximum inter-story drifts, with sufficient margin of safety for all levels of ground motions represented by IM-a through IM-h. This observation suggests that the jointed wall systems established using both the DDBD and FBD are acceptable design solutions. The maximum inter-story drifts of JWS1 were generally higher than those of JWS2 and they differ by as much as 109% (see data corresponding to IM-b in Fig. 3.15), indicating that the DDBD solution is more economical than the FBD solution. The highest values of the maximum transient inter-story drifts exhibited by JWS1 were 30%, 54%, 85% and 76% of the acceptable maximum transient inter-story drift limits for EQ-I, EQ-II, EQ-III and EQ-IV level ground motions, respectively. In contrast, JWS2 achieved 25%, 26%, 68% and 71% of the respective acceptable limits of the transient inter-story drifts. Unlike it was observed for short duration input motions, the difference between the maximum transient inter-story drifts of the two jointed walls, which is generally small, does not seem to increase as the intensity of the ground motion increases.

The dependency of the building responses on frequency contents of the input earthquake was also emphasized by the analyses results in Fig. 3.15. For example, at EQ-IV level, the responses of JWS1 and JWS2 to IM-g led to only 7% difference in the maximum transient inter-story drifts, whereas the corresponding difference was 76% for IM-f, although IM-f and IM-g ground motions were chosen to represent EQ-IV level input motions. Moreover, when the two jointed walls were subjected to IM-e, JWS2 produced larger transient inter-story drift than JWS1. Although not typical, such occurrence is expected because, among other parameters, the inelastic displacement excursion occurring in the opposite direction also influences the maximum transient drift especially in building systems that can re-center. It is to be noted that similar results were observed in Rahman and Sritharan (2006) for precast hybrid frames designed to re-center after subjected to earthquake lateral loading.

Figure 3.16 illustrates the maximum floor accelerations observed for the two jointed wall systems when subjected to all long-duration ground motions of Table 4.3 representing the EQ-I to EQ-IV level earthquakes. Generally, the maximum floor accelerations in JWS2 were higher than those observed for JWS1 because of the increased lateral stiffness. The largest difference between the maximum floor accelerations of JWS2 and JWS1 were 50%, 4%, 29% and 24%, respectively, for EQ-I, EQ-II, EQ-III and EQ-IV level earthquake motions.

The maximum floor accelerations of JWS1 were satisfactory and were 72% to 85% of the associated acceptable limits for all levels of earthquake motions. In contrast, the response of JWS2 produced floor accelerations somewhat greater than the acceptable limits for three input motions: 17%, 2.6% and 0.9% higher than the associated acceptable limits for input ground motions IM-a (EQ-I), IM-c (EQ-III) and IM-h (EQ-IV), respectively. Since the jointed wall designed using the FBD method violates the designated acceptable limits for the maximum floor acceleration for three levels of earthquakes, it appears that excessive floor accelerations could result in excessive damage to non-structural components in the building containing JWS2.

The re-centering capability of the unbonded post-tensioning tendon enabled both jointed wall systems to produce insignificant residual inter-story drifts at the end of short- as

well as long-duration ground motions. The maximum residual inter-story drifts observed for two jointed wall systems were less than 0.004%, which is much lower than the acceptable limits. The increase in transient inter-story drift exhibited by JWS1 did not cause any concerns with the re-centering ability of this wall system.

To investigate the influence of energy dissipating UFP connectors on the response of jointed wall systems, the response of JWS1 model was examined under IM-c and IM-d by changing the number of connectors. First, the sensitivity of energy dissipating mechanism on the maximum transient inter-story drift and the maximum residual inter-story drift was examined under design-level earthquake motion IM-d. As expected, Figures 3.17 (a) and (b) show that the maximum transient inter-story drift decreased with increased number of energy dissipating UFP connectors, but the maximum inter-story residual drift also increased. Increase in the residual drift was expected because there was no change in the post-tensioning force that provided the elastic restoring force needed for recentering the wall system. However, in all cases, the residual inter-story drift was within acceptable limit. Similar trends were observed when JWS1 was subjected to IM-c with various numbers of UFPs as shown in Figs. 3.18 (a) and (b).

### **3.8 Conclusions**

Seismic performances of two jointed wall systems representing a 5-story prototype building at 60% scale were analytically studied in this paper. The first jointed wall system was derived using the direct displacement-based design approach while the second jointed wall system was established from the traditional force-based approach. The design base shear of the first building was 50% lower than that of the second building. Following the validation of the analytical modeling procedure, both jointed wall systems were subjected to short- and long-duration earthquake input motions, which were comparable with acceleration response spectra corresponding to four levels of earthquake intensities. Using the analysis results, the following conclusions were drawn:

1. The seismic performance of the two jointed wall systems satisfied the performance limits of the maximum transient inter-story drift, residual inter-story drifts and maximum floor acceleration for all levels of short-duration ground motions.

2. The maximum transient inter-story drifts observed in jointed wall designed using the direct displacement-based design was generally more than those of the force-based jointed wall system, when subjected to long-and short-duration ground motions. An opposite trend was observed for the maximum floor acceleration.
3. Both jointed wall systems produced the maximum transient inter-story drifts lower than the acceptable limits when subjected to all levels of long-duration ground motions. For the same set of ground motions, the displacement-based jointed wall system (JWS1) also satisfied the floor acceleration limits, whereas the force-based jointed wall system (JWS2) failed to satisfy the acceleration limits established for EQ-I, EQ-III and EQ-IV level ground motions.
4. Due to the re-centering capability that stems from the unbonded post-tensioned tendons, both jointed wall systems showed residual inter-story drifts lower than the acceptable limits under both short- and long-duration input motions.
5. The transient inter-story drift in precast jointed wall systems can be controlled by increasing the hysteretic damping in the jointed wall system by adding more number of energy dissipating shear connectors. Although, increasing the number of shear connectors increases the residual inter-story drifts of the jointed walls, they are not expected to exceed the limiting values established for the residual inter-story drifts.
6. Based on the satisfactory performance of the jointed wall system designed using the direct displacement-based design that led to a lower design base shear force, it appears that this design method would lead to a more economical design than the force-based design method for jointed wall systems in low-rise buildings. However, analysis similar to that presented above for JWS1 should be repeated for several other low-rise buildings to generalize this conclusion.

### **3.9 Acknowledgements**

The study reported in this paper was conducted as part of a 2005-06 Daniel P. Jenny Fellowship provided by the Precast/Prestressed Concrete Institute (PCI). Dr. Ned Cleland, Dr. S. K. Ghosh and Ms. Suzanne Nakaki serve as the PCI advisors for this fellowship award. Authors also acknowledge the support of Professor Eduardo Miranda, Department of

Civil and Environmental Engineering, Stanford University, California, USA, for providing some of the ground motion data, while most of the remaining ground motion data were downloaded from the website of the Pacific Earthquake Research Center, USA.

### 3.10 References

- Aaleti, S., 2005. Design and Analysis of Unbonded Post-Tensioned Precast Wall Systems, M.S. Thesis, Department of Civil, Construction and Environmental Engineering, Iowa State University, Ames, Iowa, USA.
- Carr, A. J., 2003. RUAUMOKO - Inelastic Dynamic Analysis Program. University of Canterbury, Christchurch, New Zealand.
- Collins, R. H., 1999. Design of a Precast Concrete Building for Seismic Loading. Thesis of M.S., University of Washington, USA, 37-235.
- Conley, J., Sritharan, S., and Priestley, M. J. N., 2002. Precast Seismic Structural Systems PRESSS-3: The Five-Story Precast Test Building, Vol. 3-1: Wall Direction Response, Report Number: SSRP-99/19, University of California, San Diego, California, USA.
- Galusha, J. G., 1999. Precast, Post-tensioned Concrete Walls Designed to Rock, M.S. Thesis, Department of Civil Engineering, University of Washington, Seattle, Washington, USA.
- International Building Code (IBC), 2000. *International Code Council*, Virginia, USA, 331-377.
- ITG 5.1-XX, 2006. Acceptance Criteria for Special Unbonded Post-Tensioned Structural Walls Based on Validation Testing, *American Concrete Institute*.
- Kurama, Y., Pessiki, S., Sause, R., and Lu, L., 1999. Lateral Load Behavior and Seismic Design of Unbonded Post-Tensioned Precast Concrete Walls, *ACI Structural Journal*, July-August, Vol. 96, No. 4, 622-632.
- Kurama, Y., Pessiki, S., Sause, R., and Lu, L., 1999. Seismic Behavior and Design of Unbonded Post-Tensioned Precast Concrete Walls, *PCI Journal*, Vol. 44, No. 3, 72-88.
- Nakaki, S. D., Stanton, J. F., and Sritharan, S., 1999. An Overview of the PRESSS Five-story Precast Test Building, *PCI Journal*, 44(2), 26-39.
- Performance-Based Seismic Engineering Ad Hoc Subcommittee, 2003. Revised Interim Guidelines: Performance-Based Seismic Engineering for the SEAOC Blue Book, Structural Engineers Association of California, California, USA, 128-132.

- Priestley, M. J. N., 2002. Direct Displacement-Based Design of Precast/Prestressed Concrete Buildings, *PCI Journal*, Vol. 47, No. 6, 67-79.
- Priestley, M. J., N., Sritharan S., Conley, J. R., and Pampanin, S., 1999. Preliminary Results and Conclusions From the PRESSS Five-Story Precast Concrete Test Building, *PCI Journal*, Vol. 44, No. 6, 42-67.
- Rahman, M. A., and Sritharan, S., 2007. A Performance-Based Seismic Evaluation of Two Five-Story Precast Concrete Hybrid Frame Buildings, *Journal of Structure Engineering, American Society of Civil Engineers (ASCE)*, Vol. 133, No. 11, 2007, 1489-1500.
- Seismology Committee, 1999. Recommended Lateral Force Requirements and Commentary (Blue Book). Structural Engineers Association of California (SEAOC), California, USA, 327-421.
- Sritharan, S., and Rahman, M. A., 2004. Performance-based Seismic Assessment of Two Precast Concrete Hybrid Frame Buildings, *Proceedings of International Workshop on Performance-based Seismic Design*, Bled, Slovenia.
- Sritharan, S., 2002. Performance of Four Jointed Precast Frame Systems under Simulated Seismic Loading, *Proceedings of the Seventh National Conference on Earthquake Engineering*; Paper No. 264, Boston, USA.
- Sritharan, S., Pampanin, S., and Conley, J., 2002. Design Verification, Instrumentation and Test Procedures, PRESSS-3: The Five-Story Precast Test Building, Vol. 3-3. ISU-ERI-Ames Report ERI-03325, Iowa State University, Ames, Iowa, USA.
- Thomas, D. J., and Sritharan, S., 2004. An Evaluation of Seismic Design Guidelines Proposed for Precast Jointed Wall Systems, ISU-ERI-Ames Report ERI-04635, Iowa State University, Ames, Iowa, USA.
- Thomas, D. J., 2003. Analysis and Validation of a Seismic Design Method Proposed for Precast Jointed Wall Systems, M.S. Thesis, Department of Civil, Construction and Environmental Engineering, Iowa State University, Ames, Iowa, USA.
- Tong, M., Lee, G., Rzhovsky, V., Qi, J., and Shinozuka, M., 2004. A Comparison of Seismic Risk of Non-structural Systems in a Hospital Before and After a Major Structural Retrofit, ATC-29-2 Seminar on Seismic Design, Retrofit, and Performance of Non-

structural Components in Critical Situations <<http://shingo8.eng.uci.edu/ATC-29-2.htm>,  
date-11-17-2004>

- Uniform Building Code (UBC), 1997. *International Conference of Building Officials*, Whittier, California, USA, 2, 13-38.

Table 3.1 Dimensions of the jointed wall JWS1 and the properties of the analytical model shown in Fig. 3.5

| <b>Parameter</b>  | <b>Value</b>                          |
|---|---------------------------------------|
| Wall height   | 11.43 m                               |
| Wall length   | 2.7432 m                              |
| Wall thickness  | 203.2 mm                              |
| Initial post-tensioning force   | 765.95 kN                             |
| Area of post-tensioning tendons   | 2193.54 mm <sup>2</sup>               |
| Yield strength of post-tensioning tendons                               | 827.40 MPa                            |
| Elastic modulus of post-tensioning tendons                              | 200 GPa                               |
| Wall concrete strength  | 52.64 MPa                             |
| <b><u>Properties of spring modeling</u></b>                             |                                       |
| <b><u>moment resistance of a wall at base</u></b>                       |                                       |
| Yield moment  | 15.49 x 10 <sup>2</sup> kN-m          |
| Elastic rotational stiffness  | 12.38 x 10 <sup>5</sup> kN-m/rad      |
| Hardening ratio   | 0.043                                 |
| <b><u>Properties of spring modeling</u></b>                             |                                       |
| <b><u>UFPs at each floor level</u></b>                                  |                                       |
| Yield strength  | 129.35 kN                             |
| Elastic stiffness   | 105.08 kN/mm                          |
| Hardening ratio   | 0.035                                 |
| <b><u>Properties of spring modeling seismic column contribution</u></b> |                                       |
| Yield moment  | 327.61 kN-m                           |
| Elastic rotational stiffness  | 140.41 x 10 <sup>3</sup> kN-m/rad     |
| Hardening ratio   | 0.0356                                |
| <b><u>Properties of spring modeling gravity column contribution</u></b> |                                       |
| Yield moment  | 406.70 kN-m                           |
| Elastic rotational stiffness  | 203.35 x 10 <sup>3</sup> kN-m/rad     |
| Hardening ratio   | 0.0278                                |
| Fundamental period  | JWS1 = 0.4592 sec<br>JWS2 = 0.3251sec |

Table 3.2 Different combinations of short-duration ground motions used for the performance based seismic evaluation of precast jointed wall systems

| Combinations  | Earthquake Intensity Level |                |            |               |
|---------------|----------------------------|----------------|------------|---------------|
|               | EQ-I                       | EQ-II          | EQ-III     | EQ-IV         |
| Combination-1 | EQ-I                       | EQ-II          | EQ-III     | EQ-IVa        |
| Combination-2 | EQ-I                       | EQ-II          | EQ-III     | EQ-IVb        |
| Combination-3 | 0.22EQ-III                 | (-) 0.50EQ-III | EQ-III     | (-) 1.5EQ-III |
| Combination-4 | 0.15EQ-IVb                 | (-) 0.33EQ-IVb | 0.67EQ-IVb | EQ-IVb        |

Table 3.3 List of ground motions selected for the performance-based seismic evaluation of precast jointed wall systems

| Identification of the Input Motion | Earthquake Intensity | Earthquake Name (Year) and Station                            | Magnitude     | Direction of Component | Scale Factor | PGA after multiplying by the Scale Factor (g) |
|------------------------------------|----------------------|---|---------------|------------------------|--------------|---|
| IM-a                               | EQ-I                 | Morgan Hill (1984); Station: Gilroy # 6, San Ysidro Microwave | 6.1 ( $M_s$ ) | East-West              | 0.65         | 0.19  |
| IM-b                               | EQ-II                | Loma Prieta (1989); Station: Saratoga Aloha Avenue            | 7.1 ( $M_s$ ) | North-South            | 0.64         | 0.32  |
| IM-c                               | EQ-III               | Northridge (1994); Station: Castaic Old Ridge Route           | 6.8 ( $M_s$ ) | East-West              | 1.30         | 0.67  |
| IM-d                               | EQ-III               | Imperial valley (1940); Station: Elcentro                     | 7.2 ( $M_s$ ) | North-South            | 1.50         | 0.48  |
| IM-e                               | EQ-III               | Kobe-Japan (1995); Station: KJM                               | 6.9 ( $M_w$ ) | East-West              | 1.10         | 0.66  |
| IM-f                               | EQ-IV                | Tabas-Iran (1978)   | 7.4 ( $M_s$ ) | 344 degrees from North | 1.00         | 0.93  |
| IM-g                               | EQ-IV                | Chi-Chi-Taiwan (1999); Station: CHY                           | 7.6 ( $M_s$ ) | 80 degrees from North  | 0.95         | 0.86  |
| IM-h                               | EQ-IV                | Kobe-Japan (1995); Station: KJM                               | 6.9 ( $M_w$ ) | North-South            | 1.18         | 0.97  |

PGA = Peak Ground Acceleration,  $M_s$  = Surface Wave Magnitude,  $M_w$  = Moment Magnitude

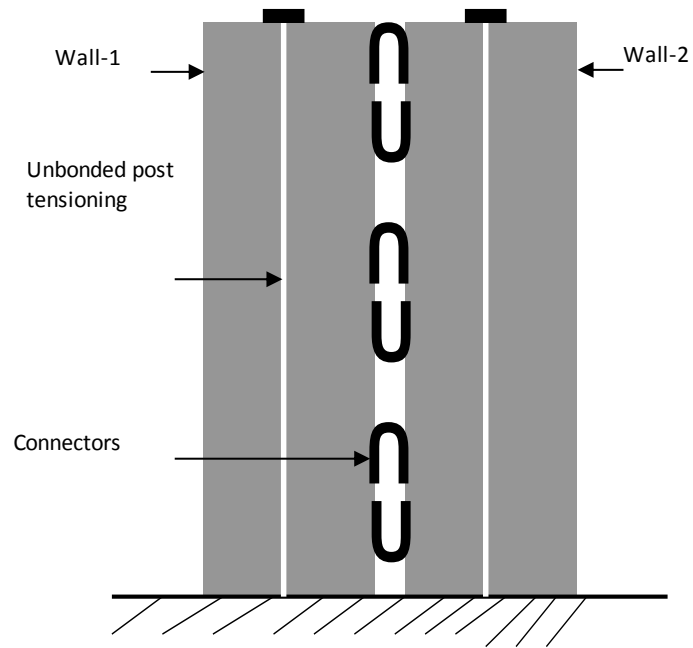


Figure 3.1 Illustration of the jointed wall system

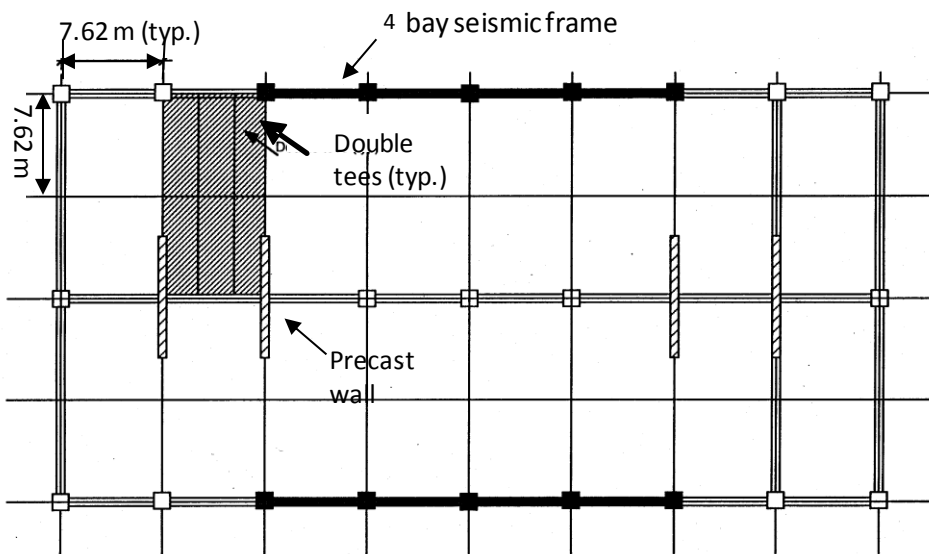


Figure 3.2 Plan view of the precast concrete prototype building (Nakaki et al. 1999)

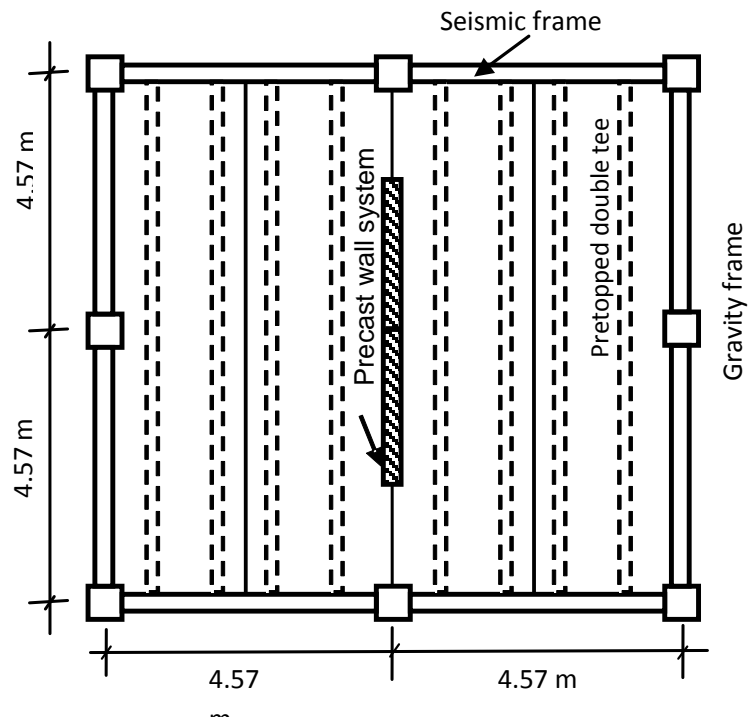


Figure 3.3 Plan view of the scaled post-tensioned precast wall system building



Figure 3.4 The PRESSS test building after erecting the jointed wall system

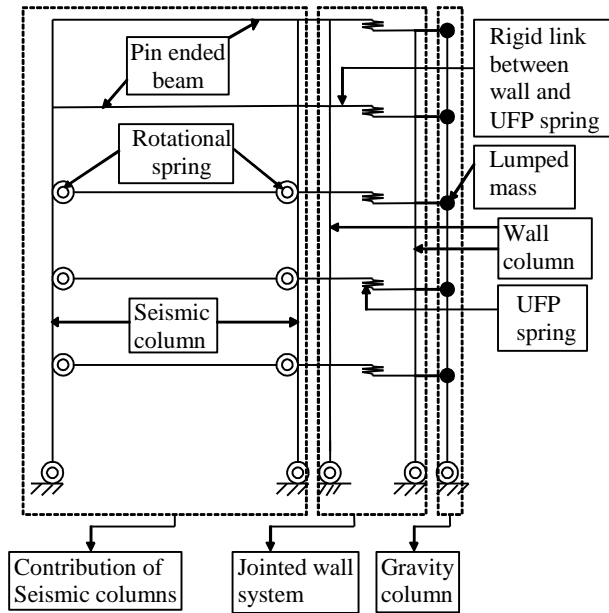


Figure 3.5 Proposed analytical model for the building with the jointed wall system shown in Fig. 3.3

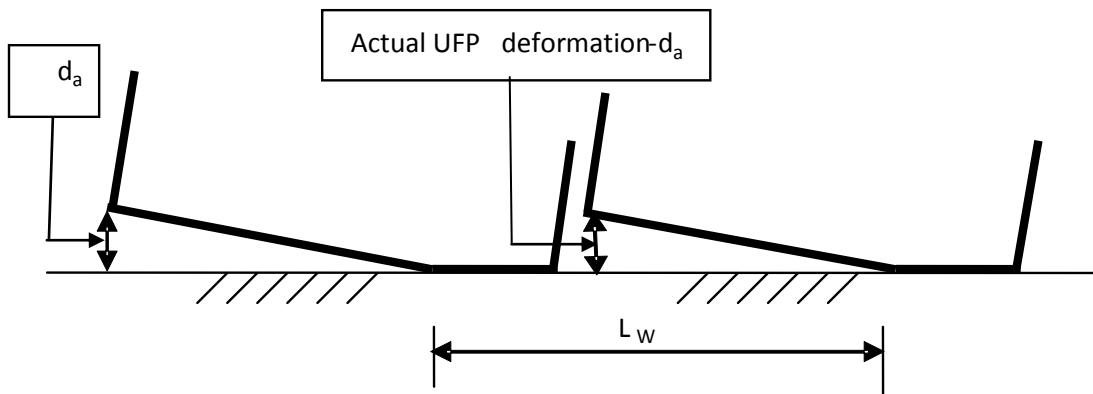


Figure 3.6 Illustration of rotations of walls and the corresponding UFP deformation at a base rotation of  $\theta$

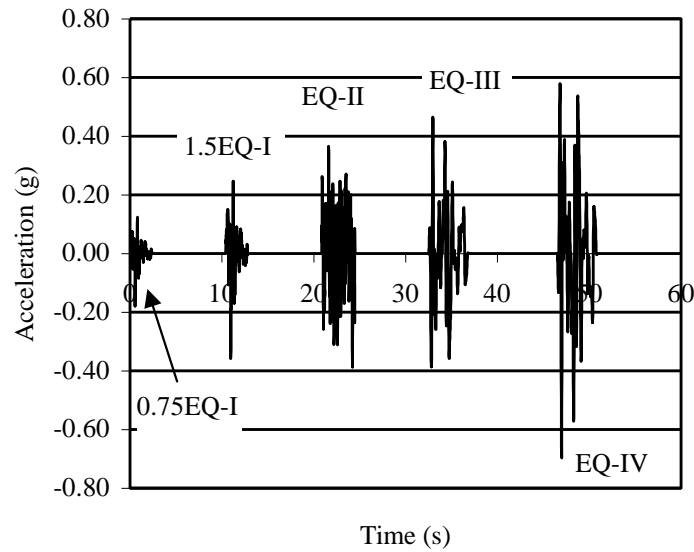


Figure 3.7 Short-duration earthquake ground motions used for testing of the PRESSS building in the jointed wall direction

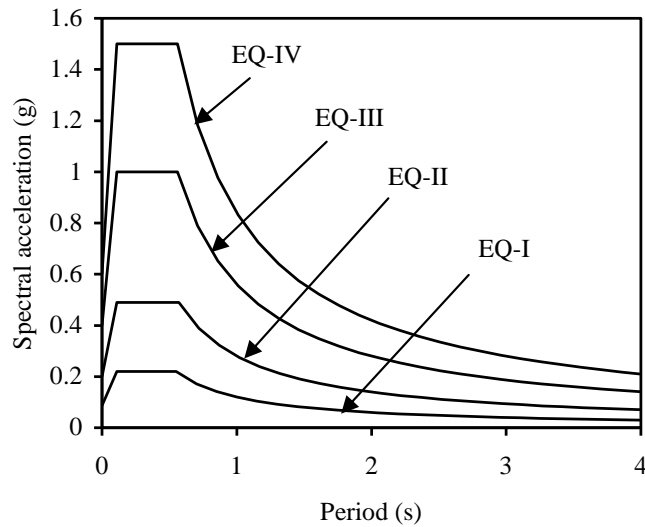


Figure 3.8 The 5% damped multiple-level acceleration response spectra suggested for soil type Sc in high seismic zone as per the Performance-Based Seismic Engineering Ad Hoc Subcommittee (2003) of SEAOC

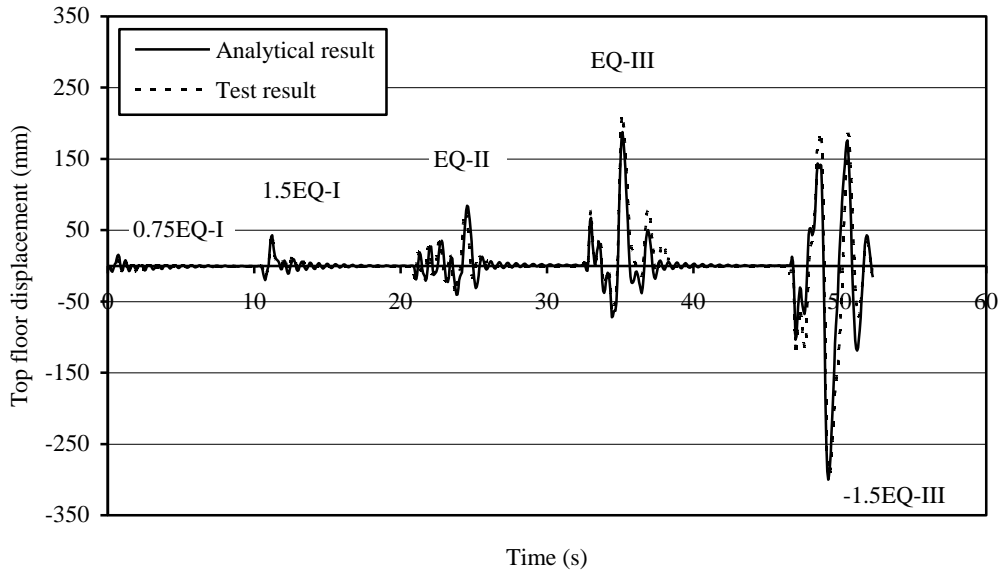


Figure 3.9 Comparison between the analytical and experimental lateral displacement at the fifth floor of the PRESSS test building in the jointed wall direction

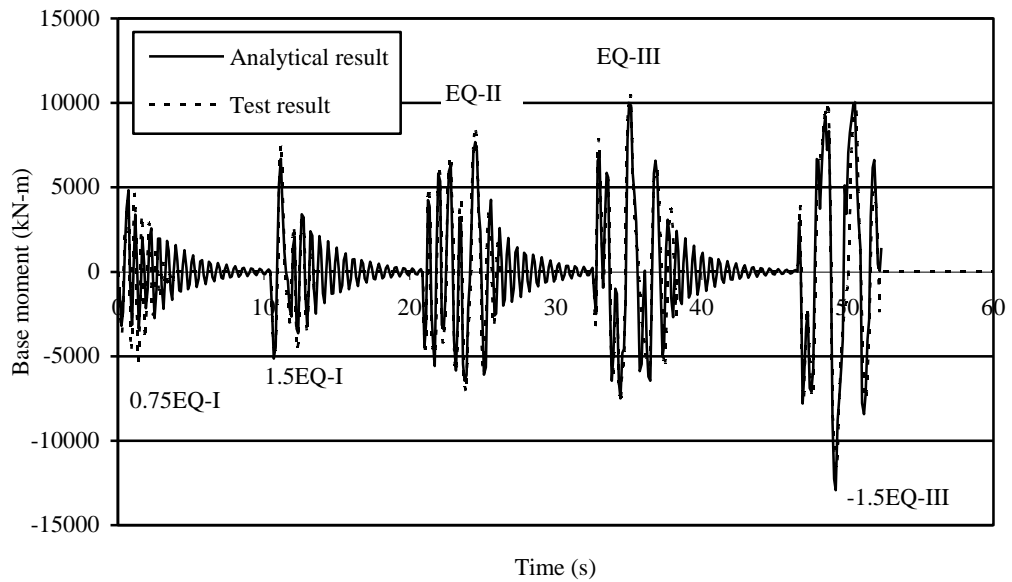


Figure 3.10 Comparison between the analytical and experimental base moment of the PRESSS test building in the jointed wall direction

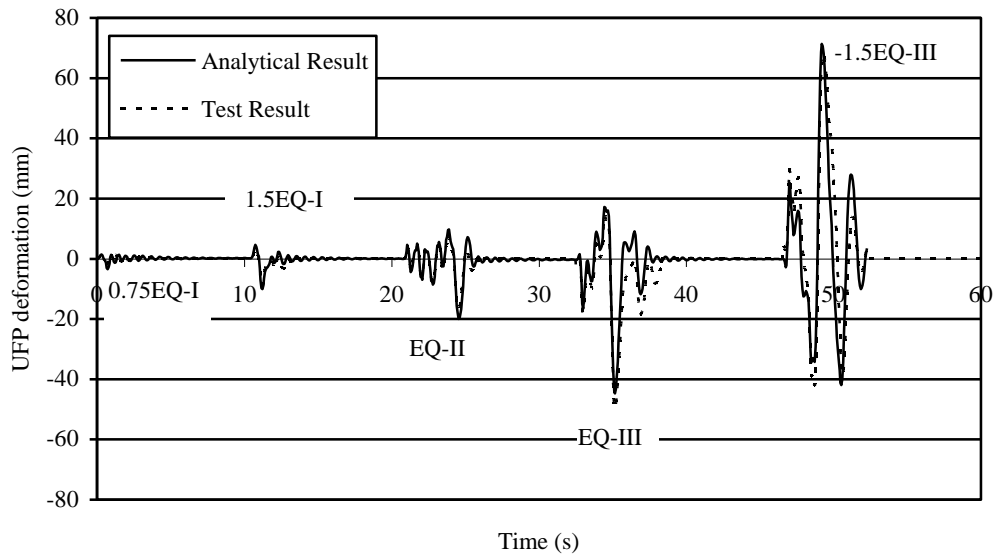


Figure 3.11 Comparison between the analytical and experimental UFP deformation at the fifth floor of the PRESSS test building in the jointed wall direction

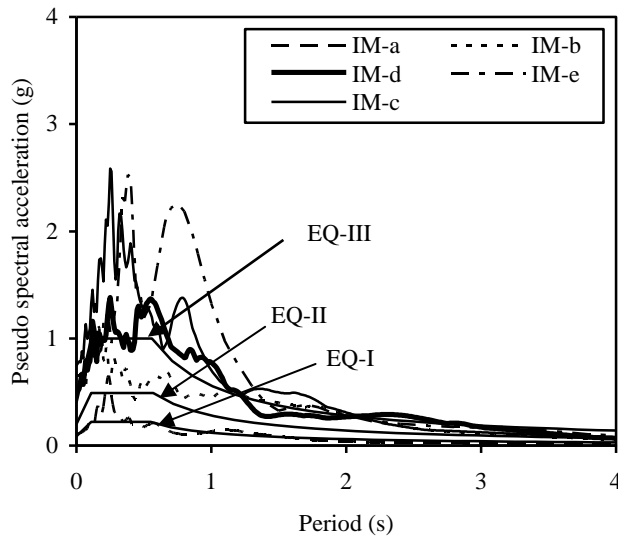


Figure 3.12 (a) The 5% damped acceleration response spectra of EQ-I, EQ-II and EQ-III with those produced for scaled ground motions IM-a through IM-e listed in Table 3.3

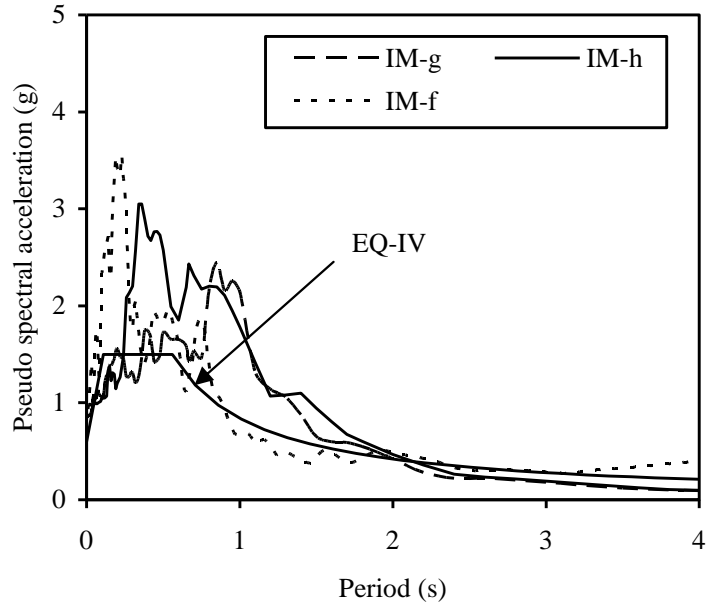


Figure 3.12 (b) The 5% damped acceleration response spectra of EQ-IV with those produced for scaled ground motions IM-f through IM-h listed in Table 3.3

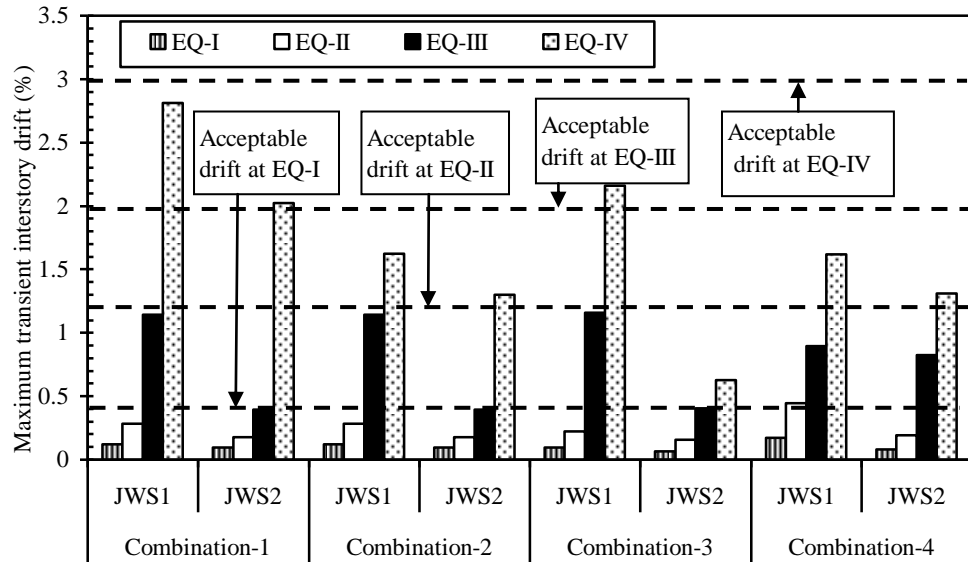


Figure 3.13 The maximum transient interstory drifts obtained for JWS1 (DDBD) and JWS2 (FBD) when subjected to various combinations of short-duration ground motions summarized in Table 3.2

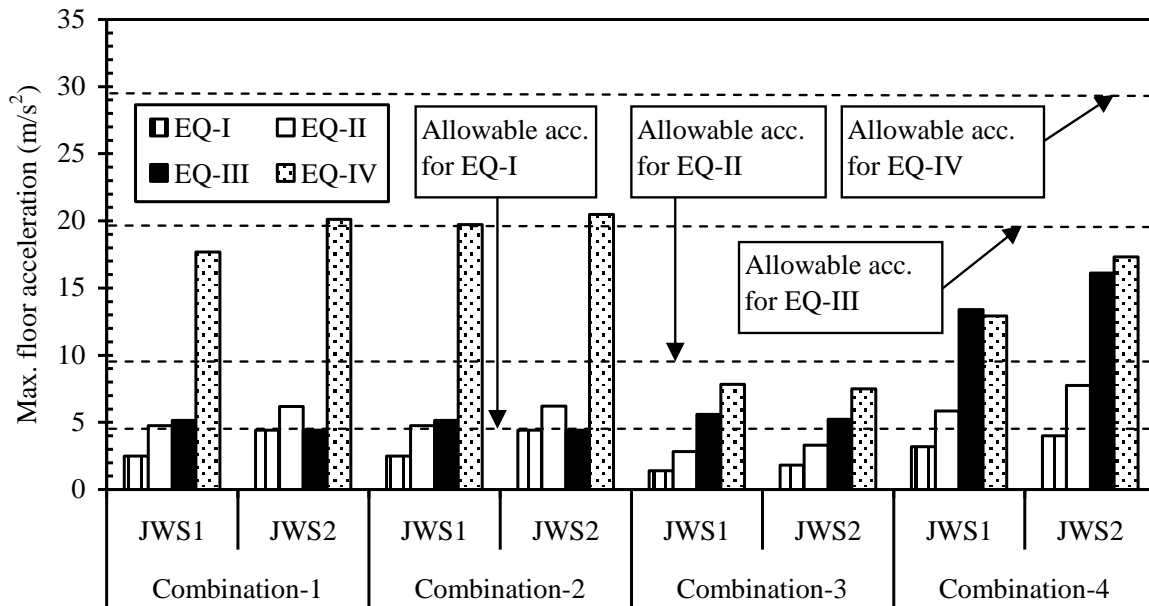


Figure 3.14 The maximum floor accelerations obtained for JW1 (DDBD) and JW2 (FBD) when subjected to various combinations of short-duration ground motions summarized in Table 3.2

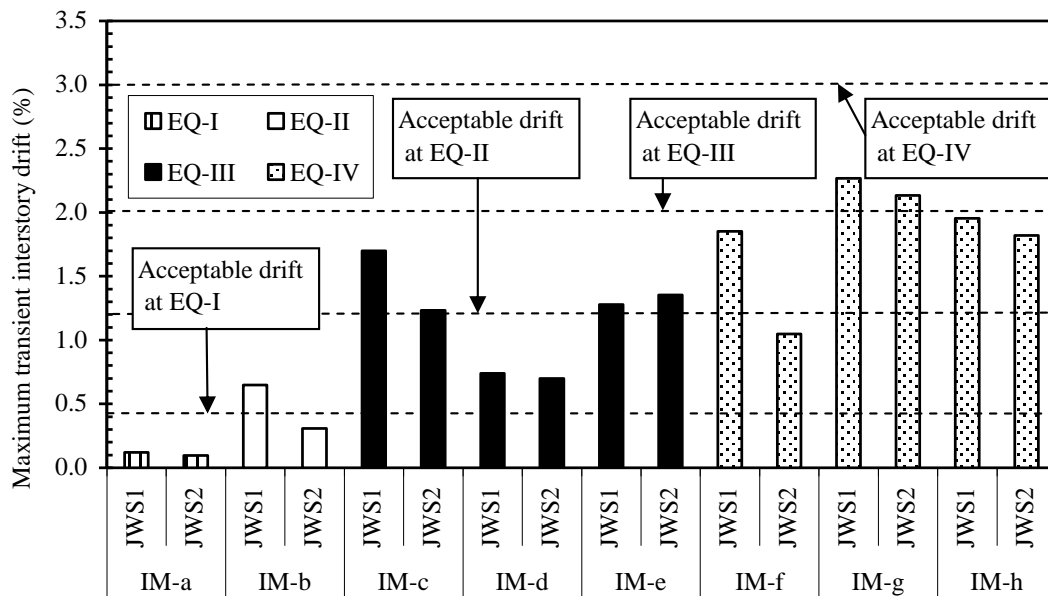


Figure 3.15 The maximum transient interstory drifts obtained for JWS1 (DDBD) and JWS2 (FBD) when subjected to various long-duration ground motions summarized in Table 3.3

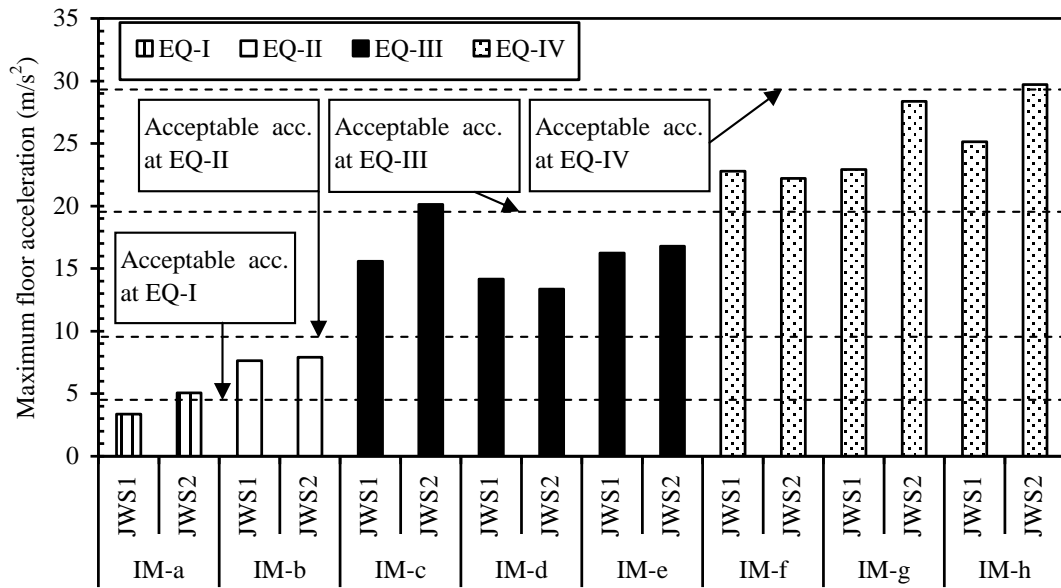


Figure 3.16 The maximum floor accelerations obtained for JWS1 (DDBD) and JWS2 (FBD) when subjected to various long-duration ground motions summarized in Table 3.3

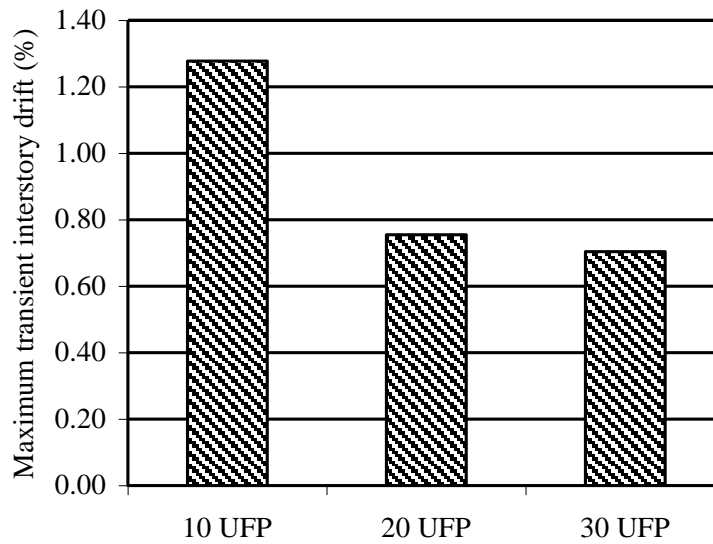


Figure 3.17 (a) Illustration of the influence of the number of UFP connectors on the maximum transient interstory drift of JWS1 using input motion IM-d

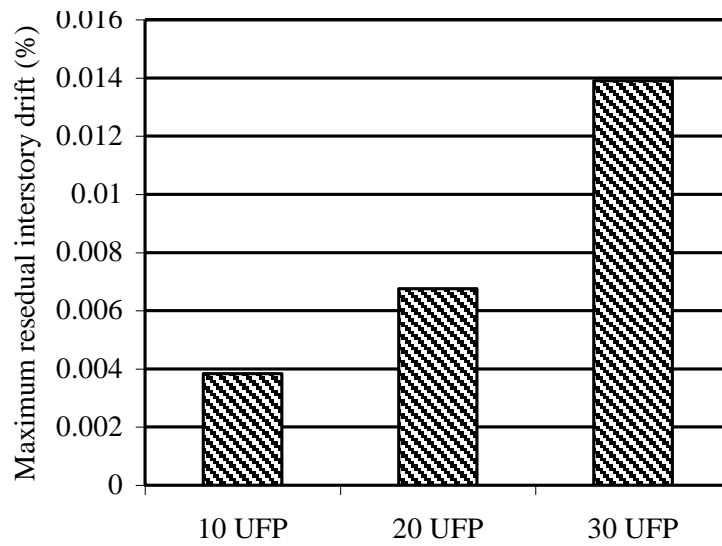


Figure 3.17 (b) Illustration of the influence of the number of UFP connectors on the maximum residual interstory drift of JWS1 using input motion IM-d

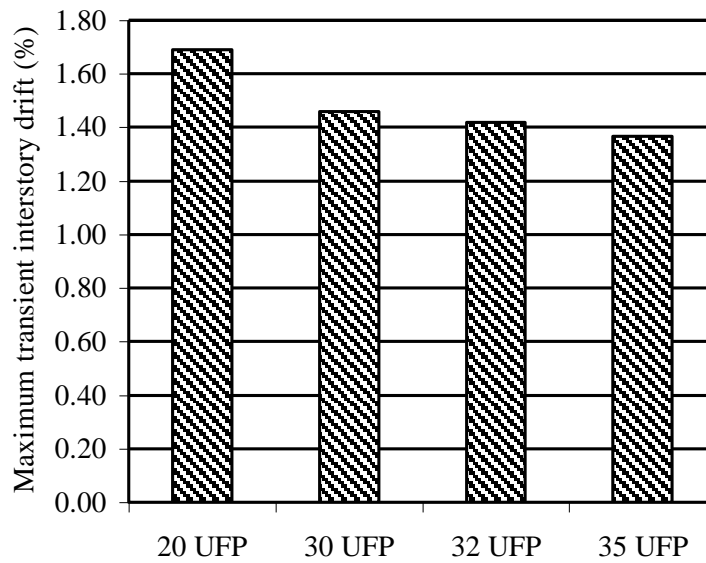


Figure 3.18 (a) Illustration of the influence of the number of UFP connectors on the maximum transient interstory drift of JWS1 using input motion IM-c

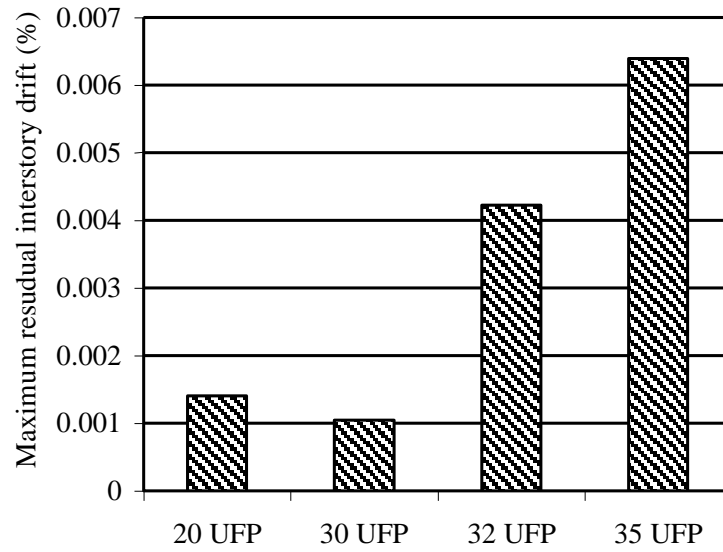


Figure 3.18 (b) Illustration of the influence of the number of UFP connectors on the maximum residual interstory drift of JWS1 using input motion IM-c

# **CHAPTER 4: SEISMIC RESPONSE OF PRECAST POST-TENSIONED JOINTED WALL SYSTEMS DESIGN FOR LOW TO MID-RISE BUILDINGS USING THE DIRECT DISPLACEMENT-BASED APPROACH**

(A paper to be submitted in *Earthquake Spectra Journal* )

**M. Ataur Rahman<sup>1</sup> and Sri Sritharan<sup>2</sup>**

## **Abstract**

This paper presents an investigation on the seismic performance of precast post-tensioned jointed wall systems designed for a five-, seven- and ten-story building using the direct displacement-based design approach. Using earthquake motions of different intensities, the performance of the buildings was evaluated using response parameters, such as the maximum transient interstory drift, floor acceleration, and residual interstory drift. The three buildings performed satisfactorily in terms of the maximum transient interstory drift and residual interstory drift. The maximum floor accelerations exceeded the acceptable limits in some analyses of the seven- and ten-story buildings. Therefore, a strategy to control floor accelerations in these buildings is suggested by modifying the wall dimensions. It was identified that low-rise building achieved transient interstory drifts closer to the acceptable limits compared to the taller building. An opposite trend was observed regarding floor acceleration. In taller jointed wall systems, the average interstory drift of the building was less sensitive to the increase in the maximum interstory drift compared to that in a low-rise jointed wall system.

---

<sup>1</sup>PhD Candidate, Department of Civil, Construction and Environmental Engineering, e-mail: [ataur70@iastate.edu](mailto:ataur70@iastate.edu), Iowa State University, Ames, IA 50011, USA

<sup>2</sup>Associate Professor, Department of Civil, Construction and Environmental Engineering, e-mail: [sri@iastate.edu](mailto:sri@iastate.edu), tel.: 515-294-5238, fax:515-294-7424, Iowa State University, Ames, IA 50011, USA

## 4.1 Introduction

Precast concrete wall systems have shown to be an excellent choice for designing earthquake resistant buildings, which benefits from the quality and cost-efficiency of prefabrication. A concept for a precast unbonded post-tensioned concrete wall system has been investigated in consideration of its potential benefits over an emulative precast concrete wall for seismic applications (Priestley et al. 1999; Thomas 2003; Thomas and Sritharan 2004). In this jointed wall system, individual precast walls are secured to the foundation using unbonded prestress tendons running from the top of the wall to the foundation. Shear connectors distributed vertically along the height connects two or more walls together horizontally as shown in Fig. 4.1. The use of unbonded post-tensioning allows the walls to rock individually at the base and minimizes the residual displacements of the wall system when subjected to earthquake lateral loading by providing a restoring force (Priestley et al. 1999; Thomas and Sritharan 2004). In addition, the prestress contributes to the overturning moment resistance and transfer of shear forces at the wall bases, where the shear transfer is ensured, based on a friction mechanism. Hysteretic energy dissipation for the wall system is primarily provided by the connectors placed between the walls.

Design base shear of jointed precast wall systems may be established by using two different methods. The first approach is the traditional force-based design (FBD) method as recommended in design codes, such as the Uniform Building Code (UBC) (1997) and the International Building Code (IBC) (2000). In this approach, the design base shear is obtained from the estimated fundamental period of the structure in the elastic region and the total seismic mass, while incorporating the influence of seismic intensity in terms of a design spectral acceleration. The target lateral displacement of the building is not used in quantifying the design base shear. The second approach is the direct displacement-based design (DDBD) method, which uses a target displacement selected to ensure the expected performance of the building when establishing the design base shear. In this approach, the base shear is determined using an effective period for the fundamental mode and seismic intensity in terms of a design spectral displacement representing design-level earthquakes (Priestley 2002). By representing the expected hysteretic energy dissipation with equivalent viscous damping, the effective period is established using an effective mass for the

fundamental mode of the building, which is determined based on an assumed displacement profile for this mode. The effective period is used to determine the effective stiffness of the building. Finally, the design base shear is calculated by multiplying the equivalent target displacement and effective stiffness. A more detailed presentation of the DDBD method proposed specifically for prestressed structural systems may be found in Priestley (2002).

Using acceptance criteria defined in terms of interstory drift, residual drift, and floor acceleration, a multiple-level performance-based seismic evaluation was conducted on a FBD and DDBD solution for a five-story precast unbonded post-tensioned jointed wall system (Rahman and Sritharan 2006). This study was motivated to exploit the economical benefit of the DDBD for the design of jointed precast wall systems because the design base shear derived for the wall system using DDBD was 50% less than that obtained from the FBD method, although the jointed wall systems designed by both FBD and DDBD methods exhibited acceptable seismic performance. The economical benefit of the DDBD method for designing post-tensioned jointed wall systems is the motivation for the research of the present paper.

The objective of the study presented herein is to evaluate the seismic performance of jointed precast post-tensioned wall systems designed for low to mid-rise buildings using the DDBD approach. For practical construction constraints and in accordance with the current precast industry practice, the height of building is limited to ten stories. Consequently, the focus of this study was on five-, seven-, and ten-story jointed wall systems and their performance evaluation under multiple level earthquakes in terms of the maximum transient interstory drift, floor acceleration and residual interstory drift

## **4.2 Unbonded Post Tensioning Precast Wall Systems in Five-, Seven-, and Ten-Story Buildings**

The plan view of the three prototype precast concrete buildings is shown in Figure 4.2. A 60% scale model of the five-story building was designed, built, and tested in the PRESSS program to verify the conceptual viability of using unbonded post tensioning precast wall systems under multiple levels short-duration seismic input motions (Nakaki et al. 1999; Priestley et al. 1999; Sritharan 2002). Thus, the chosen plan view ensured manifestation of constructible precast concrete buildings.

As identified in Fig. 4.2, four jointed wall systems are used to resist lateral seismic forces in the transverse direction of each building. Each wall system is comprised of two precast walls secured to the foundation using unbonded post-tensioning bars located at the centroid axis. The walls are connected horizontally by U-shaped stainless steel flexural plates known as UFP connectors. Expected structural responses and construction details of UFP connectors may be found elsewhere (Galusha 1999; Nakaki et al. 1999; Thomas and Sritharan et al. 2007). The jointed wall systems for five-, seven- and ten-story buildings were designed by following the design methodology presented in (Aaleti 2005) for a target interstory design drift of 2% to satisfy the specifications of ITG 5.1-XX (2006), Seismology Committee (1999), and Performance-Based Seismic Engineering Ad Hoc Subcommittee (2003) of the Structural Engineers Association of California (SEAOC)). Design base shear forces for the three buildings were calculated using the DDBD method for a high seismic zone defined by the Performance-Based Seismic Engineering Ad Hoc Subcommittee (2003) of SEAOC, assuming very dense soil or rock with shear wave velocity in the range of 366 m/s to 762 m/s identified as Site Class C in IBC (2000).

Table 4.1 shows design base shear force calculated by FBD and DDBD methods. Design base shear force calculated by the FBD method (IBC 2000) for one jointed wall system in five- and ten- story buildings were 4819 kN and 7089 kN, respectively. In contrast, the DDBD method resulted in a significantly lower amount of design base shear i.e., 2409 kN and 4565 kN for the five- and ten-story buildings, respectively. It appears that the design base shear force was reduced by 50% and 36% for the five- and ten-story buildings, respectively, by choosing the DDBD method instead of the FBD method. Such substantial reduction in base shear force obtained by using DDBD method will result in an economical solution for constructing these structures.

### **4.3 Dynamic Analysis Models**

In an earlier study (Rahman and Sritharan 2006), a 2-D analysis model for a jointed precast wall system was developed for the wall system of the PRESSSS test building using the non-linear finite element computer program RAUMOKO (Carr 2003). The adequacy of the model was validated using the PRESSSS test data. Therefore, a similar procedure was

followed to establish the analysis models of the five-, seven-, and ten-story jointed wall systems.

Figure 4.3 illustrates the analytical model of the jointed wall system for the ten-story building, where each wall system was comprised of two unbonded post-tensioned precast walls. These walls were represented in the model using elastic beam-column elements positioned at the wall centerlines. The moment-rotation behavior of each unbonded post-tensioned wall was represented by a non-linear elastic rotational spring at the base of the beam-column element. Although there were fifty-three UFP connectors positioned between the two unbonded walls, their combined effect was concentrated at the floor level using ten identical non-linear inelastic shear springs along the height of the walls. These springs were connected to rigid beam-column elements extending from the centerline of each wall towards the centerline of the jointed wall system as seen in Figure 4.3. Figure 4.4 illustrates idealized non-linear elastic moment-rotation and non-linear inelastic force-displacement hysteric behavior of rotational and axial springs representing rotational and displacement resistance capacities of post-tensioned walls and UFP shear connectors, respectively. A beam-column element per floor was added to the right side of the jointed wall system model to account for the effect of the gravity columns (see Figure 4.3). Seismic mass of the building lumped at all ten floor levels was assigned to the nodes of the elements modeling the gravity columns. A similar procedure was followed to develop the analytical models for the five- and seven-story jointed wall system buildings.

Properties of various elements, used in the analytical model, were derived based on their material properties and geometric dimensions included in Table 4.2. Since each wall in the jointed system was expected to undergo negligible damage with inelastic actions concentrated at the wall base, the walls in the analytical model were represented by elastic beam-column elements with their stiffness based on their gross section properties. Each wall element was connected to the foundation using an elastic bi-linear rotational spring to model the flexural resistance of the wall at the base and the corresponding concentrated crack opening at this location. Moment-rotation behavior of the rotational springs found by analyzing the individual response of the walls under monotonic loading using the procedure recommended in (Aaleti 2005) are reported in Table 4.2. This procedure is identical to that

used for an earlier model and validated using experimental data from Rahman and Sritharan (2006).

#### **4.4 Performance-Based Seismic Evaluation**

Seismic performance of the five-, seven- and ten-story jointed wall system buildings designed using DDBD was evaluated using four levels of earthquake intensities, namely EQ-I, EQ-II, EQ-III and EQ-IV (see Fig. 4.5). These intensity levels representing different earthquake hazards were proposed by the Performance-Based Seismic Engineering Ad Hoc Subcommittee (2003) of the Structural Engineers Association of California (SEAOC), such that EQ-III represents the design-level earthquake ground motions. Whereas, EQ-IV, which is equivalent to 1.5 times EQ-III, corresponds to the maximum considered earthquakes. According to the performance-based seismic design concept presented by the SEAOC Seismology Committee (1999), ordinary buildings with conventional structural systems when subjected to ground motions compatible with EQ-I, EQ-II, EQ-III and EQ-IV may be expected to produce operational, occupiable, life safety and near collapse performances for both structural and non-structural components. The precast jointed wall systems were expected to meet the same performance levels at the minimum.

The acceptable performance of the jointed wall systems was determined by comparing the maximum values of the transient interstory drift, residual interstory drift and floor acceleration against the permissible values. The permissible values for the transient interstory drifts and residual interstory drifts were defined in accordance with the recommendations of the Seismology Committee (1999) and ITG 5.1-XX (2006), whereas the acceptable floor accelerations were defined using an IBC (2000) recommendation for the design of non-structural components. Details of the earthquake input ground motions and the permissible values of the parameters defining the building performance are presented below.

#### **4.5 Input Ground Motions**

The five-, seven-, and ten-story jointed wall system buildings were evaluated by using two sets of earthquake input motions. The first set consisted of eight long-duration scaled input motions recorded in past earthquakes, while the second set consisted of four combinations of short-duration spectrum compatible earthquake motions. The motivation for

using the second set of input motions was it followed the procedure adopted for the pseudo dynamic testing of the PRESSS building (Sritharan et al. 1999) and provided an opportunity to examine the validity of using short-duration input motions in performance-based seismic testing of structural systems.

Table 4.3 provides details of eight scaled long-duration input motions used for evaluating the performance of the jointed wall systems. The originals of these input motions were recorded at free field stations of soil profile type  $S_C$  as defined in UBC 1997. All original recorded motions were scaled as detailed in Table 4.3. Therefore, their spectra would be comparable to the target spectra following the procedure presented by Rahman and Sritharan (2007). More detailed information about these ground motions along with the depiction of the acceleration response spectra for all modified long-duration ground motions may be found in Rahman and Sritharan (2007).

Table 4.4 lists different combinations of short-duration ground motions used in the seismic evaluation of the jointed wall systems performed using each combination of records as one sequence with zero acceleration for duration of twenty-five seconds between the records. This procedure enabled the examination of the free vibration response of the jointed wall systems after subjecting them to each earthquake segment. The original motions used to create the short-duration spectrum compatible ground motions of 1.5EQ-I, EQ-II, EQ-III, EQ-IVa and EQ-IVb were recorded at stations with soil profile type  $S_C$  in the 1974 Hollister, 1971 San Fernando, 1940 Imperial Valley, 1993 Northridge and 1978 Tabas earthquakes, respectively. More descriptions of the input records and the process used for creating these short-duration input motions may be found in Sritharan et al. (1999); Sritharan et al. (2002); Rahman and Sritharan (2007).

## **4.6 Interstory Drift Limits**

To evaluate the jointed wall system performance at the four earthquake intensity levels, the following interstory drift limits were used as permissible limits maximum transient interstory drifts of 0.4% (EQ-I), 1.2% (EQ-II), 2.0% (EQ-III), and 3.0% (EQ-IV); and maximum residual interstory drifts of 0.1% (EQ-I), 0.3% (EQ-II), 0.5% (EQ-III) and 0.75% (EQ-IV). These limits were those recommended by Rahman and Sritharan (2006),

based on the guidance given by the SEAOC Blue Book (Seismology Committee 1999), ITG 5.1-XX (2006) and considering the re-centering nature of the jointed wall systems.

#### **4.7 Floor Acceleration Limits**

The permissible floor accelerations for the jointed wall system buildings were established to limit earthquake damage to non-structural elements, which may be anchored to the floors. These limits were derived by Rahman and Sritharan (2007) using the recommendations of Tong et al. (2004) and the IBC (2000) provision for estimating design forces required to anchor different types of non-structural elements to building floors under seismic conditions. A controlling parameter of these floor acceleration limits is the spectral acceleration corresponding to a short period used to define the design response acceleration spectrum (IBC 2000). Accordingly, the permissible limits of the floor accelerations are 2.60 m/s<sup>2</sup> (EQ-I), 5.77 m/s<sup>2</sup> (EQ-II), 11.79 m/s<sup>2</sup> (EQ-III), and 17.68 m/s<sup>2</sup> (EQ-IV).

#### **4.8 Analysis Results**

Figures 4.6(a), (b) and (c) depict the deflected shapes of the five-, seven-, and ten-story jointed wall systems for the long-duration earthquake motions that produced the maximum interstory drift in each intensity level. The five-story wall system shows a linear increase in floor displacement as the floor height increases for all four levels of ground motions. This trend changes to a nonlinear variation as the number of stories in the wall system increases. For example, the ten-story wall system exhibits a linear increase in lateral floor displacement with height for the EQ-I ground motion. However, this trend changes to a nonlinear shape, increasing the interstory drift with story height for EQ-II through EQ-IV ground motions. Although less pronounced, observations similar to those observed for the ten-story wall system can be seen in the response of the seven-story wall system. Two conclusions drawn from these figures are: 1) the fundamental mode of response controlled the maximum floor displacements in all three buildings and 2) the contribution of the flexural response of the walls in the jointed system increased with respect to the lateral displacement induced by the rotation at the base of walls as the number of story in the wall system increased.

As the earthquake intensity increased from EQ-I to EQ-II, from EQ-II to EQ-III, and from EQ-III to EQ-IV, displacements at all floors were amplified by 186%, 200% and 10% in the seven-story building, by 305%, 160% and 13% in the five story building, respectively (see Figs. 4.6(a) and (b)). Due to the aforementioned elevation of earthquake intensity, the ten-story building experienced the amplifications of floor displacements by 201%, 171% and 64% (see Fig. 4.6(c)). The five- and seven-story buildings experienced as much as 12-20 times higher levels of rate of increase in floor displacement, due to the elevation of ground motion from EQ-II to EQ-III compared to that as a consequence of elevation of ground motion in the range of EQ-III - EQ-IV. In contrast, the ten-story building demonstrated only 2.67 times higher level of rate of increase in floor displacement, due to elevation of ground motion from EQ-II to EQ-III compared to elevation of ground motion in the range of EQ-III - EQ-IV. It seems that abruptness of difference in floor displacement, due to increase of ground motion in the range of EQ-II to EQ-III and EQ-III to EQ-IV, depletes in buildings having higher heights like ten stories. In addition, for a common floor level in all of the three buildings, the ten-story building demonstrated lower floor displacement consistently for all four levels of ground motions EQ-I through EQ-IV.

Figure 4.7 shows correlations between average drift and the maximum interstory drift for the five-, seven-, and ten-story buildings. These correlations were established based on lateral floor displacements of the three buildings obtained by using eight long-duration ground motions. In all cases, a relationship between the maximum interstory drift and average drift can be characterized by using a linear function. Furthermore, both the average and the maximum interstory drifts are less for the ten-story wall system than the five- and seven-story wall systems. For a given value of the maximum interstory drift, the average interstory drift reduces with increasing height of the wall system. It also appears that in taller jointed wall systems, the average interstory drift of the building is less sensitive to the increase in the maximum interstory drift compared to that in a low-rise jointed wall system. The correlation between the maximum interstory drift and average drift will be helpful for designing jointed wall systems by providing a trend to obtain the maximum interstory drift for an average interstory drift.

Figures 4.8(a), (b) and (c) represent the maximum interstory drifts obtained for the five-, seven-, and ten-story jointed wall system buildings when subjected to long-duration ground motions. In each case, the building interstory drifts were less than the acceptable limits for all four levels of earthquakes. Furthermore, it was found that as the building height increased, the ratio between the maximum transient drift to the acceptable limit generally decreased. These observations suggest that a) the design base shear established for the low to mid-rise jointed wall systems buildings based on DDBD is adequate and b) further reduction to the design base shear is possible for the mid-rise buildings.

The differences in the maximum transient interstory drifts obtained between buildings for the same event were more pronounced at large earthquake intensities. For the design level ground motions (i.e., for EQ-III events), the five-story building produced the maximum transient interstory drift in the range of 0.74 – 1.7%, whereas, the ten-story building exhibited the maximum transient interstory drift in the range of 0.37 – 0.85%. These drift ratios indicate the five-story jointed wall system building experienced about twice the maximum transient drifts experienced by the ten-story building. At EQ-IV events, the corresponding ranges for the maximum transient drifts were 1.85 – 2.27% and 0.62 – 0.76%, respectively, exhibiting a factor of almost three between the two building responses. However, for EQ-I and EQ-II input motions, the ten-story building experienced the maximum transient interstory drifts of 0.11% and 0.34%, which compared 0.12% and 0.65% for the five-story jointed wall system building.

Table 4.5 presents the maximum residual interstory drifts achieved by all three jointed wall system buildings. The re-centering capability provided by unbonded post-tensioning enabled the buildings to produce an insignificant amount of residual interstory drifts after subjecting to earthquakes of all intensities.

Figures 4.9(a), (b), and (c) depict the maximum floor accelerations obtained for the five-, seven-, and ten-story jointed wall system buildings when subjected to the long-duration ground motions. The maximum floor accelerations obtained for the five-story building were within the permissible limits, ensuring safety of nonstructural components of the building at all four levels of earthquakes. For the seven-story building, the floor acceleration limits satisfied for all ground motions except for IM-c and IM-a. A similar trend was observed for

the ten-story building with an additional violation of the acceptable limit for the IM-h ground motion representing an EQ-IV event. These observations, which suggest that taller jointed wall systems designed based on DDBD procedure, have a higher tendency to violate the acceptable limits of floor accelerations, are consistent with an earlier finding that the design base shear obtained for the seven- and ten-story building could be reduced so that they can produce larger transient drifts and smaller floor accelerations.

Due to the design level ground motions of earthquake level EQ-III, the five-story building showed the maximum floor acceleration in the range of  $8.50 \text{ m/s}^2$ -  $9.76 \text{ m/s}^2$ , whereas the ten-story building exhibited the maximum floor acceleration in the range of  $10.56 \text{ m/s}^2$ -  $17.06 \text{ m/s}^2$ . Thus, the moderately high building, comprised of ten stories, experienced as much as 74.80% and as low as 24.23% of the higher value of the maximum floor acceleration compared to the low rise building, comprised of five stories, under design level ground motions. However, for EQ-I, EQ-II and EQ-IV, the moderately high-rise (ten-story) building showed the maximum floor acceleration of  $2.85 \text{ m/s}^2$ ,  $5.31 \text{ m/s}^2$  and  $15.36 \text{ m/s}^2$  -  $19.87 \text{ m/s}^2$  and the low rise (five-story) building demonstrated the maximum floor acceleration of  $2.03 \text{ m/s}^2$ ,  $4.56 \text{ m/s}^2$  and  $13.67 \text{ m/s}^2$  -  $15.10 \text{ m/s}^2$ , respectively. It shows that the moderately high building exhibited 40.40%, 16.45% and 12.36% - 31.60% higher level of the maximum floor acceleration compared to the low rise building when subjected to long-duration ground motions of earthquake levels EQ-I, EQ-II and EQ-IV. In addition, the dependency of the building responses on frequency contents of the input earthquake was also emphasized by the analyses results. For example, at EQ-III level, the difference in responses of the ten and five story buildings for the maximum floor acceleration subjected by IM-c was 82.26%, whereas the corresponding difference was only 24.23% for IM-d, although both of these ground motions were chosen to represent EQ-III level ground motions.

Traditionally, short duration ground motions are used in experimental research. Therefore, the present study also investigated the performance of the jointed wall system buildings under short-duration spectrum compatible ground motions representing EQ-I to EQ-IV events. Figures 4.10(a), (b), and (c) depict the maximum transient interstory drift of the five-, seven- and ten-story jointed wall system buildings when subjected to the four

combinations of short-duration ground motions. All three buildings showed satisfactory performance in terms of the maximum transient interstory drift with sufficient margin of safety with respect to their permissible limits. Short-duration ground motions from combination-2 were chosen to compare the transient interstory drift and floor acceleration performance of the buildings under short- and long-duration ground motions. Generally, short-duration ground motions resulted in lower values of the maximum transient interstory drift compared to long duration motions for all of the three buildings except for the EQ-I level short-duration ground motion in the seven- and five-story buildings where both short and long-duration ground motions created identical transient interstory drift. The largest differences between the maximum transient interstory drift due to long and short-duration motions were 116.77%, 173.31% and 2.62% for the ten story building; 48.79%, 91.71% and 135.89% for the seven story building; 129.80%, 48.47% and 39.65% for the five story building when subjected to EQ-II, EQ-III and EQ-IV level ground motions, respectively. This shows the difference was increased consistently with taller buildings for design level ground motion.

Figures 4.11(a), (b) and (c) show the maximum floor accelerations resulted from for the five-, seven-, and ten-story jointed wall system buildings under the short-duration ground motions. The floor accelerations obtained for all three buildings were satisfactory. Comparing Figs. 4.11(a), (b), and (c) with Figs. 4.9(a), (b), and (c) revealed that long-duration ground motions resulted in higher floor accelerations than the short-duration ground motions. The largest differences in the maximum floor accelerations obtained between the long and short-duration ground motions were 43.5%, 22.4%, 274% and 40.5% for the ten story building; 13.4%, 40.7% and 166.3% and 22% for the seven story building; 35.6%, 59.7%, 215.2% and 27.7% for the five story building when subjected by EQ-I, EQ-II, EQ-III and EQ-IV level ground motions, respectively, with the largest different being for the EQ-III level earthquakes. Therefore, it appears that subjecting the building to realistic long-duration motions are necessary to obtain the maximum transient interstory drifts and floor accelerations, and use of short-duration ground motions may underestimate these parameters sometimes by a significant amount.

Figures 4.12 shows the maximum transient interstory drift at four levels of long-duration ground motions normalized by the respective allowable limits of interstory drift, in the five-, seven-, and ten story buildings. The largest achievement in transient interstory drifts were 30%, 54%, 85% and 76% of the associated acceptable limit for the five story building when subjected by EQ-I, EQ-II, EQ-III and EQ-IV level ground motions, respectively. These achievements were 34%, 34%, 59% and 77% for the seven story building, and 27%, 29%, 43% and 25% for the ten-story building. Figure 4.13 represents the maximum floor acceleration at four levels of long-duration ground motions, normalized by the respective allowable limits of floor acceleration, in the three buildings. The largest attainment in floor acceleration were recorded as 78%, 79%, 83% and 85% of the associated acceptable limit for the five story building when subjected by EQ-I, EQ-II, EQ-III and EQ-IV level ground motions, respectively. However, the achievements in floor acceleration were 129%, 91%, 90% - 112% and 80% - 99% for the seven-story building, and 110%, 92%, 90% - 145% and 87% - 112% for the ten-story building.

To ensure protection against damage to nonstructural elements in jointed wall system buildings, keeping the floor acceleration within the acceptable limit is essential. To address this issue, the highest level of violation of the maximum floor acceleration limit, observed in the ten-story building, was chosen to resolve by decreasing the moment of inertia of the walls through decreasing the thickness of the walls resulting in a more flexible structure. Figures 4.14 and 4.15 show the maximum floor acceleration was consistently reduced, due to the reduction of moment of inertia of the walls in the ten story building when subjected to ground motions IM-h and IM-c. Figure 4.14 shows that reduction in moment of inertia of walls by 10% helped the building to achieve the maximum floor acceleration lower than the acceptable limit under ground motion IM-h. Similarly, for IM-c, reduction of moment of inertia of walls by 40% led the building to satisfy acceptable limits of floor acceleration (see Fig. 4.15). The maximum transient interstory drifts and residual interstory drifts were also within the acceptable limits after the aforementioned modification of the walls.

## 4.9 Conclusions

Seismic performances of low- to mid-rise post-tensioned jointed wall system buildings designed by the direct displacement-based design approach were analytically investigated in this paper. Using a validated analytical modeling procedure, the five, seven and ten-story post-tensioned jointed wall system buildings with an identical plan view were subjected to long and short-duration earthquake input motions having an acceleration response spectra representative of four levels of earthquake intensities. Using the analysis results the following conclusions were drawn:

1. All three jointed wall systems designed for low- to mid-rise buildings deflected predominantly by the fundamental mode. For a common floor level, the taller building exhibited less floor displacement compared to low-rise building.
2. The sensitivity of the average drift to the increase of the maximum interstory drift was reduced in jointed wall systems as the number of stories in the building increased. For a given value of the maximum transient interstory drift, the taller building exhibited a lower average drift.
3. Irrespective of the height, all three buildings demonstrated satisfactory performance in terms of the maximum transient interstory drift, when subjected to both short- and long-duration ground motions representing the four levels of earthquake intensities.
4. The maximum transient interstory drift was reduced for taller buildings. The difference in capacity to resist interstory drift between the tallest (ten-story) and smallest (five-story) buildings increased with the elevation of intensity of ground motions.
5. The re-centering capacity of the unbonded post-tensioning bars enabled the buildings to produce negligible amount of residual interstory drifts after subjecting them to both the long- and short-duration ground motions.
6. For all long-duration ground motions, the five-story building showed lower values of the maximum floor accelerations compared to the respective acceptable limits for four levels of earthquakes. But, the seven and ten-story buildings violated the limits for few ground motions. Generally, the values of the maximum floor acceleration increased for taller buildings.

7. Short-duration ground motions generated smaller values of the maximum transient interstory drift and floor accelerations compared to long-duration ground motions. It appears necessary to use actual-long duration ground motions for analyzing the real full scale buildings to avoid the possibility of under estimating transient interstory drift and floor acceleration.
8. For short-duration ground motions, all three buildings performed satisfactorily in terms of allowable floor acceleration.
9. Low-rise building tends to achieve the maximum transient interstory drifts closer to the acceptable limits compared to the taller building. The Taller building has a stronger tendency to approach and exceed unity of normalized floor acceleration compared to the low-rise building.
10. By making necessary modifications in the precast wall dimensions of jointed wall system as recommended in this paper, the maximum floor acceleration of taller buildings may be brought to an acceptable limit.
11. Based on the satisfactory performance of the jointed wall systems designed by direct displacement-based design that led to lower base shear (Rahman and Sritharan 2006; Rahman and Sritharan 2007), it appears this design method would result in a more economical design than the traditional force-based design method.

#### **4.10 Acknowledgments**

The study reported in this paper was conducted as part of a 2005-06 Daniel P. Jenny Fellowship provided by the Precast/Prestressed Concrete Institute (PCI). Dr. Ned Cleland, Dr. S. K. Ghosh, and Ms. Suzanne Nakaki serve as the PCI advisors for this fellowship award. Authors also acknowledge the support of Professor Eduardo Miranda, Department of Civil and Environmental Engineering, Stanford University, California, USA, for providing some of the ground motion data, while most of the remaining ground motion data were downloaded from the website of the Pacific Earthquake Research Center, USA.

## 4.11 References

- Aaleti, S., 2005. Design and analysis of unbonded post-tensioned precast wall systems, M.S. Thesis, Department of Civil, Construction and Environmental Engineering, Iowa State University, Ames, Iowa, USA.
- Carr, A. J., 2003. *RUAUMOKO - Inelastic Dynamic Analysis Program*. University of Canterbury, Christchurch, New Zealand.
- Conley, J., Sritharan, S., and Priestley, M. J. N., 2002. Precast Seismic Structural Systems PRESSS-3: The Five-Story Precast Test Building, Vol. 3-1: Wall Direction Response, Report Number: SSRP-99/19, University of California, San Diego, California, USA.
- Galusha, J. G., 1999. Precast, Post-tensioned Concrete Walls Designed to Rock, M.S. Thesis, Department of Civil Engineering, University of Washington, Seattle, Washington, USA.
- International Building Code (IBC), 2000. *International Code Council*, Virginia, USA, 331-377.
- ITG 5.1-XX, 2006. Acceptance criteria for special unbonded post-tensioned structural walls based on validation testing, *American Concrete Institute*.
- Kurama, Y., Sause, R., Pessiki, S., and Lu, L., 2002. Seismic response evaluation of unbonded post-tensioned precast walls, *ACI Structural Journal*, September-October, **99 (5)**, 641-651.
- Kurama, Y., Pessiki, S., Sause, R., and Lu, L., 1999a. Lateral load behavior and seismic design of unbonded post-tensioned precast concrete walls, *ACI Structural Journal*, July-August, **96 (4)**, 622-632.
- Kurama, Y., Pessiki, S., Sause, R., and Lu, L., 1999b. Seismic behavior and design of unbonded post-tensioned precast concrete walls, *PCI Journal*, May-June, **44 (3)**, 72-88.
- Nakaki, S. D., Stanton, J. F., and Sritharan, S., 1999. An overview of the PRESSS five-story precast test building, *PCI Journal*, **44(2)**, 26-39.

- Performance-Based Seismic Engineering Ad Hoc Subcommittee, 2003. Revised Interim Guidelines: Performance-Based Seismic Engineering for the SEAOC Blue Book, Structural Engineers Association of California, California, USA, 128-132.
- Priestley, M. J. N., 2002. Direct displacement-based design of precast/prestressed concrete buildings, *PCI Journal*, **47 (6)**, 67-79.
- Priestley, M. J. N., Sritharan, S., Conley, J., R., and Pampanin, S., 1999. Preliminary results and conclusions from the PRESSSS five-story precast concrete test building, *PCI Journal*, **44 (6)**, 42-67.
- Priestley, M. J. N., Tao, J. R., 1993. Seismic response of prestressed concrete frames with partially debonded tendons, *PCI Journal*, Jan-Feb.
- Rahman, M., A., and Sritharan, S., 2007, A performance-based seismic evaluation of two five-story precast concrete hybrid frame buildings, accepted in *ASCE Structural Journal*, Vol. 133, No. 11, 2007, p. 1489-1500.
- Rahman, M., A., and Sritharan, S., 2006, An evaluation of force-based design vs. direct displacement-based design of jointed precast post-tensioned wall systems, *Earthquake Engineering and Engineering Vibration* **5(2)**, 285-296.
- Seismology Committee, 1999. Recommended Lateral Force Requirements and Commentary (Blue Book). Structural Engineers Association of California (SEAOC), California, USA, 327-421.
- Sritharan, S., 2002. Performance of four jointed precast frame systems under simulated seismic loading, *Proceedings of the Seventh National Conference on Earthquake Engineering*, Paper No. 264, Boston, USA.
- Sritharan, S., Pampanin, S., and Conley, J., 2002. Design Verification, Instrumentation and Test Procedures, PRESSSS-3: The Five-Story Precast Test Building, Vol. 3-3. ISU-ERI-Ames Report ERI-03325, Iowa State University, Ames, Iowa, USA.
- Thomas, D., J., and Sritharan, S., 2004. An Evaluation of Seismic Design Guidelines Proposed for Precast Jointed Wall Systems, ISU-ERI-Ames Report ERI-04635, Iowa State University, Ames, Iowa, USA, June.

- Thomas, D., J., 2003. Analysis and Validation of a Seismic Design Method Proposed for Precast Jointed Wall Systems, M.Sc. Thesis, Department of Civil, Construction and Environmental Engineering, Iowa State University, Ames, Iowa, USA.
- Tong, M., Lee, G., Rzhovsky, V., Qi, J., and Shinozuka, M., 2004. A comparison of seismic risk of non-structural systems in a hospital before and after a major structural retrofit, *ATC-29-2 Seminar on Seismic Design, Retrofit, and Performance of Non-structural Components in Critical Situations*, <<http://shingo8.eng.uci.edu/ATC-29-2.htm>, date-11-17-2004>
- Uniform Building Code (UBC), 1997. *International Conference of Building Officials*, Whittier, California, USA, **2**, 13-38.

Table 4.1 Design base shear force calculated by force-based and direct displacement-based methods for low and mid-rise buildings

| Story of Buildings | Force-based Design Method (kN) | Direct Displacement-based Design Method (kN) |
|--------------------|--------------------------------|--|
| Five-story         | 4819                           | 2384   |
| Ten-story          | 7089                           | 4565   |

Table 4.2 Dimensions of the jointed wall systems and the properties of the analytical models shown in Fig. 4.3 for the five-, seven-, and ten-story buildings

| Parameter   | Value                           |                                  |                                  |
|---|---------------------------------|----------------------------------|----------------------------------|
|   | Five-story                      | Seven-story                      | Ten-story                        |
| Wall height   | 19.05 m                         | 26.67 m                          | 38.01 m                          |
| Wall length   | 4.57 m                          | 4.57 m                           | 6.10 m                           |
| Wall thickness  | 337 mm                          | 381mm                            | 381mm                            |
| Initial post-tensioning force   | 1530 kN                         | 2892.54 kN                       | 9096.04 kN                       |
| Area of post-tensioning tendons   | 3838.70 mm <sup>2</sup>         | 5483.86 mm <sup>2</sup>          | 15903.20 mm <sup>2</sup>         |
| Yield strength of post-tensioning tendons                                       | 827.40 MPa                      | 827.40 MPa                       | 827.40 MPa                       |
| Elastic modulus of post-tensioning tendons                                      | 200 GPa                         | 200 GPa                          | 200 GPa                          |
| Wall concrete strength  | 41.37 MPa                       | 41.37 MPa                        | 41.37 MPa                        |
| <b><i>Properties of spring modeling moment resistance of a wall at base</i></b> |                                 |                                  |                                  |
| Yield moment  | 80.50 x 10 <sup>2</sup> kN-m    | 129.67 x 10 <sup>2</sup> kN-m    | 378.22 x 10 <sup>2</sup> kN-m    |
| Elastic rotational stiffness  | 6.85 x 10 <sup>6</sup> kN-m/rad | 11.12 x 10 <sup>6</sup> kN-m/rad | 35.93 x 10 <sup>6</sup> kN-m/rad |
| Hardening ratio   | 0.0200                          | 0.0012                           | 0.0095                           |
| <b><i>Properties of spring modeling UFPs at each floor level</i></b>            |                                 |                                  |                                  |
| Yield strength  | 464.55 kN                       | 448.29 kN                        | 615.54 kN                        |
| Elastic stiffness   | 39.42 kN/mm                     | 38.04 kN/mm                      | 52.24 kN/mm                      |
| Hardening ratio   | 0.035                           | 0.035                            | 0.035                            |

Table 4.3 List of long-duration ground motions selected for the performance-based evaluation of the ten-, seven-, and five-story precast jointed wall system buildings

| Identification of the Input Motion | Earthquake Intensity | Earthquake Name (Year) | Magnitude     | Scale Factor | PGA after multiplying by the Scale Factor (g) |
|------------------------------------|----------------------|------------------------|---------------|--------------|---|
| IM-a                               | EQ-I                 | Morgan Hill (1984)     | 6.1 ( $M_s$ ) | 0.65         | 0.19  |
| IM-b                               | EQ-II                | Loma Prieta (1989)     | 7.1 ( $M_s$ ) | 0.64         | 0.32  |
| IM-c                               | EQ-III               | Northridge (1994)      | 6.8 ( $M_s$ ) | 1.30         | 0.67  |
| IM-d                               | EQ-III               | Imperial valley (1940) | 7.2 ( $M_s$ ) | 1.50         | 0.48  |
| IM-e                               | EQ-III               | Kobe-Japan (1995)      | 6.9 ( $M_w$ ) | 1.10         | 0.66  |
| IM-f                               | EQ-IV                | Tabas-Iran (1978)      | 7.4 ( $M_s$ ) | 1.00         | 0.93  |
| IM-g                               | EQ-IV                | Chi-Chi-Taiwan (1999)  | 7.6 ( $M_s$ ) | 0.95         | 0.86  |
| IM-h                               | EQ-IV                | Kobe-Japan (1995)      | 6.9 ( $M_w$ ) | 1.18         | 0.97  |

PGA = Peak Ground Acceleration,  $M_s$  = Surface Wave Magnitude,  $M_w$  = Moment Magnitude

Table 4.4 List of combinations of short-duration ground motions used for the performance-based evaluation of the ten-, seven-, and five-story precast jointed wall system buildings

| Identification of Combinations | Earthquake Intensity |                     |                      |                     |
|--------------------------------|----------------------|---------------------|----------------------|---------------------|
|                                | Earthquake Level-I   | Earthquake Level-II | Earthquake Level-III | Earthquake Level-IV |
| Combination-1                  | EQ-I                 | EQ-II               | EQ-III               | EQ-IVa              |
| Combination-2                  | EQ-I                 | EQ-II               | EQ-III               | EQ-IVb              |
| Combination-3                  | 0.22EQ-III           | (-) 0.50EQ-III      | EQ-III               | (-) 1.5EQ-III       |
| Combination-4                  | 0.15EQ-IVb           | (-) 0.33EQ-IVb      | 0.67EQ-IVb           | EQ-IVb              |

Table 4.5 Maximum residual interstory drift of the seven- and ten-story buildings under long-duration motions

| Identification of the Input Motion | Earthquake Intensity | Maximum residual interstory drift (%) |             | Acceptable residual interstory drift (%) |
|------------------------------------|----------------------|---------------------------------------|-------------|--|
|                                    |                      | Ten story                             | Seven story |  |
| IM-a                               | EQ-I                 | 0.0113                                | 0.0051      | 0.10                                     |
| IM-b                               | EQ-II                | 0.0156                                | 0.0083      | 0.30                                     |
| IM-c                               | EQ-III               | 0.0049                                | 0.0093      | 0.50                                     |
| IM-d                               | EQ-III               | 0.0236                                | 0.0438      | 0.50                                     |
| IM-e                               | EQ-III               | 0.0205                                | 0.0197      | 0.50                                     |
| IM-f                               | EQ-IV                | 0.0237                                | 0.0089      | 0.75                                     |
| IM-g                               | EQ-IV                | 0.0044                                | 0.0016      | 0.75                                     |
| IM-h                               | EQ-IV                | 0.0095                                | 0.0021      | 0.75                                     |

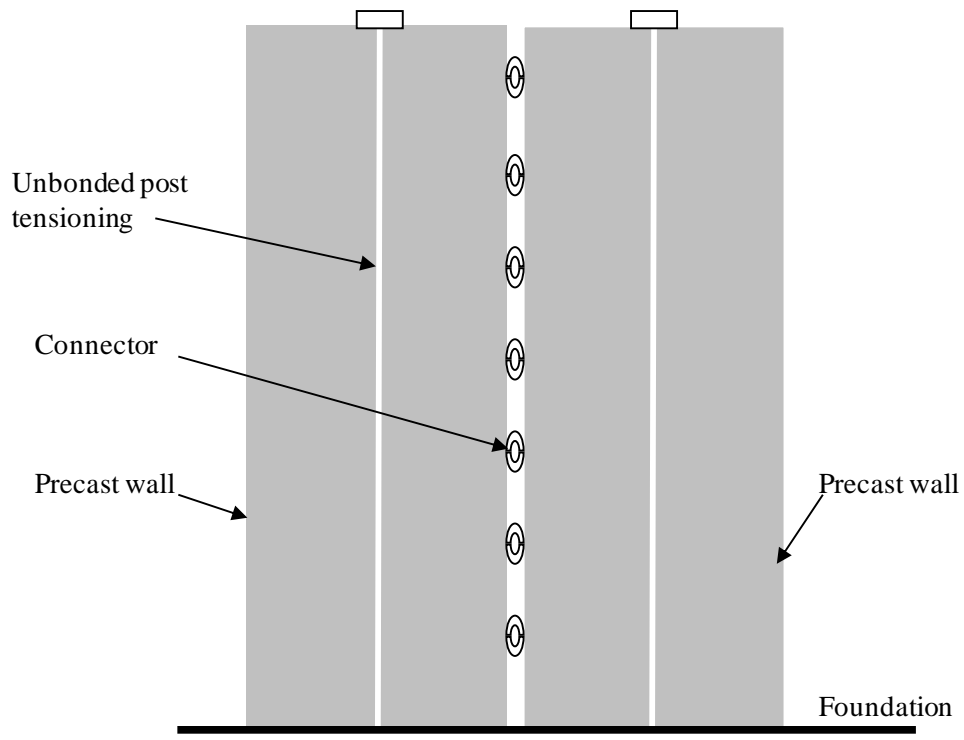


Figure 4.1 Illustration of a unbonded precast post tensioned jointed wall system

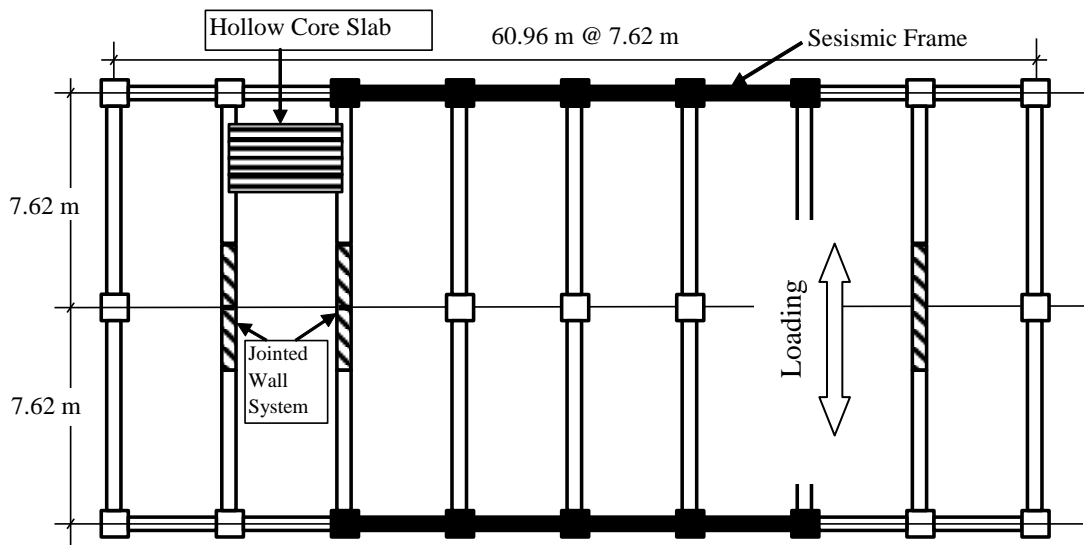


Figure 4.2 Plan view for the five-, seven-, and ten-story prototype buildings

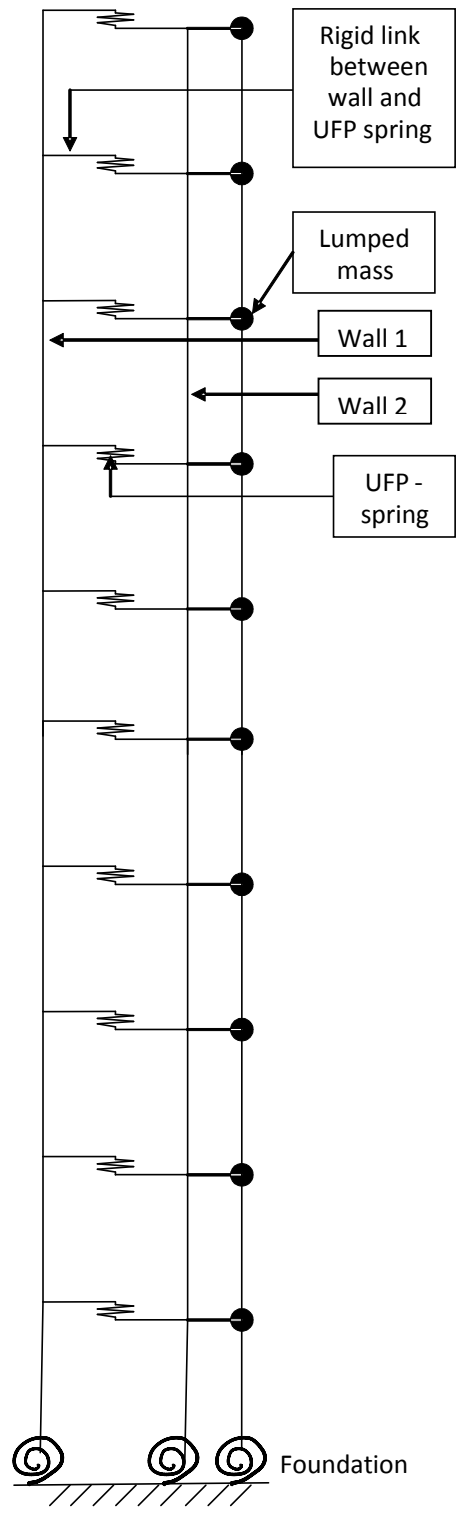


Figure 4.3 Analytical model of the wall system in the ten-story building

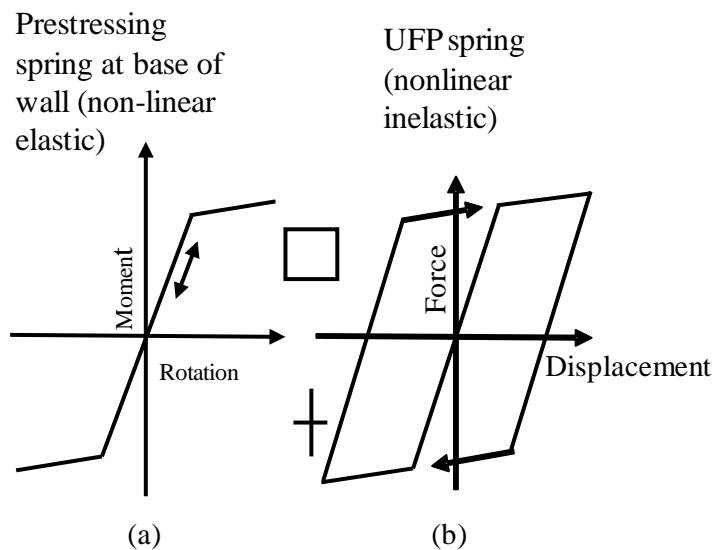


Figure 4.4 Illustration of typical moment-rotation response of post-tensioning spring located at each wall base and force-displacement response of UFP spring placed between two walls

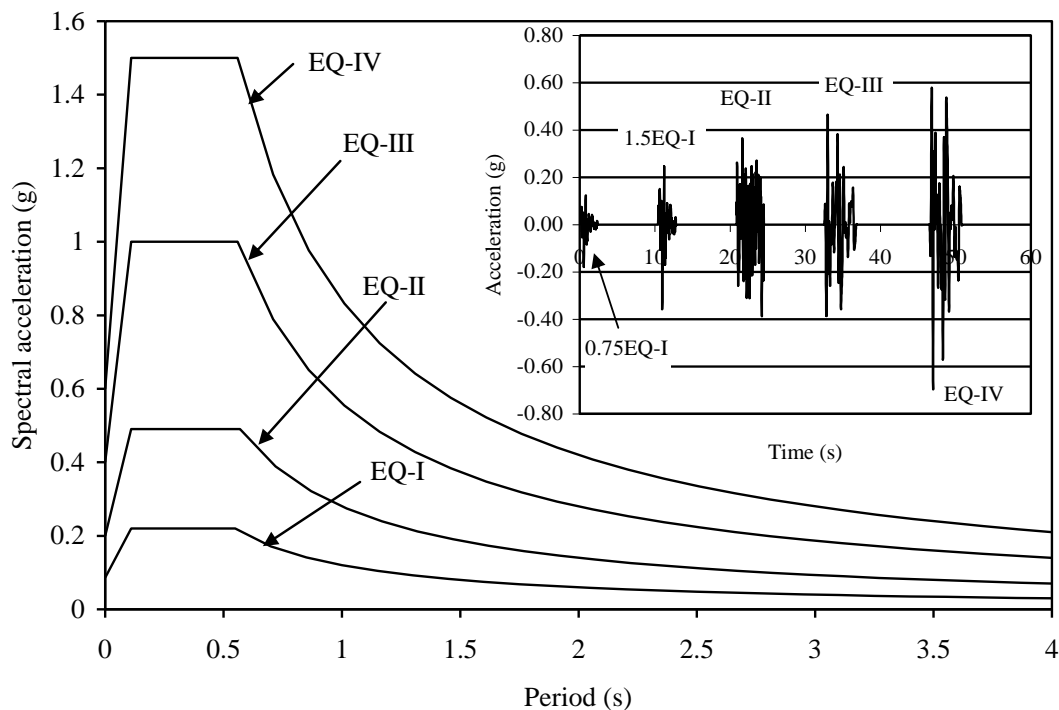


Figure 4.5 The 5% damped multiple-level acceleration response spectra suggested for soil type Sc in high seismic zone as per the Performance-Based Seismic Engineering Ad Hoc Subcommittee (2003) of SEAOC. (The insert in the figure shows short-duration earthquake ground motions.)

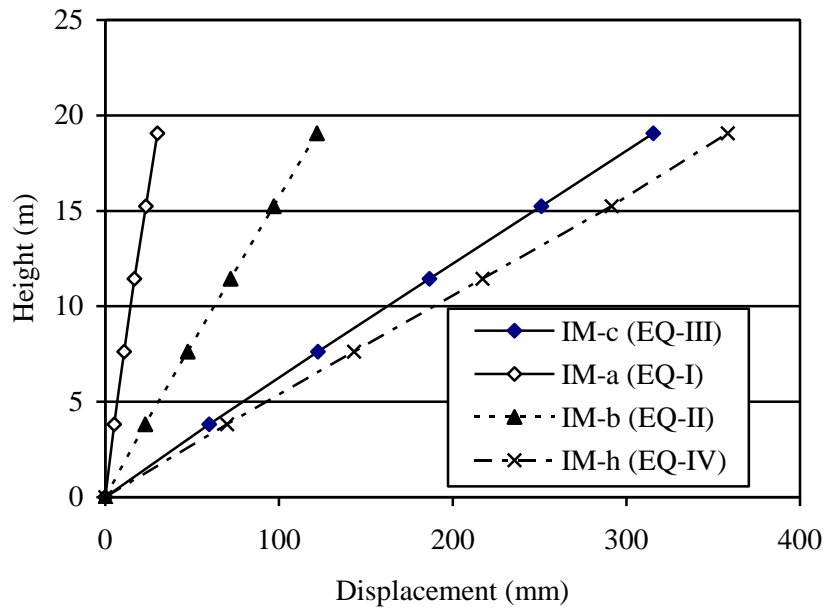


Figure 4.6 (a) Deflected shape of the five-story building when achieving at the maximum interstory drifts imposed by the four levels of ground motions

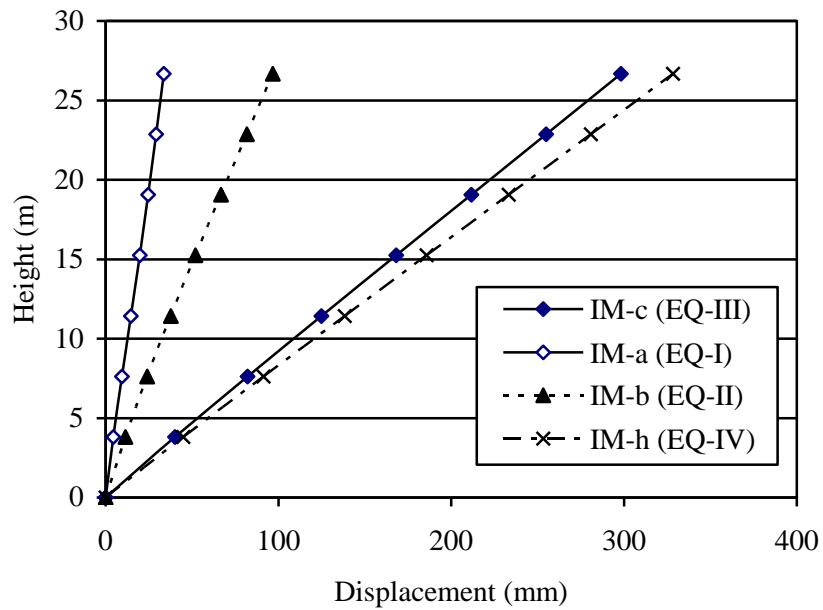


Figure 4.6 (b) Deflected shape of the seven-story building when achieving at the maximum interstory drifts imposed by the four levels of ground motions

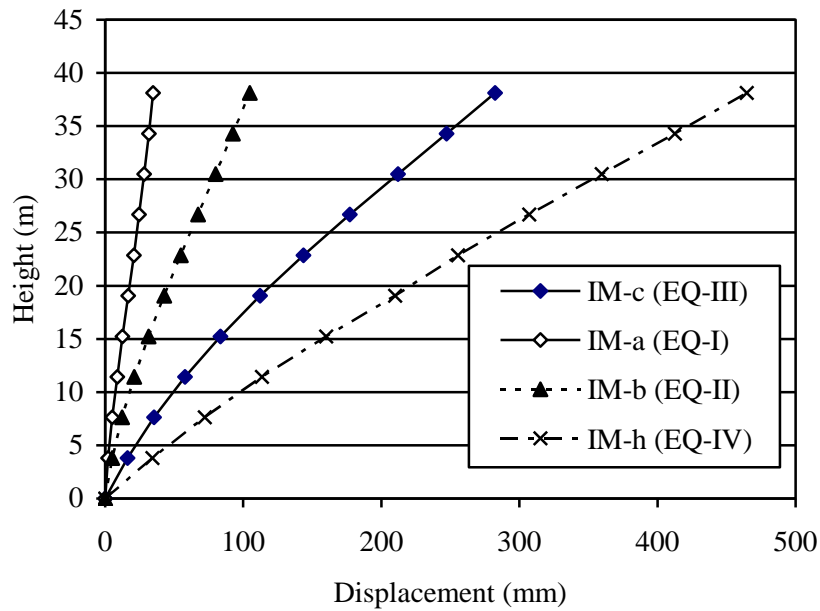


Figure 4.6 (c) Deflected shape of the ten-story building when achieving at the maximum interstory drifts imposed by the four levels of ground motions

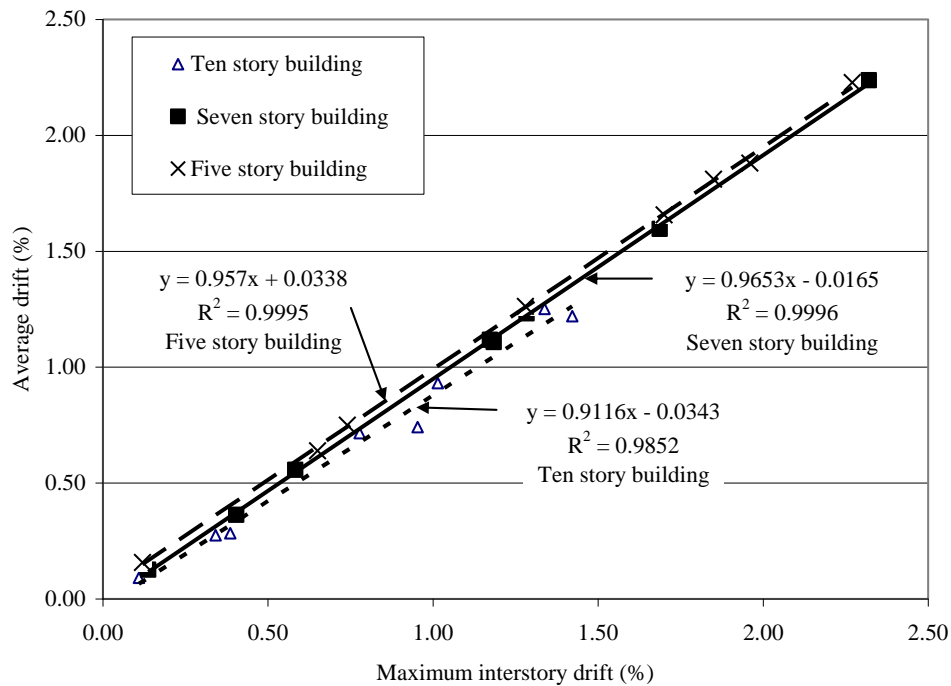


Figure 4.7 Correlation between the average and maximum interstory drifts obtained for the five-, seven-, and ten-story post-tensioned jointed wall system based on the responses to long-duration ground motions

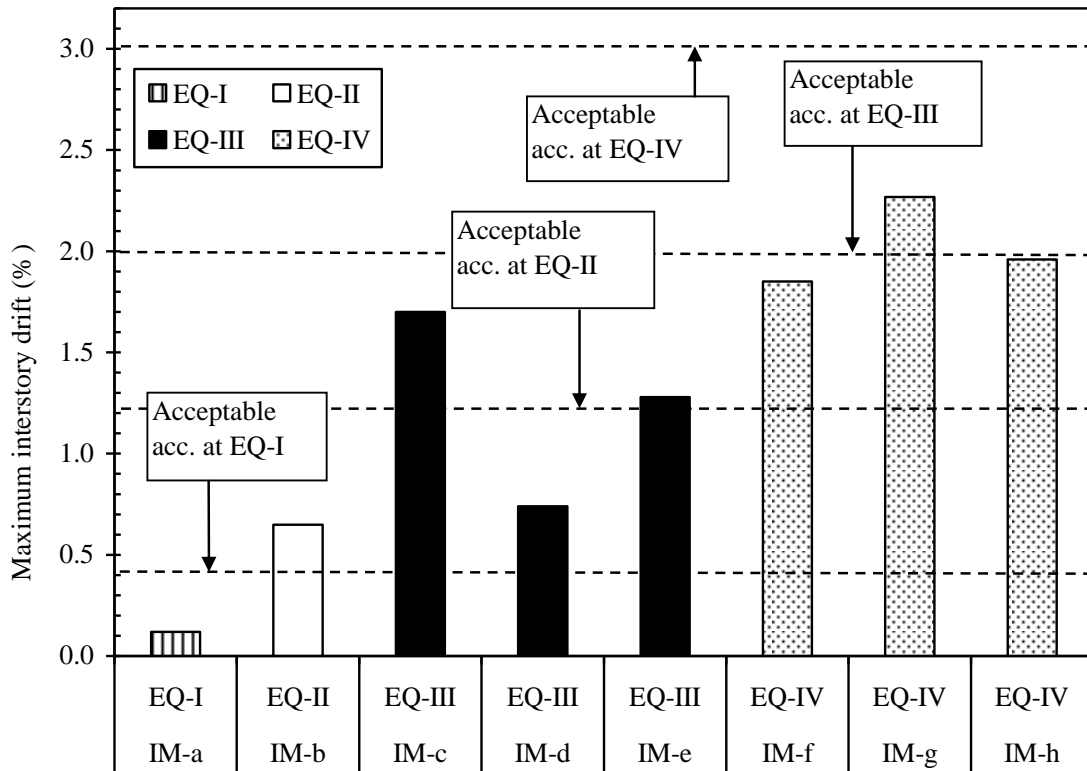


Figure 4.8 (a) Maximum transient interstory drift obtained for the five-story jointed wall system building subjected to the long-duration ground motions

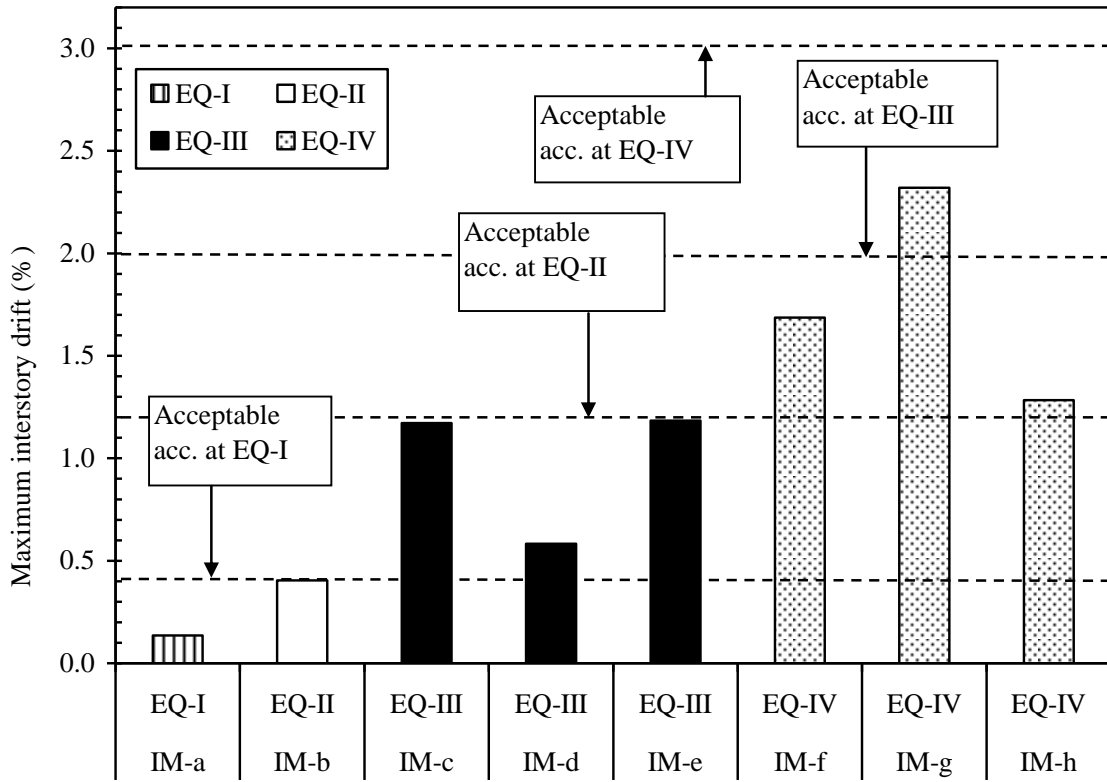


Figure 4.8 (b) Maximum transient interstory drift obtained for the seven-story jointed wall system building subjected to the long-duration ground motions

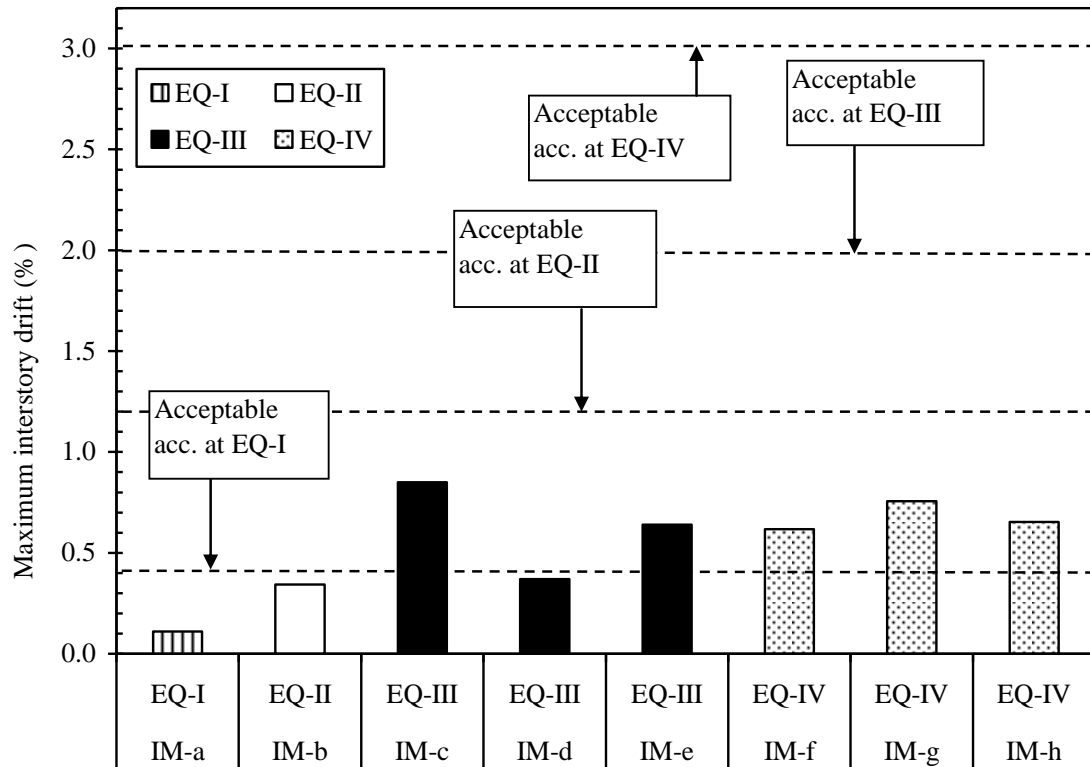


Figure 4.8 (c) transient interstory drift obtained for the ten stories jointed wall system building subjected to long-duration ground motions

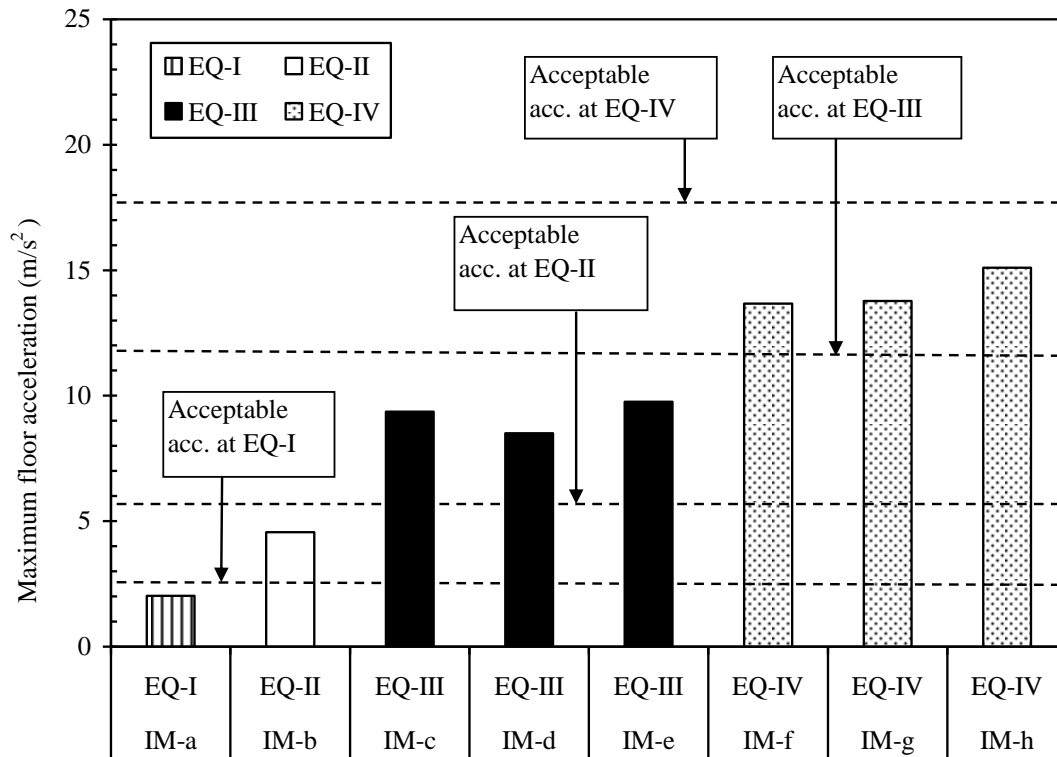


Figure 4.9 (a) Maximum floor acceleration obtained for the five-story jointed wall system building subjected to the long-duration ground motions

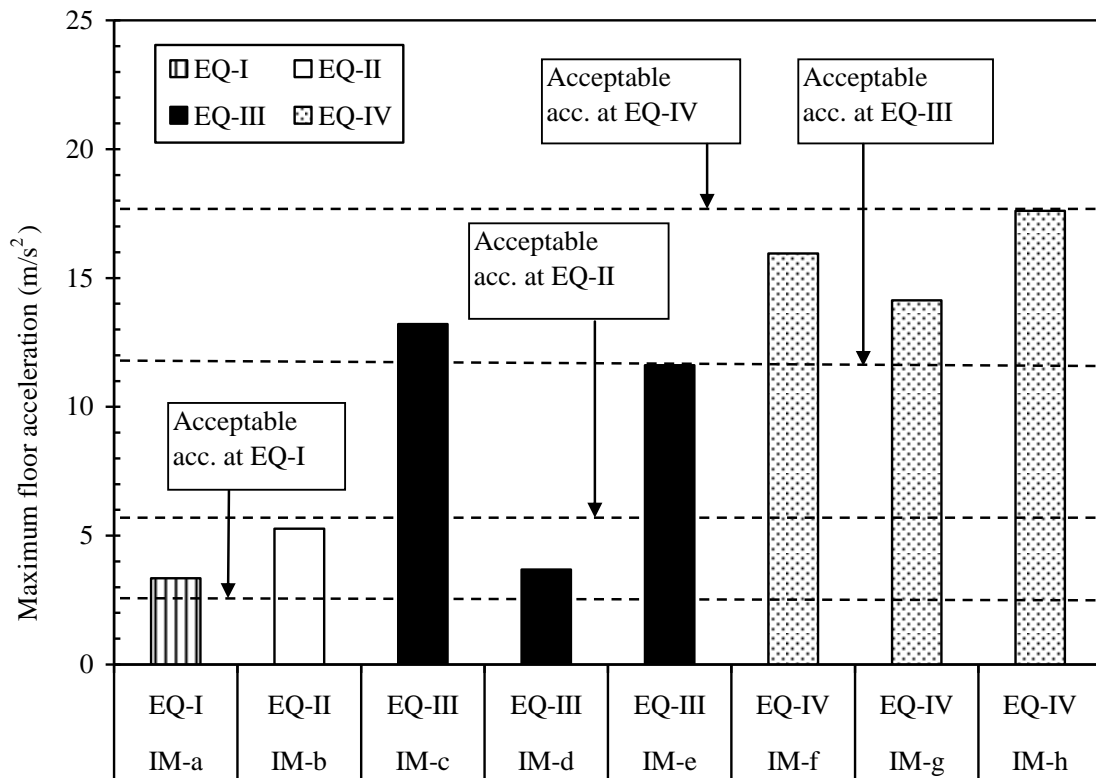


Figure 4.9 (b) Maximum floor acceleration obtained for the seven-story jointed wall system building subjected to the long-duration ground motions

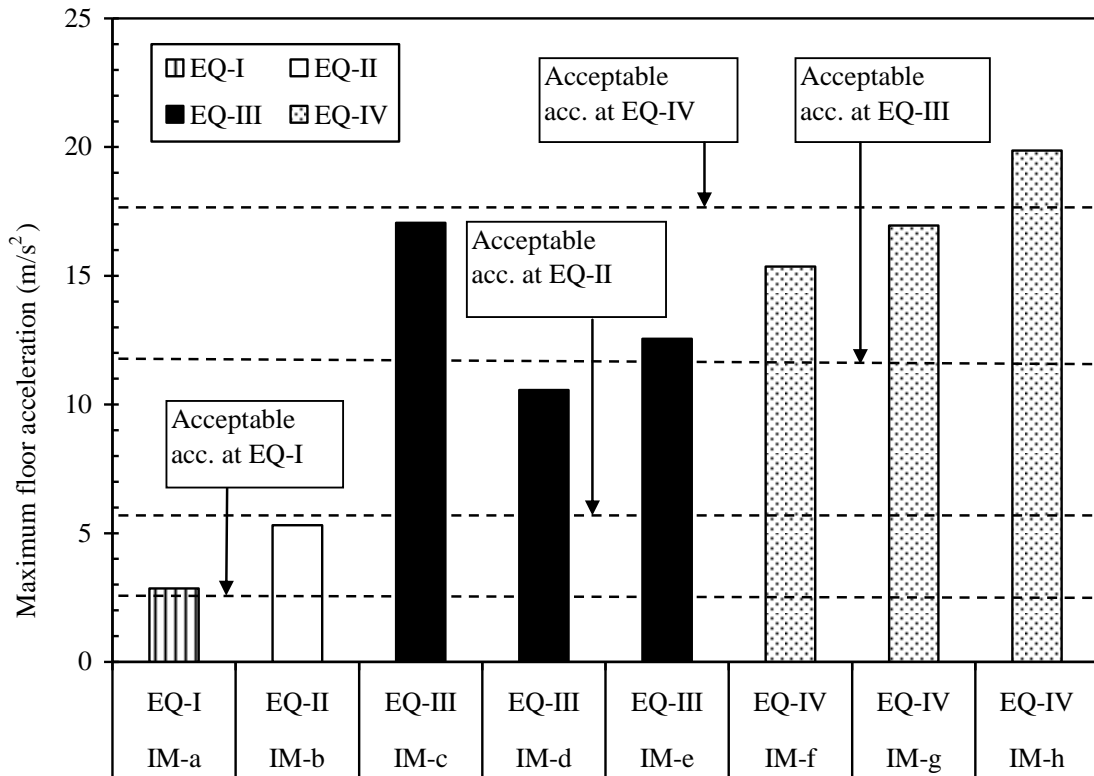


Figure 4.9 (c) Maximum floor acceleration obtained for the ten-story jointed wall system building subjected to the long-duration ground motions

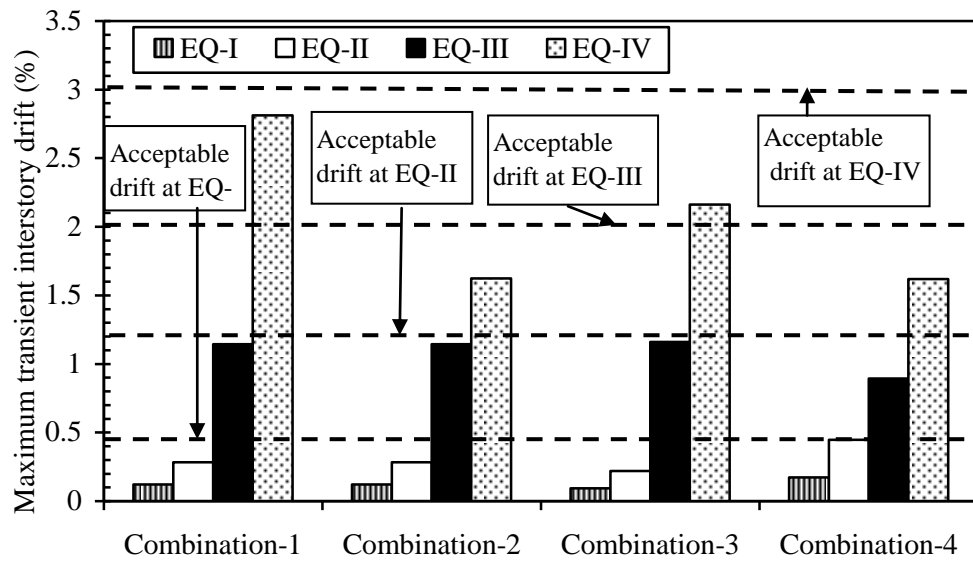


Figure 4.10 (a) Maximum transient interstory drift obtained for the five-story building when subjected to short-duration ground motions

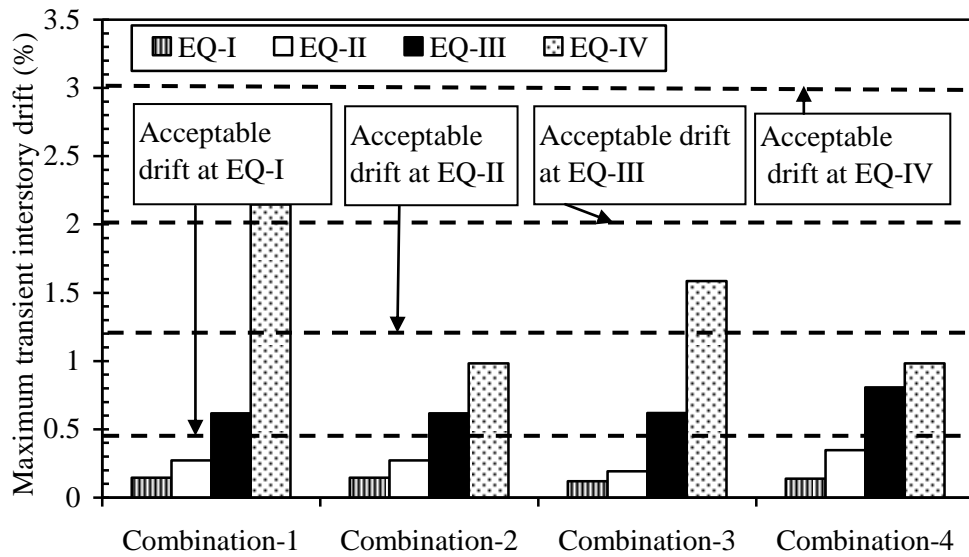


Figure 4.10 (b) Maximum transient interstory drift obtained for the seven-story building when subjected to short-duration ground motions

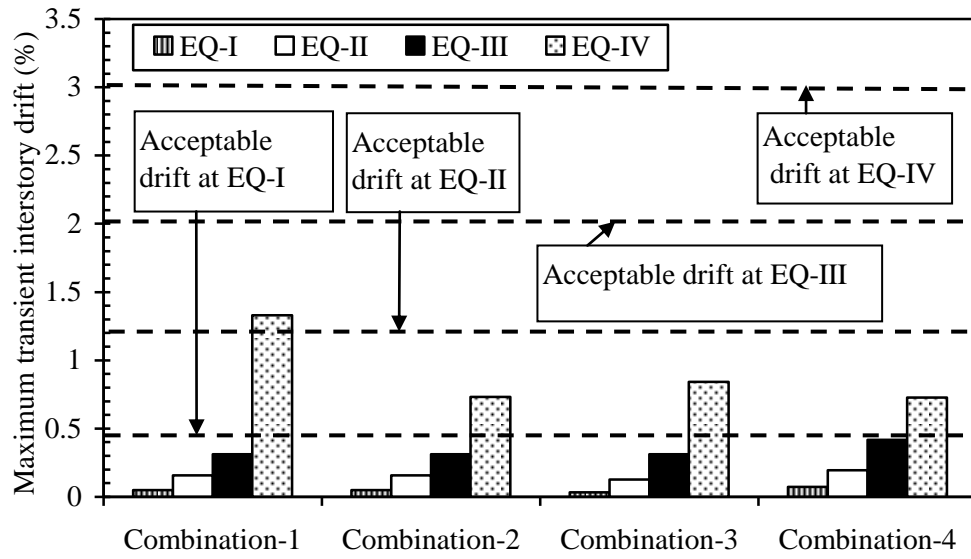


Figure 4.10 (c) Maximum transient interstory drift obtained for the ten-story building when subjected to short-duration ground motions

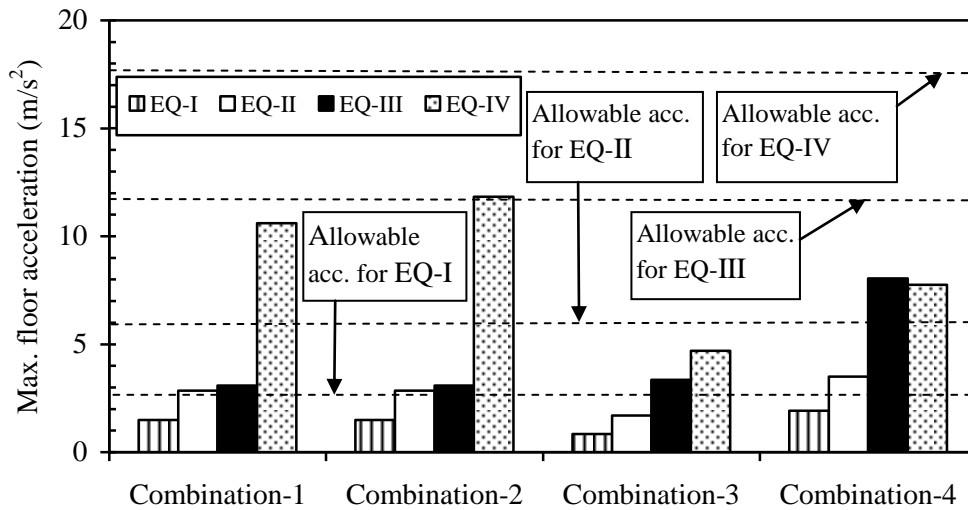


Figure 4.11(a) Maximum floor acceleration obtained for the five-story building when subjected to short-duration ground motions

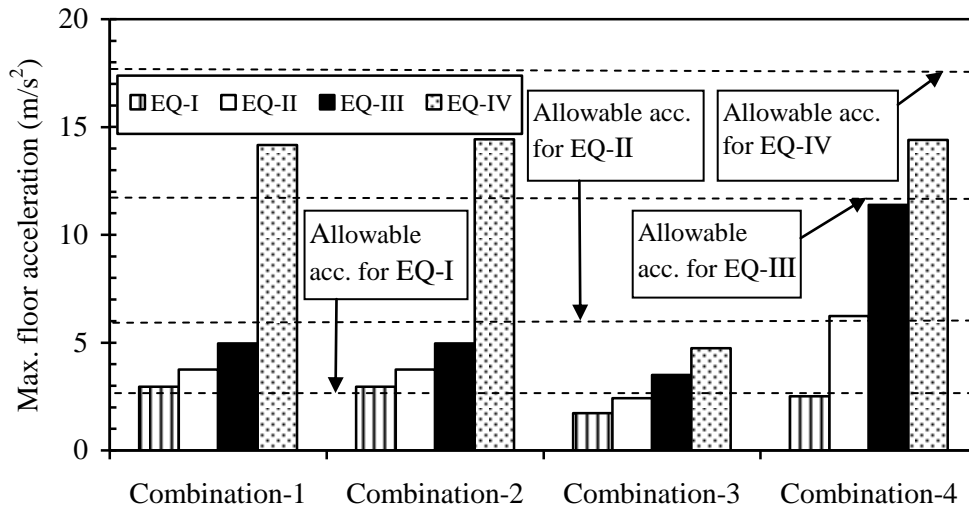


Figure 4.11 (b) Maximum floor acceleration obtained for the seven-story building when subjected to short-duration ground motions

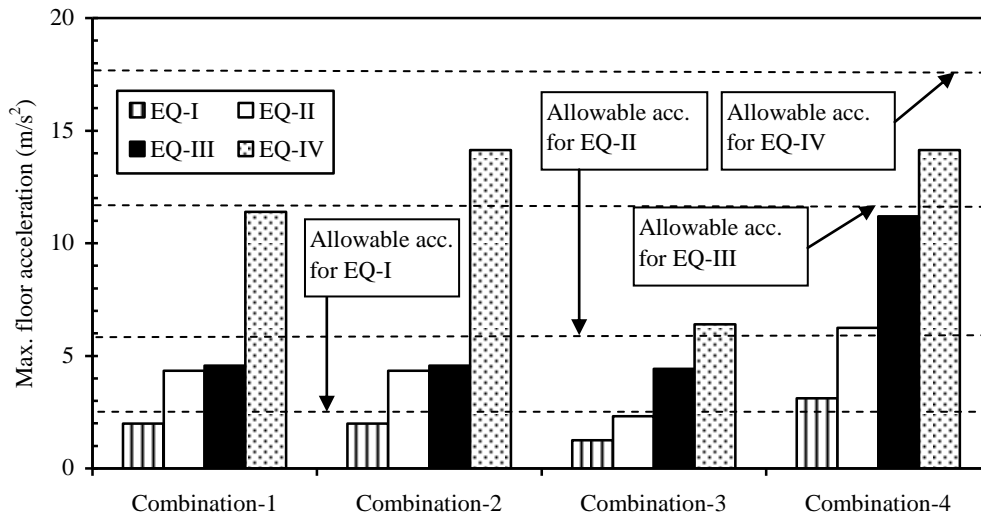


Figure 4.11 (c) Maximum floor acceleration obtained for the ten-story building when subjected to short-duration ground motions

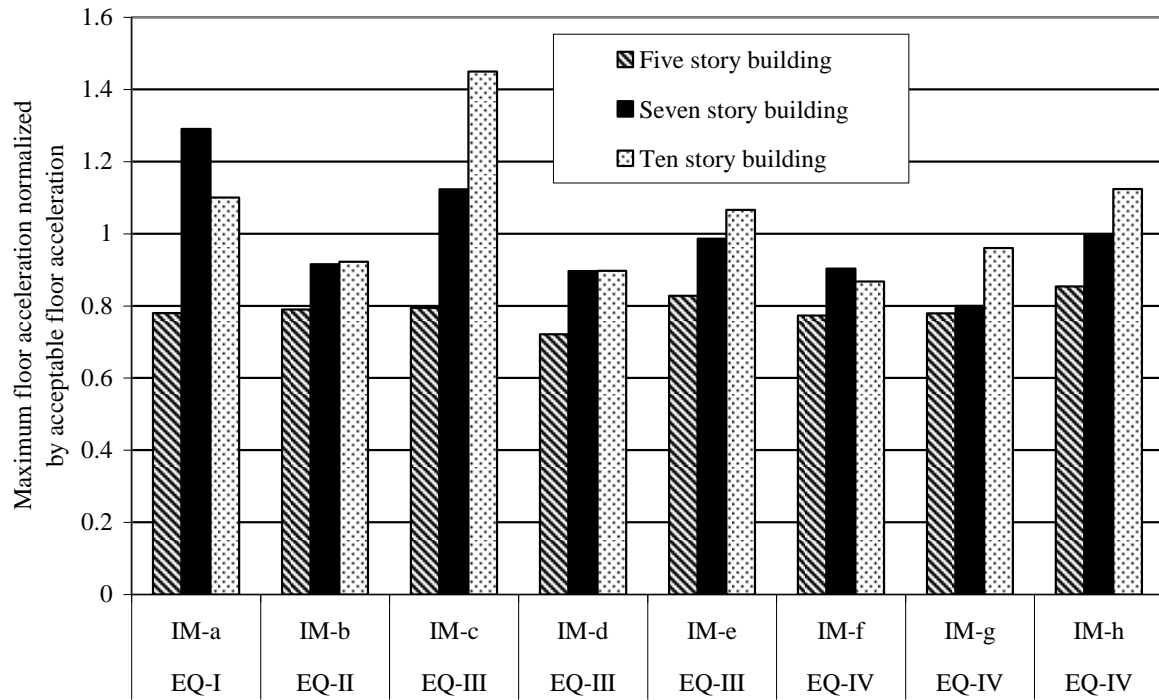


Figure 4.12 The maximum transient interstory drift normalized by the acceptable interstory drift.

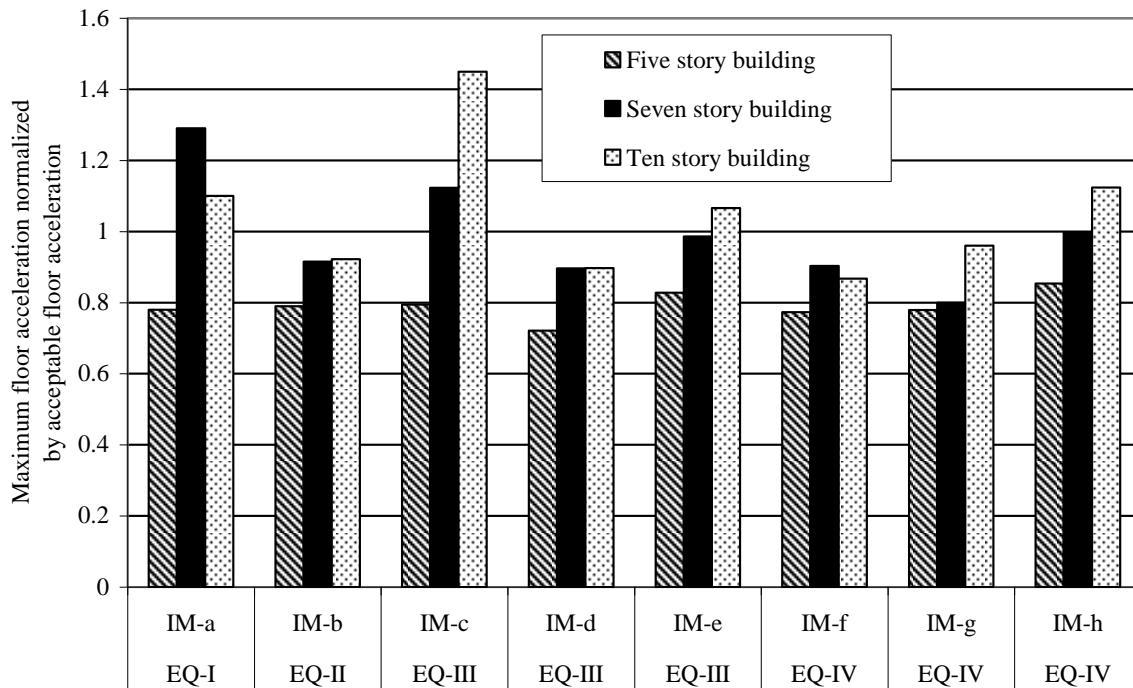


Figure 4.13 The maximum floor acceleration normalized by the acceptable floor acceleration

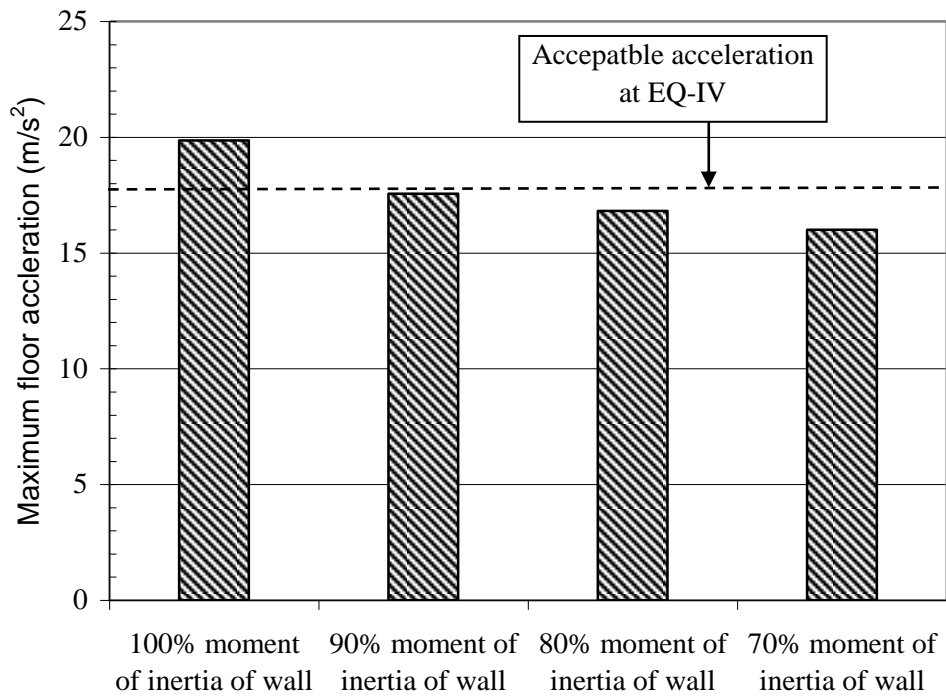


Figure 4.14 Effect of moment of inertia of wall in controlling the maximum floor acceleration when the ten-story building was subjected to ground motion IM-h

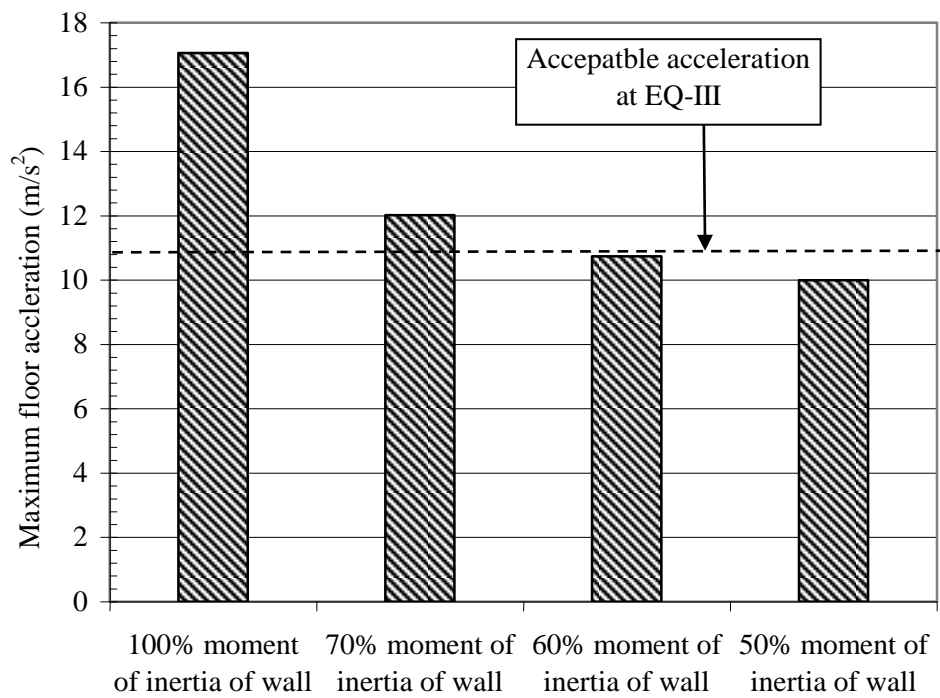


Figure 4.15 Effect of moment of inertia of wall in controlling the maximum floor acceleration when the ten-story building was subjected to ground motion IM-c

## **CHAPTER 5: CONCLUSIONS**

### **5.1 Overview**

Precast concrete structural systems have several advantages, including high quality, efficient use of materials, reduced construction time, and cost efficiency. Lack of sufficient knowledge about the intrinsic structural capacity of precast prestressed concrete structural systems kept structural design professionals away from using these structural systems in seismic zones. Traditional design codes have also imposed penalties on use of precast concrete, due to unknown fears and the lower level of performance of precast structures in past earthquakes, although such lower levels of performance resulted from using poor connection details between precast elements and a lack of sufficient number of lateral load resistance systems in the structures. Recent research shows that hybrid frames and unbonded jointed post-tensioned walls have the capacity to show acceptable seismic performance.

The present study introduced analytical models for jointed precast post-tensioned wall systems with validation. This study investigated the viability of use of unbonded jointed post-tensioned walls in buildings from low- to mid-rise in most intensive seismic region of the United States zone-4, considering the performance parameters of the maximum transition interstory drift, maximum floor acceleration and residual interstory drift. This system contained unique properties of re-centering and energy dissipation capacity. It was determined that the use of a jointed wall system is an economical solution for resisting seismic loads, if the direct displacement-based design method is used instead of the traditional force-based design method for designing these structural systems. In addition, the direct displacement-based design method has better ties with the actual performance of the structure compared to the force-based design method. The specific conclusions derived through this study are presented below.

### **5.2 Conclusions**

Two five-story jointed precast post-tensioned wall systems designed by direct displacement-based and force-based approaches at 60% scale were studied analytically. In this case, the direct displacement-based design approach resulted in a base shear 50% less

than for the force-based design method. Both wall systems performed satisfactorily in terms of the maximum interstory drift, maximum floor acceleration, and residual interstory drift. The transient interstory drift of the jointed wall system reduced with a higher number of energy dissipating shear connector without exceeding the limits of residual interstory drift.

Following the study of the five-story jointed wall system at 60% scale, performance-based seismic evaluation of jointed precast post-tensioned wall systems for low- to mid-rise buildings designed by the direct displacement-based approach was conducted using analytical models of the five-, seven-, and ten-story full scale buildings. For four levels of ground motions, the three buildings performed satisfactorily in terms of the maximum transient interstory drift and residual interstory drift. Few violations in the maximum floor acceleration of the ten- and seven-story buildings were observed, which could be mitigated by modifying the wall dimensions. Sensitivity was observed of the average drift to the increase of the maximum transient interstory drift reduced in jointed wall systems with the increase of the building's height. The taller building demonstrated a stronger tendency to approach and exceed unity of normalized floor acceleration as compared to the low-rise building. The low-rise building achieved the maximum transient interstory drifts closer to the acceptable limits compared to the taller building.

In summary, this study suggests that post-tensioned jointed walls are effective lateral load resistance systems and they can be used to adequately protect low- to mid-rise buildings experiencing seismic damages of structural and non-structural elements. These two systems have the capability to show satisfactory seismic performance not only under design level earthquakes but also under multiple levels of earthquakes, a high priority for keeping the buildings serviceable. In addition, the direct displacement-based design approach appears to be the preferred design methodology compared to the traditional force-based approach for designing post-tensioned jointed wall systems because of its coherent tie with the performance of buildings and the economy of construction as well.

### **5.3 Future Research**

In future research, a combined use of hybrid frame and jointed precast post-tensioned wall systems in the same direction of building may be considered. It appears combined use of

hybrid frame and jointed precast post-tensioned wall systems in the same direction may lead to improved performance by producing optimized values of the maximum transient interstory drift and maximum floor acceleration leading to economical structural solution. In addition, similar research may be conducted for seismic zones other than zone-4 and soil class C. Reconciliation of such recommended research may help the structural design professionals by providing them a comprehensive direction to take technological advantage of precast concrete hybrid frame and jointed precast post-tensioned wall systems as primary seismic load resistance systems.

*Intentionally blank*